The Frequency of Failures within a Group of Similar Structures

A. H. CHILVER, Ph.D.

(*Department of Civil Engineering, University of Bristol*)

Summary: An attempt is made to assess the rate at which failures occur within a group of similar structures, or structural components, when each structure is subjected to the same set of applied loads. The structures are similar in every respect except for small inherent differences in strength from one structure to another. On infrequent occasions the applied loads may be so intense as to destroy the weaker members of the group. For the problem in which the structural strengths are distributed within the group in a " normal " fashion, and when the frequency of severe loads diminishes exponentially, it is found that the rate at which failures occur within the group of structures is governed by two simple non-dimensional parameters. Numerical values of these parameters are studied more fully.

1. Introduction

In the design of engineering structures it is assumed generally that all components of the same type, and manufactured from the same material, have equal strengths. It is well known, however, that all constructional materials—whether produced naturally or manufactured—show distinct variations in strength from one test sample to another, even when special efforts are made to produce a material of consistent strength. With a set of structural components manufactured from a natural material, such as timber, the variations in strength from one component to another may be considerable; those materials which are manufactured—such as steel, aluminium alloy and, to a limited extent, concrete—may be controlled in quality more carefully, and for these materials it is possible to prescribe certain minimum strengths with reasonable accuracy. However, even for the manufactured materials the testing of a number of structural components reveals inevitable variations in strength from one component to another, although the range of strength scatter may be relatively small. In addition to inherent material variations, there is the further difficulty that manufacturing processes cannot provide structural components which are exactly similar in geometrical form, in surface finish, and so on. It may be concluded that, although the mean strength of a number of similar structural components is usually defined closely, the scatter of strength among those components is governed by the quality of the material and the extent to which the manufacture of the components is controlled.

A further important consideration in assessing the safety of a group of similar structures is that extremely severe loads—more intense than the design loads—may be encountered by a few of the structures during their working lives. The infrequent occurrence and uncertain nature of these loads may tempt the designer to ignore

Originally received March 1954.

their effects, because the life expected of each structure may be so short that there is little chance of severe loads being encountered. For example, hurricanes and earthquakes may destroy completely certain light types of building; obviously it is not economical to design the less important structures to withstand the most severe effects of such disturbances. To take account of these severe loads and to provide the structures with the necessary additional strength, would mean that a longer life is expected of each structure, and in many instances this is unjustifiable. A more logical approach to this problem is to accept an occasional failure of one of a group of structures, and at the same time to provide the structures with sufficient strength to give a frequency of failures which is not unreasonable for structures of that particular type. In the aeronautical field the design of aircraft wings involves a similar problem; on rare occasions an aircraft may encounter extremely severe upward or downward gusts. The frequency of occurrence of gusts of such intensities is so small that it is not economical to encumber every aircraft with the additional structural weight necessary to provide against these severe loads.

On considering these two aspects of the problem, only qualitative conclusions can be deduced about their relative importance at this stage. However, a discussion of the frequency of failures among a group of similar structures will revolve obviously around considerations of

(*i*) the variation of strength within the group of structures, and

(*ii*) the frequency of occurrence of severe loads.

If the strength variation is considerable, then it may be found that both moderate and severe loads destroy some of the structures. On the other hand, if the strength variation is small, then only the severest loads cause destruction among the group of structures.

The first writer to study the problem in simple terms was Pugsley[1] who discussed the case of a group of aircraft wings of variable strength, each wing encountering gust loads of varying intensities. The approach used by Pugsley is extended in the present paper to give finally a method of analysis which is wider in scope.

Notation

N	number of structures within the group
P	intensity of load applied to a structure
λ	number of structures of strength less than P
E	number of loads of intensity greater than P applied to each structure in unit time
F	number of failures in N units of time
f	frequency of failures
P_m	mean strength of the group
σ	standard deviation of strengths within the group

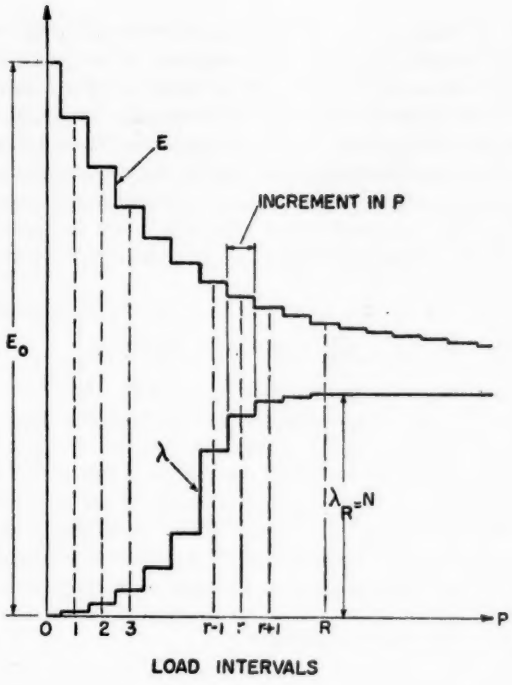

Fig. 1.

Distribution of strength and variation of applied loads on the basis of finite differences.

y	normal distribution function
k	a constant related to the applied loads
$\phi(x)$	standardised normal distribution function
$\Phi(x)$	standardised normal cumulative distribution function
α	non-dimensional strength parameter $(=\sigma/P_m)$
β	non-dimensional load parameter $(=kP_m)$

2. Solution in Terms of Finite Differences

2.1. Distribution of strength and variation of applied loads

Consider a group of N structures, or structural components, similar in all respects except that the strengths may vary from one structure to another. Suppose λ_r structures have strengths less than that corresponding to P_r (Fig. 1); for convenience the load scale is divided into a number of equal finite intervals. If the structure is a simple tension member of a framework, then all structures would be expected to withstand loads greater than zero load; in this case, $\lambda_0=0$. Also there must be an upper limit for the strength, and it is assumed that all structures are weaker than some finite strength P_R; then $\lambda_R=N$.

The number of loads applied to each structure in unit time, and in excess of P_r, is taken as E_r. It is assumed that each structure of the group is called upon to withstand the same set of loads. The unit of time is defined quite arbitrarily; in some problems, such as those associated with aircraft wings, the unit of time is replaced for convenience by a suitable unit of distance. The time unit is simply the most convenient basis for comparing the relative frequencies of the applied loads. Since all the applied loads must be greater than zero intensity, E_0 represents the total number of loads applied to a structure in unit time. The variation of the function E_r must be derived from the measurement of loads in actual structures of the type under consideration.

2.2. *Increments in strength (Pugsley's method)*

Consider the number of structures of strength P_r; there are λ_r structures of strength less than P_r, and λ_{r+1} structures of strength less than P_{r+1}. So that $(\lambda_{r+1}-\lambda_r)$ structures have strengths within the interval P_r; these structures are destroyed only by loads which exceed P_r in intensity, that is, by E_r loads in unit time for each structure. If it is assumed* that whenever structures of a certain strength are destroyed then they are replaced by new structures of the same strength, the effects of the loads on the structures can be imagined as a continuous process of destruction and replenishment at constant strength. The number of failures suffered by structures of strength P_r is $E_r(\lambda_{r+1}-\lambda_r)$; so that the total number of failures suffered by structures of all strengths is

$$F_1=\sum_{r=0}^{r=\infty} E_r(\lambda_{r+1}-\lambda_r)=E_0\lambda_1+\sum_{r=1}^{r=R-1} E_r(\lambda_{r+1}-\lambda_r), \quad . \quad . \quad . \quad (1)$$

since $\lambda_0=0$, and $(\lambda_{r+1}-\lambda_r)=0$ for $r\geqslant R$; the failures F_1 occur in N units of time Equation (1) is a formal statement of the method used by Pugsley[1].

2.3. *Increments in applied load (alternative method)*

There is an alternative method of deriving the total number of failures suffered by the structures; consider, for example, the damage caused by the loads of intensity P_r. The number of loads applied to each structure in unit time and in excess of P_{r-1} is E_{r-1}, while the number of loads in excess of P_r is E_r. So that in the interval P_r there are $(E_{r-1}-E_r)$ applied loads, which destroy structures of strength less than P_r. On the basis of replenishment at constant strength, the number of failures caused by these loads is $\lambda_r(E_{r-1}-E_r)$. The total number of failures caused by all applied loads is therefore

$$F_2=\sum_{r=0}^{r=\infty}\lambda_r(E_{r-1}-E_r)=\sum_{r=1}^{r=R-1}\lambda_r(E_{r-1}-E_r)+\lambda_R E_{R-1}, \quad . \quad . \quad (2)$$

since $\lambda_0=0$, $\lambda_R=\lambda_{R+1}=\lambda_{R+2}=\ldots=\lambda_\infty$, and E_∞ is assumed equal to zero. The failures F_2 occur again in N units of time.

*This assumption is considered by Pugsley[1] to be a reasonable approximation to practical conditions.

2.4. *Comparison of the two methods*

Both methods give values of the total number of failures occurring within the group of N structures. The former method (Pugsley's approach) gives the number of failures suffered by the group of structures, while the latter method gives the number of failures caused by the applied loads. Since the total number of failures in each case is the same, F_1 and F_2 are equal; to demonstrate this, equation (2) is written first in its expanded form

$$F_2=\lambda_1(E_0-E_1)+\lambda_2(E_1-E_2)+\ldots.+\lambda_{R-1}(E_{R-2}-E_{R-1})+\lambda_R E_{R-1}.$$

The terms in this series may be rearranged to give

$$F_2=\lambda_1 E_0+E_1(\lambda_2-\lambda_1)+E_2(\lambda_3-\lambda_2)+\ldots.+E_{R-1}(\lambda_R-\lambda_{R-1}),$$

so that

$$F_2=E_0\lambda_1+\sum_{r=1}^{r=R-1}E_r(\lambda_{r+1}-\lambda_r)=F_1.$$

TABLE I

ESTIMATION OF THE FREQUENCY OF FAILURES AMONG A GROUP OF STRUCTURES

λ_r=number of structures of strength less than P_r,

E_r=number of loads in excess of P_r applied to each structure in unit time.

Interval r	λ_r	E_r	*Increments in* λ $\Delta\lambda$	$E\Delta\lambda$	*Increments in* E ΔE	$\lambda\Delta E$
—	—	—	—	—	—	—
5	0	—	0	0	—	0
6	0	2,525	0	0	—	0
7	0	1,591	0	0	934	0
8	0	1,004	0	0	587	0
9	0	634	2	1,268	370	0
10	2	400	9	3,600	234	468
11	11	252	27	6,804	148	1,628
12	38	159	65	10,335	93	3,534
13	103	100	121	12,100	59	6,077
14	224	63	176	11,088	37	8,288
15	400	40	200	8,000	23	9,200
16	600	25	176	4,400	15	9,000
17	776	16	121	1,936	9	6,984
18	897	10	65	650	6	5,382
19	962	6	27	162	4	3,848
20	989	4	9	36	2	1,978
21	998	3	2	6	1	998
22	1,000	2	0	0	1	1,000
23	1,000	1	0	0	1	1,000
24	1,000	0	0	0	1	1,000
25	1,000	0	0	0	0	0
—	—	—	—	—	—	—
				60,385		60,385

Total number of failures=60,385 in 10^3 time units
=60+ in 1 time unit.

KRESGE-HOOKER
WAYNE
UNIVERSITY
SCIENTIFIC LIBRARY

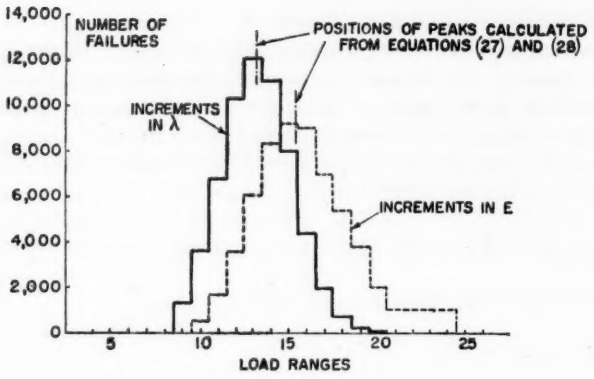

Fig. 2.
Distribution of failures for the example of Table I.

Although the summations of the two series are the same, corresponding terms in each series are not equal. The sum of terms of equation (1) up to $r=q$ is

$$F_1(q)=E_0\lambda_1+\sum_{r=1}^{r=q} E_r(\lambda_{r+1}-\lambda_r).$$

From equation (2), the sum of terms up to $r=q$ is

$$F_2(q)=\sum_{r=1}^{r=q} \lambda_r\,(E_{r-1}-E_r), \qquad [q<R],$$

$$\text{so that} \qquad F_1(q)-F_2(q)=E_q\lambda_{q+1}. \qquad . \quad . \quad . \quad . \quad (3)$$

It is deduced that $F_1(q)\geqslant F_2(q)$; at the low end of the strength range and the upper end of the applied load range the two functions are equal.

The two methods are compared in the solution of the frequency of failures for the group of structures outlined in Table I. The group consists of 1,000 structures with a symmetrical distribution of strengths about a mean value of 15. The variation of applied loads is not necessarily typical of any practical problem; it is used in this example to illustrate the important differences between the two methods of solution. The individual terms of the two series given by equations (1) and (2) are plotted in Fig. 2. The largest term in equation (1) corresponds to those structures suffering the greatest damage; in this light Pugsley's method is useful in indicating the weakest range of strength. On the other hand the largest term of equation (2) corresponds to those applied loads causing the greatest failure frequency; equation (2) indicates, therefore, the range of loads causing the greatest damage.

The examples discussed by Pugsley[1] may be analysed by either equation (1) or equation (2); although the total summations given by these equations are the same, there is again a marked difference between the positions of the largest terms in the two series.

3. The Use of the Differential Calculus

The main purpose of the present paper is to determine those factors which govern the frequency of failures; it is advantageous to simplify the preceding analysis by replacing the finite intervals of load and strength by infinitesimal increments. This will give continuous functions for strength distribution and applied load variation.

Suppose $E(P)$ represents the number of times the applied load P is exceeded in intensity on each structure in unit time; suppose also that in the group of N structures there are $\lambda(P)$ having strengths less than P. The functions E and λ have the continuous forms shown in Fig. 3; E_0 defines again the total number of loads applied to each structure in unit time; it is assumed that $E \longrightarrow 0$ as $P \longrightarrow \infty$. The total variation of strengths is finite, so that $\lambda(0)=0$ and $\lambda(\infty)=N$; that is, all structures are stronger than zero strength and weaker than infinite strength.

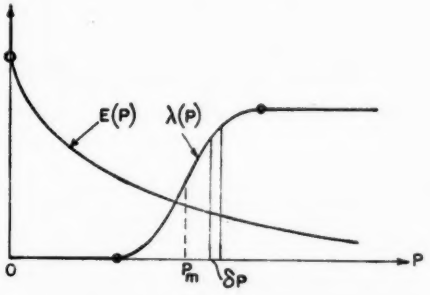

Fig. 3.
Continuous variations in E and λ.

3.1. *Infinitesimal increments in strength*

Of the N structures in the group, $\delta\lambda$ have strengths in the range from P to $(P+\delta P)$. Each of these structures withstands E loads in excess of P in unit time. On assuming as before that a destroyed structure is replaced by a structure of the same strength, the number of failures suffered by structures in the strength range δP is $E\delta\lambda$. The total number of failures suffered by all structures is

$$F_1 = \int_{P=0}^{P=\infty} E\,d\lambda = \int_0^{\infty} E\lambda' dP, \qquad \text{(in } N \text{ time units)}, \quad . \quad . \quad . \quad (4)$$

where $\lambda' = d\lambda/dP$. The number of failures in unit time, or the frequency of failures, is therefore

$$f_1 = \frac{1}{N} F_1 = \frac{1}{N} \int_0^{\infty} E\lambda' dP. \quad . \quad . \quad . \quad . \quad (5)$$

3.2. *Infinitesimal increments in applied load*

Again, consider the applied loads in the range from P to $(P+\delta P)$; there are E loads in excess of P, and $(E+\delta E)$ loads in excess of $(P+\delta P)$. So that in the range δP there are $-\delta E$ applied loads. The number of structures destroyed by the $-\delta E$ loads is $-\lambda\delta E$, since λ structures are weaker than P. On the basis of replenishment at constant strength the total destruction due to all applied loads is

$$F_2 = \int_{t=0}^{P=\infty} -\lambda\, dE = -\int_0^{\infty} E\lambda' dP, \qquad \text{(in } N \text{ time units)}, \quad . \quad . \quad . \quad (6)$$

where $E' = dE/dP$. The number of failures in each unit of time is

$$f_2 = \frac{1}{N} F_2 = -\frac{1}{N} \int_0^{\infty} \lambda E' dP. \quad . \quad . \quad . \quad . \quad (7)$$

3.3. *Comparison of the two frequencies of failure*

On integrating equation (6) by parts,

$$F_2 = -\int_0^{\infty} \lambda E' dP = -\left[\lambda E - \int E\lambda' dP\right]_0^{\infty} = -\left[\lambda E\right]_0^{\infty} + \int_0^{\infty} E\lambda' dP.$$

But $E(\infty) = 0$, and $\lambda(0) = 0$; so that $\left[\lambda E\right]_0^{\infty} = 0$, and

$$F_2 = \int_0^{\infty} E\lambda' dP = F_1.$$

As for the finite difference method, the total number of failures suffered by all structures may be derived by either equation (5) or equation (7).

On the basis of increments in strength, the total number of failures suffered by all structures of strength less than P is

$$F_1(P) = \int_0^{P} E\lambda' dP. \quad . \quad . \quad . \quad . \quad . \quad . \quad (8)$$

Alternatively, for increments in applied load, the total number of failures caused by loads less than P is

$$F_2(P) = -\int_0^{P} \lambda E' dP. \quad . \quad . \quad . \quad . \quad . \quad (9)$$

Equation (9) may be written

$$F_2(P) = -\left[\lambda E - \int E\lambda' dP\right]_0^P = -\lambda E + F_1(P),$$

since $\lambda(0) = 0$.

Then $$F_1(P) - F_2(P) = \lambda E. \quad . \quad . \quad . \quad . \quad (10)$$

It is concluded that $F_1(P)$ is always greater than $F_2(P)$, unless λ or E is zero.

4. Idealised Variations of Strength and Applied Load

4.1. Strength variations

The analysis of Section 3 can be used most profitably if it is possible to define more precisely the forms of strength distribution on the one hand, and the variation of applied loads on the other.

For the distribution of strengths of the structures a normal distribution about the mean strength is assumed. This assumption disregards any deviations from symmetry which actual strength variations may show. On this basis, the number of structures having strengths in the range from P to $(P+\delta P)$ is $y\delta P$, where y is the normal distribution function defined by

$$y = \frac{N}{\sigma\sqrt{(2\pi)}} \exp\left\{-\frac{(P-P_m)^2}{2\sigma^2}\right\} \quad . \quad . \quad . \quad . \quad (11)$$

in which N = total number of structures in the group,

P_m = mean strength of the group, and

σ = standard deviation of the strengths of the group.

$\lambda(P)$ has been defined as the number of structures of strength less than P; so that

$$\delta\lambda = y\delta P, \quad \text{or} \quad \lambda' = y. \quad . \quad . \quad . \quad . \quad . \quad (12)$$

Then λ is the normal cumulative distribution function.

4.2. Load variations

For the definition of the applied loads it is assumed that severe loads occur far less frequently than more moderate loads; extensive studies[2] of gust loads on aircraft wings suggest that the function E is defined closely by the relation

$$E(P) = E_0 \exp(-kP), \quad . \quad . \quad . \quad . \quad . \quad (13)$$

in which $E(P)$ = total number of loads in excess of P in unit time,

E_0 = total number of loads in excess of zero load, and

k = a positive constant [having the dimensions of (load)$^{-1}$].

Equation (13) is by no means true of all structural loading conditions; for example, it has been suggested[3] that wind loads on buildings are distributed normally about a mean wind velocity of approximately 23 m.p.h.; problems such as this require special study.

4.3. *The frequency of failures*

The idealised strength distribution and applied load variations are shown in Fig. 4; the strength function λ is anti-symmetrical about the mean strength P_m. Hypothetically the total range of strength scatter is from $P=-\infty$ to $P=+\infty$.

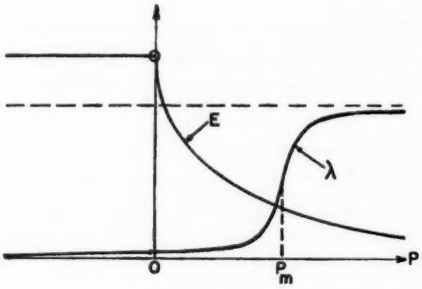

Fig. 4.

Idealised representation of the strength distribution and applied load variations.

The variation of positive loads is given by equation (13); suppose, for convenience, that all loads are negative initially, and increase progressively up to their maximum values; then for $P<0$, we have $E(P)=E_0$.

In terms of increments in the strength function λ, the total number of failures is

$$F_1=\int_{-\infty}^{+\infty} E\lambda' dP=E_0\int_{-\infty}^{0}\lambda' dP+\int_{0}^{\infty} E\lambda' dP, \qquad \text{(in } N \text{ time units)}.$$

The frequency of failures is

$$f_1=\frac{1}{N}\left[E_0\lambda_0+\int_0^{\infty} E\lambda' dP\right], \qquad \text{(in unit time)}, \quad . \quad . \quad . \quad (14)$$

where λ_0 is the value of λ at $P=0$.

On the basis of increments in the applied load function E, the frequency of failures is

$$f_2=-\frac{1}{N}\int_{-\infty}^{+\infty}\lambda E' dP=-\frac{1}{N}\int_0^{\infty}\lambda E' dP, \qquad \text{(in unit time)}. \quad . \quad . \quad (15)$$

since $E'(P)=0$ for $P<0$.

Equation (15) may be written

$$f_2 = -\frac{1}{N}\left[\lambda E - \int E\lambda' dP\right]_0^\infty = \frac{1}{N}\left[E_0\lambda_0 + \int_0^\infty E\lambda' dP\right] = f_1. \quad . \quad (16)$$

On substituting for λ and E the values given by equations (11) and (13),

$$\lambda = \int_{-\infty}^{P} \frac{N}{\sigma\sqrt{(2\pi)}} \exp\left\{-\frac{(P-P_m)^2}{2\sigma^2}\right\} dP, \qquad E = E_0 \exp(-kP). \quad . \quad (17)$$

Then

$$f_1 = \frac{E_0}{\sigma\sqrt{(2\pi)}}\left[\int_{-\infty}^{0} \exp\left\{-\frac{(P-P_m)^2}{2\sigma^2}\right\} dP + \int_0^\infty \exp(-kP)\exp\left\{-\frac{(P-P_m)^2}{2\sigma^2}\right\} dP\right],$$

which may be written

$$f_1 = E_0\left[\frac{1}{\sqrt{(2\pi)}}\int_{-\infty}^{-P_m/\sigma} \exp(-x^2/2)\,dx + \exp(\tfrac{1}{2}\sigma^2k^2 - kP_m)\frac{1}{\sqrt{(2\pi)}}\int_{\left(\sigma k - \frac{P_m}{\sigma}\right)}^{\infty} \exp(-x^2/2)\,dx\right]. \quad . \quad (18)$$

Now, $\frac{1}{\sqrt{(2\pi)}}\int_{-\infty}^{x} \exp(-x^2/2)\,dx$ is the standardised normal cumulative distribution function, written here for convenience as $\Phi(x)$. Then equation (18) takes the form

$$f_1/E_0 = \Phi\left(-\frac{P_m}{\sigma}\right) + \exp(\tfrac{1}{2}\sigma^2k^2 - kP_m)\,\Phi\left(\frac{P_m}{\sigma} - \sigma k\right), \quad . \quad (19)$$

since $$\frac{1}{\sqrt{(2\pi)}}\int_{-\infty}^{\infty} \exp(-x^2/2)\,dx = \frac{1}{\sqrt{(2\pi)}}\int_{-\infty}^{x} \exp(-x^2/2)\,dx = \Phi(x).$$

When the first term, $\Phi(-P_m/\sigma)$, in equation (19) becomes large in relation to the second term, the idealised representation of the frequency of failures loses all practical significance, because the weaker members of the group, for which $P < 0$, become important. A study of the relative values of the two terms in equation (19) indicates the stage at which the idealised problem is meaningless.

4.4. *Distribution of failures*

The failures suffered by structures up to strength P is

$$F_1(P) = \int_{-\infty}^{P} E\lambda' dP.$$

We are interested in values of $P>0$; so that

$$F_1(P)=E_0\int_{-\infty}^{0}\lambda' dP+\int_{0}^{P}E\lambda' dP=E_0\lambda_0+\int_{0}^{P}E\lambda' dP.$$

Then $$dF_1(P)/dP=F_1'(P)=E\lambda'=Ey, \quad . \quad . \quad . \quad . \quad (20)$$

where y is the normal distribution function. On substituting for y,

$$F_1'(P)=\frac{E_0N}{\sigma\sqrt{(2\pi)}}\exp(\tfrac{1}{2}\sigma^2k^2-kP_m)\exp\left\{-\frac{1}{2\sigma^2}[P-(P_m-\sigma^2k)]^2\right\}, \quad (21)$$

so that $F_1'(P)$ is a type of normal distribution function with values disposed symmetrically about a mean value $P=P_m-\sigma^2k$; the maximum value of $F_1'(P)$ is

$$F_1'(P)_{max}=\frac{E_0N}{\sigma\sqrt{(2\pi)}}\exp(\tfrac{1}{2}\sigma^2k^2-kP_m). \quad . \quad . \quad . \quad (22)$$

It may be concluded that the most heavily damaged strength range occurs at $P=P_m-\sigma^2k$, that is, at a value of P below the mean strength P_m of the structures.

The total number of failures caused by loads up to an intensity P is

$$F_2(P)=-\int_{-\infty}^{P}\lambda E' dP.$$

We are interested in values of $P>0$; so that

$$F_2(P)=-\int_{0}^{P}\lambda E' dP,$$

and $$dF_2(P)/dP=F_2'(P)=-\lambda E'.$$

On substituting for λ and E

$$F_2'(P)=E_0k\exp(-kP)\frac{N}{\sigma\sqrt{(2\pi)}}\int_{-\infty}^{P}\exp\left[-\frac{(P-P_m)^2}{2\sigma^2}\right]dP$$

$$=E_0Nk\exp(-kP)\,\Phi\left(\frac{P}{\sigma}-\frac{P_m}{\sigma}\right). \quad . \quad . \quad . \quad . \quad (23)$$

The maximum value of $F_2'(P)$ occurs when $F_2''(P)=0$. Now

$$F_2''(P)=\frac{1}{\sigma}E_0Nk\exp(-kP)\left[\phi\left(\frac{P}{\sigma}-\frac{P_m}{\sigma}\right)-\sigma k\Phi\left(\frac{P}{\sigma}-\frac{P_m}{\sigma}\right)\right],$$

where $\phi(x)=\sqrt{(1/2\pi)}\exp(-x^2/2)$, the standardised normal distribution function.

Then $F_2''(P)$ is zero when

$$\frac{\phi\left(\frac{P}{\sigma}-\frac{P_m}{\sigma}\right)}{\Phi\left(\frac{P}{\sigma}-\frac{P_m}{\sigma}\right)}=\sigma k. \quad . \quad . \quad . \quad . \quad . \quad . \quad (24)$$

The required value of P is the root of equation (24), which cannot be solved exactly in a simple fashion. It is interesting to note that $F_2'(P)$, unlike the function $F_1'(P)$, is not a normal distribution.

5. Basic Parameters of the Idealised Problem

The important feature which emerges from the idealised representation of the strength distribution and the applied load variation is that the frequency of failures, as given by equation (19), is governed by the two parameters (σ/P_m) and (kP_m).

$$\text{Suppose} \qquad \sigma/P_m=\alpha, \qquad kP_m=\beta. \quad . \quad . \quad . \quad . \quad (25)$$

Then the frequency of failures is given by

$$(f_1/E_0)=\Phi\left(-\frac{1}{\alpha}\right)+\exp\left(\tfrac{1}{2}\alpha^2\beta^2-\beta\right)\Phi\left(\frac{1}{\alpha}-\alpha\beta\right). \quad . \quad . \quad (26)$$

The function (f_1/E_0) defines the number of failures in unit time for each load applied to a structure; α is a non-dimensional parameter which gives a measure of the scatter of strength within the group of structures; the parameter β defines the frequency with which the applied load P_m is exceeded. If there is no scatter of strength then $\sigma=0$, $1/\alpha=\infty$, and

$$(f_1/E_0)=\Phi(-\infty)+\exp(-\beta)\,\Phi(+\infty)=\exp(-\beta).$$

In this case, $f_1=E_0\exp(-\beta)=E_0\exp(-kP_m)$, which is the frequency with which P_m is exceeded; of course, this would be expected to correspond to the frequency of failures when all the structures have the same strength P_m.

In terms of α and β, the most heavily damaged strength range is given by

$$\frac{P}{P_m}=1-\frac{\sigma^2 k}{P_m}=1-\alpha^2\beta. \quad . \quad . \quad . \quad . \quad (27)$$

Moreover, the most heavily damaging load range is given by the solution of the equation

$$\frac{\phi\left[\frac{1}{\beta}\left(\frac{P}{P_m}-1\right)\right]}{\Phi\left[\frac{1}{\beta}\left(\frac{P}{P_m}-1\right)\right]}=\frac{1}{\alpha\beta}. \quad . \quad . \quad . \quad . \quad (28)$$

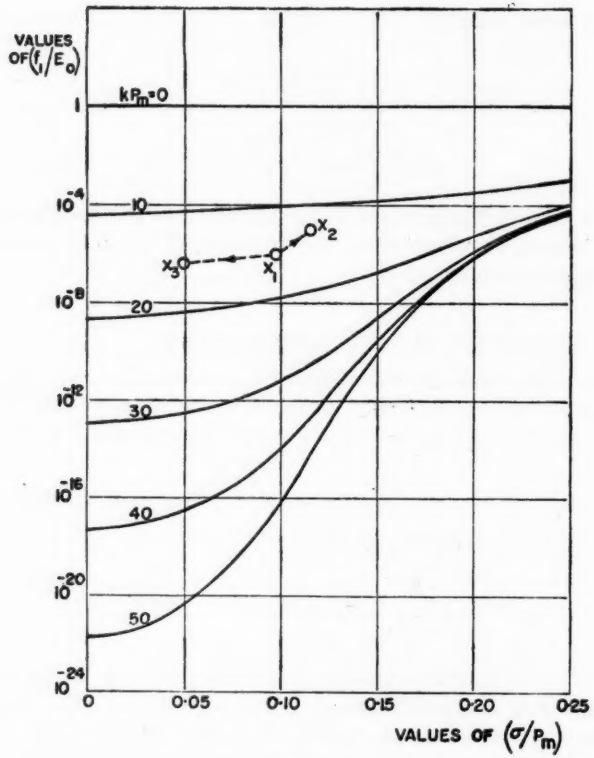

Fig. 5.
Chart of idealised frequencies of failure. Points X_1, X_2, X_3 refer to Pugsley[1].

Since the function f_1/E_0 is governed by only two parameters according to equation (26), values of f_1/E_0 may be studied on a single chart, as indicated in Fig. 5. In this diagram the failure frequencies are given for values of the "strength" parameter σ/P_m from 0·00 to 0·25, and for values of the "applied load" parameter kP_m from 0 to 50. Low values of kP_m have no practical significance, but are included for completeness. In many problems σ/P_m is very small; Fig. 5 shows clearly the extent to which the failure rate is increased by the presence of even small scatters of strength; for example, if $kP_m=40$, an increase of the strength parameter σ/P_m from 0 to 0·05 produces a tenfold increase in the failure rate.

The three numerical problems discussed by Pugsley[1] are indicated in Fig. 5 by the points X_1, X_2 and X_3; in the first example the strength properties of the structures give $\sigma/P_m=0·097$, while the applied loading conditions approximate to $kP_m=15·0$. These values of the two parameters correspond to the point X_1 in Fig. 5; the frequency of failures given by Fig. 5 is 31 per unit time, compared with 32 per unit time computed from Pugsley's finite difference formula. In the second example the mean strength of the group of structures is reduced to give $\sigma/P_m=0·115$; the value of

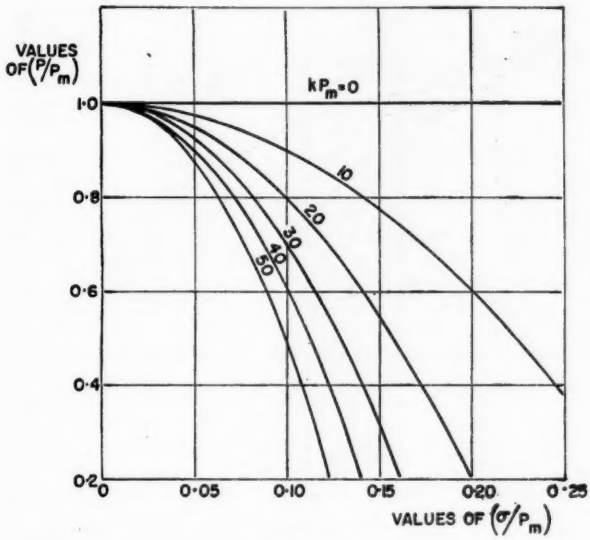

Fig. 6.

Position of the most heavily damaged strength range.

kP_m is reduced to 12·7; these correspond to the point X_2 of Fig. 5. There is obviously a concomitant increase in the frequency of failures. In the third example Pugsley considers the effect of reducing the standard deviation of the strength distribution; in this case $\sigma/P_m=0{\cdot}049$ and $kP_m=15{\cdot}0$, giving the point X_3 in Fig. 5. The change in failure frequency is not so pronounced because the change from X_1 to X_3 takes place along the flat portion of the kP_m contour.

From equation (27) can be derived the most heavily damaged strength range in terms of σ/P_m and kP_m; Fig. 6 gives values of P/P_m which satisfy equation (27). In all practical problems the most heavily damaged strength range is below the mean strength P_m; this can be checked for the three examples discussed by Pugsley[1]. For the most heavily damaging applied loads equation (28) is solved for P/P_m; the results of a number of computations are given in Fig. 7. For the numerical example studied in Table I, the positions of the turning points of the two curves, as calculated from equations (27) and (28), are indicated in Fig. 2; in that example the variation of applied loads follows the exponential law of equation (13). The estimated positions of the maxima are in excellent agreement with the actual turning points.

6. Conclusions

The solution of the problem in terms of infinitesimal increments in strength and applied load leads to results which may be used to considerable advantage in studying the problem more generally. The frequency of failures can be derived in two ways—the one based on strength increments and the other on applied load

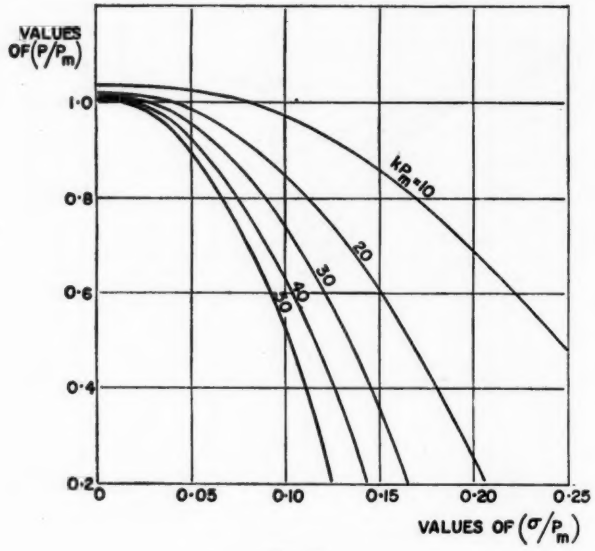

Fig. 7.
Position of the most heavily damaging range of applied loads.

increments; the result is the same in each case, although there are different distributions of failures among the load ranges. The one method indicates the most heavily damaged range of strengths, and hence the weakest section within the group of structures, while the other method shows clearly the most damaging range of applied loads.

For the idealised variations of strength and applied load, the frequency of failures is governed by "strength" and "applied load" parameters; in this respect Fig. 5 is useful in indicating changes in the frequency of failures which accompany alterations of either the mean strength or the scatter of strength of the group of structures.

Acknowledgment

The author is indebted to Professor A. G. Pugsley, F.R.S., for a number of helpful suggestions in the preparation of this paper.

References

1. Pugsley, A. G. (1942). A Philosophy of Aeroplane Strength Factors. R. & M. 1906.
2. Taylor, J. (1953). Measurement of Gust Loads in Aircraft. *Journal Royal Aeronautical Society*, p. 78, February 1953.
3. Horne, M. R. (1950). Wind Loads on Structures. *Journal of the Institution of Civil Engineers*, Vol. 33, p. 155, 1950.

The Effect of Delta Vanes on Supersonic Wings

M. A. GORGUI

(Department of Mathematics, University of Manchester)*

Summary: For supersonic wings it is known that the presence of a tip reduces the lift and the performance compared with the corresponding values for the two-dimensional wing. It appeared from some work by K. Stewartson[3] that the addition of a vane at the wing tip might counteract this effect. The purpose of this paper is to determine the effect due to the presence of the vane. For this purpose a wing in the form of a semi-infinite wedge whose leading edge is swept back is supposed placed at incidence to the flow, with a symmetric triangular vane with diamond-shaped base attached to it, its vertex being at the tip of the leading edge, and its plane of symmetry parallel to the flow. The problem is of the " conical field " type and is solved by the method of S. Goldstein and G. N. Ward[1].

The problem is divided into its anti-symmetrical and symmetrical parts. The results obtained in Ref. 1 are applied to determine the field in each case, both outside and inside the Mach cone of the vertex.

In the anti-symmetrical part, three cases are considered, with a different vane in each case, and the lift coefficient for the parts of the wing inside the Mach cone is determined. In the symmetrical part, only the case when the vane lies entirely inside the Mach cone is considered, and the drag force is obtained. The performance is then calculated, and curves are drawn to show how it is affected by the existence of the vane.

1. Introduction

In supersonic flow the lifting force at the tip of a finite plane wing with a straight leading edge is less than the value for a two-dimensional wing with the same angle of sweep of the leading edge. The two-dimensional value of the lift is attained at points on the wing which lie just outside the Mach cone with vertex at the tip of the leading edge. If the tip is straight and parallel to the undisturbed stream, then the lift falls from the two-dimensional value at the Mach cone to zero at the tip. The drag changes in a similar way but much less rapidly; it decreases from the corresponding two-dimensional value at the Mach cone to a value that depends on the angle of sweep. It seems then that the performance of such a wing is not as good as that of the corresponding two-dimensional wing. But from some results obtained by K. Stewartson[3] it appeared that if a vane is attached to the wing tip, it might counteract this effect. For the reduction in lift is due to flow around the tip from the pressure to the suction side, and this would presumably be reduced by the presence of a vane. These considerations suggested the problem of studying how the addition of a vane to a wing will affect the lift, the drag and hence the performance.

For this purpose, the wing is taken in the form of a semi-infinite wedge, whose straight leading edge is swept back and whose tip is along the undisturbed stream.

*Now Department of Mathematics, Alexandria University.

Originally received December 1952.

[The Aeronautical Quarterly, Vol. V, November 1954]

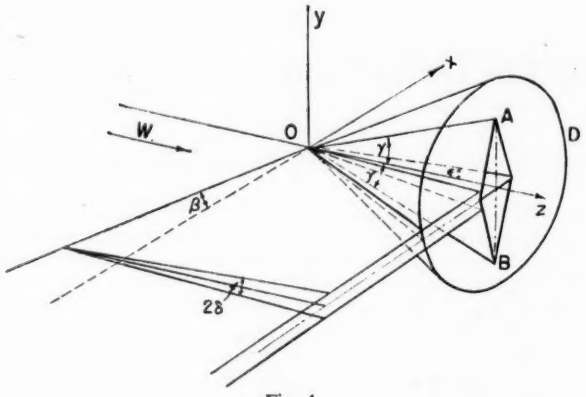

Fig. 1.

The vane has a triangular plan form and a diamond-shaped base; it is attached to the wing tip such that its vertex is at the tip of the leading edge, and their planes of symmetry are perpendicular to each other. The whole is placed in the flow with the wing at incidence α, and the vane at zero incidence. A sketch of the wing and the vane when it lies entirely inside the Mach cone is shown in Fig. 1.

The edges of the wing and the vane are taken straight, so that the problem is of the conical flow type, and it will be assumed that the incidence of the wing and the thickness of both the wing and the vane are small, so that the linearised theory of conical fields as set out in Ref. 1 can be used. Moreover, for the purpose of calculation, the wing and the vane are supposed to extend to infinity downstream. If the wing and the vane have supersonic trailing edges, the solution thus obtained will be valid upstream from the trailing edges, and the solution for a system of finite extent in the stream direction is determined.

The problem is solved by dividing the velocity field into its anti-symmetrical and symmetrical parts and treating each independently; the results may then be superposed to give the complete solution. The anti-symmetrical part corresponds to a wing of infinitesimal thickness at incidence α with a plane vane normal to the wing, and from this solution the lift is calculated. The symmetrical part corresponds to a wing and vane of small finite thickness, of the shape described earlier, but at zero incidence. This solution will give no lift, but only a drag force.

The results of the calculation show that the effect of the vane on the lift is to counteract the loss of lift caused by the presence of the wing tip. The magnitude of this effect depends on the angle of sweepback as well as the vertex angle of the vane. This effect is shown in Figs. 7 and 8, and the formula for the lift coefficient when the trailing edges are perpendicular to the stream is given by equations (60), (61) and (62). The formula for the drag is obtained in equation (93), and its variation with the vertex angle of the vane is shown in Fig. 10.

An index of merit for the performance (the lift/drag ratio) is then calculated, and it is found that it first increases and then decreases as the semi-angle of the

vertex of the vane increases up to the Mach angle. The maximum performance for a particular vane is found to increase with the decrease of the vane thickness. It appears that a wing-tip vane, if its dimensions are suitably chosen, could be used in practice to improve the performance of a supersonic wing.

Notation

a constant defined in equation (20)

b constant defined in equation (23)

$2c$ length of the cross section of the vane by the plane $z=\cot\mu$

$f(p)$ arbitrary periodic function of $\sigma+\theta$

k, k' modulus and complementary modulus of elliptic functions in Section 6

l, m, n integers in Section 4

p a variable of integration in equation (8), and the degree of the function $H(z)$ in equations (27) and (65)

r, θ polar co-ordinates in the x_1y_1-plane

t complex variable defined in equation (17)

t' imaginary part of t

t_0, t_1 real values of t

u, v, w perturbation velocity components

x, y, z rectangular Cartesian co-ordinates

x_1, y_1 rectangular co-ordinates in the plane $z=\cot\mu$

z complex variable defined in equation (22)

z_0 value of z defined in equation (23)

} in Sections 4-7

A, B real constants defined in equations (30), (29)

C, C_1, C_2 real constants defined in equations (76), (69)

C_L lift coefficient

D total drag

D_1 drag over the wing

D_2 drag over the vane

D_3 drag due to the suction force

$\mathrm{E}(\chi), \mathrm{E}$ incomplete and complete elliptic integrals of the second kind to modulus k

$\mathrm{F}(\chi), \mathrm{F}$ incomplete and complete elliptic integrals of the third kind to modulus k

$F(p)$ arbitrary periodic function of $\sigma-\theta$ in equation (8)

G_1, G_2, G_3 functions of t

H_1, H_2, H_3 functions of z

K, K'	complete elliptic integrals of the first kind to modulus k, k'
L	lift force
M	Mach number
P	perturbation pressure
W	velocity of undisturbed stream
α	angle of incidence of the wing
β	angle of sweepback of the leading edge of the wing
γ	semi-vertex angle of the vane
γ_0	value of γ at which the lift is a maximum
γ_1	value of γ at which the lift is restored to the two-dimensional value
2δ	thickness of the wing
2ε	thickness of the vane
$\varepsilon_1, \varepsilon_2$	constants defined in Section 7
$\varepsilon_1', \varepsilon_2'$	values of ε_1 and ε_2 respectively in the plane $z=\cot\mu$
θ	a variable of integration in equation (73)
λ	a constant defined in Section 7
μ	Mach angle
ρ	density of the undisturbed flow
σ, θ	variables defined in equation (6)
σ_0	value of σ for the leading edge of the wing
σ_1	value of σ for the upper tip of the vane
χ	complex variable defined in equation (72)
ψ	variable of integration in equation (74)
η	performance
$\mathscr{R}$	"real part of"
$\mathscr{I}$	"imaginary part of"

2. The Linearised Theory of Conical Fields

Let (x, y, z) be a system of rectangular co-ordinates with the origin at the vertex of the conical field (the tip of the leading edge in this problem) and the z-axis in the direction of the undisturbed stream, M its Mach number, and $\mu(=\operatorname{cosec}^{-1} M)$ its Mach angle. The flow is assumed to be irrotational, so that the perturbation velocity is the gradient of a potential function ϕ. Then to a linear approximation, the rectangular components u, v, w of the perturbation velocity and the potential ϕ satisfy the differential equation

$$\left(\frac{\partial^2}{\partial x^2}+\frac{\partial^2}{\partial y^2}-\cot^2\mu\,\frac{\partial^2}{\partial z^2}\right)(u, v, w, \phi)=0, \quad . \quad . \quad . \quad (1)$$

and from the linear approximation to Bernoulli's equation,

$$P = -\rho W w, \quad . \quad . \quad . \quad . \quad . \quad . \quad (2)$$

where P is the perturbation pressure, and ρ is the density of the undisturbed stream.

New co-ordinates (x_1, y_1) and (r, θ) are now defined by

$$\left.\begin{aligned} x_1 &= r\cos\theta = \frac{x}{z\tan\mu}, \\ y_1 &= r\sin\theta = \frac{y}{z\tan\mu}. \end{aligned}\right\} \quad . \quad . \quad . \quad . \quad . \quad . \quad (3)$$

The Mach cone of the vertex then corresponds to the circle $r=1$ in the x_1y_1-plane.

In conical flows the velocity components u, v, w are functions of (x_1, y_1) or (r, θ) only, since they are homogeneous functions of degree zero in (x, y, z). In terms of (r, θ) the equations (1) satisfied by u, v and w become

$$\left[r^2(r^2-1)\frac{\partial^2}{\partial r^2} + r(2r^2-1)\frac{\partial}{\partial r}\right](u, v, w) = \frac{\partial^2}{\partial\theta^2}(u, v, w). \quad . \quad . \quad (4)$$

The theory of such flows is developed in detail in Ref. 1 and such results as are needed for the present problem are quoted from this.

3. The Anti-symmetrical Part

The wing and the vane in this case are of infinitesimal thickness. The wing is at incidence α while the vane is at zero incidence, so that the boundary conditions of zero normal velocity on both the upper and lower surfaces of the wing and on both sides of the vane, are respectively

$$\left.\begin{aligned} v &= -W\alpha \\ \text{and} \quad u &= 0. \end{aligned}\right\} \quad . \quad . \quad . \quad . \quad . \quad . \quad (5)$$

The solution of equation (4) satisfying the boundary conditions (5) varies for the different values of r. It is therefore necessary to obtain the solution for the cases $r>1$ and $r<1$ separately. In other words the two fields (outside and inside the Mach cone) must be solved separately.

The field outside the Mach cone of the origin

The general theory is dealt with in Ref. 1. The x_1y_1-plane is transformed to the $\sigma\theta$-plane, defined by

$$\left.\begin{aligned} x_1 &= \sec\sigma\cos\theta, \\ y_1 &= \sec\sigma\sin\theta. \end{aligned}\right\} \quad . \quad . \quad . \quad . \quad . \quad . \quad (6)$$

Then equation (4) for $r>1$ will be transformed into

$$\left(\frac{\partial^2}{\partial\sigma^2}-\frac{\partial^2}{\partial\theta^2}\right)(u,v,w)=0. \quad . \quad . \quad . \quad . \quad (7)$$

The part of the x_1y_1-plane for which $r>1$ corresponds, in the $\sigma\theta$-plane, to a strip between $\sigma=0$ and $\sigma=\frac{1}{2}\pi$. The axis $y_1=0$ corresponds to $\theta=0$ (for $x_1>0$) and to $\theta=\pi$ (for $x_1<0$). The characteristics of equation (7) are the two sets of straight lines $\sigma+\theta=$constant and $\sigma-\theta=$constant. The first set corresponds in the x_1y_1-plane to those parts of the tangents to $r=1$ on which θ increases as the circle is approached, and the second set corresponds to those parts of the tangents on which θ decreases when the circle is approached. The solution of equation (7) for irrotational flow was found in Ref. 1 in the form

$$\left.\begin{aligned} u&=\int^{\sigma+\theta} f(p)\cos p\,dp+\int^{\sigma-\theta} F(p)\cos p\,dp,\\ v&=\int^{\sigma+\theta} f(p)\sin p\,dp+\int^{\sigma-\theta} F(p)\sin p\,dp,\\ w&=-\tan\mu\int^{\sigma+\theta} f(p)\,dp-\tan\mu\int^{\sigma-\theta} F(p)\,dp, \end{aligned}\right\} \quad . \quad . \quad . \quad (8)$$

where $f(p)$ and $F(p)$ are periodic functions of period 2π. They are continuous everywhere, except perhaps on crossing certain specified characteristics.

Let σ_0 (shown in Fig. 2) be related to the angle of sweepback β by the relation

$$\sec\sigma_0=\cot\mu\cot\beta \quad . \quad . \quad . \quad . \quad . \quad (9)$$

and let $2c$ be the length of the cross section of the vane by the plane $z=\cot\mu$, so that

$$c=\tan\gamma\cot\mu, \quad . \quad . \quad . \quad . \quad . \quad (10)$$

where 2γ is the vertex angle of the vane. Three different cases must then be distinguished:—

(1) $c<1$, the vane lies entirely inside the Mach cone,

(2) $1<c<\operatorname{cosec}\sigma_0$; in this case the edges of the vane lie in the regions 1 and 2 in Fig. 2,

(3) $c>\operatorname{cosec}\sigma_0$; and the edges of the vane lie in region 7 in Fig. 2.

Case 1. $c<1$

In this case the field outside the Mach cone is not affected by the vane, but by the wing alone, and this will affect only the part of the field bounded by the simple wave and the shock wave produced by the leading edge of the wing in the upper

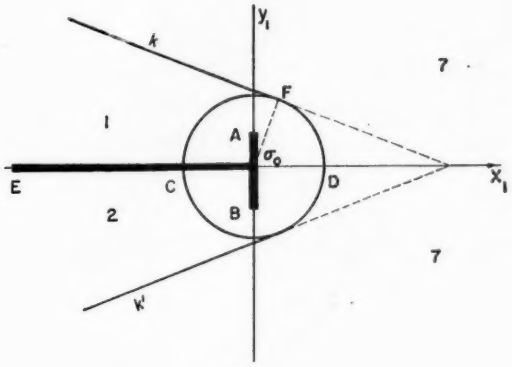

Fig. 2.

and lower half space. The approximation used in the linearised theory reduces these waves to surfaces of discontinuity represented by the characteristics k, k' (Fig. 2). Hence the velocity components are[1] zero everywhere outside the Mach cone, except in regions 1 and 2 in Fig. 2, where they are

Region	u	v	w
1	$-W\alpha\cot\sigma_0$	$-W\alpha$	$W\alpha\operatorname{cosec}\sigma_0\tan\mu$
2	$W\alpha\cot\sigma_0$	$-W\alpha$	$-W\alpha\operatorname{cosec}\sigma_0\tan\mu$

. . (11)

Case 2. $1 < c < \operatorname{cosec}\sigma_0$

This case is shown in Figs. 3(*a*) and 3(*b*). The corresponding regions in the x_1y_1-plane and the $\sigma\theta$-plane are numbered to correspond; the tip of the vane in Fig. 3(*a*) corresponds to the point $(\pi/2,\ \pi/2-\sigma_1)$ in the $\sigma\theta$-plane.

In the region 1 the velocity components are the same as in the first case and are given in equation (11). For u to be zero on the vane, $\int^{\sigma+\theta} f(p)\cos p\,dp$ must decrease discontinuously by $-W\alpha\cot\sigma_0$ as $(\sigma+\theta)$ decreases through $\pi-\sigma_1$, *i.e.* when region 3 in the $\sigma\theta$-plane is entered along $\sigma-\theta=$ constant; also $\int^{\sigma-\theta} F(p)\cos p\,dp$ must decrease discontinuously by $-W\alpha\cot\sigma_0$ as $\sigma-\theta$ decreases through σ_1, *i.e.* when region 4 in the $\sigma\theta$-plane is entered along $\sigma+\theta=$ constant. Hence for region 3

$$-\cos\sigma_1 \lim_{\epsilon\to 0}\int_{\pi-\sigma_1-\epsilon}^{\pi-\sigma_1+\epsilon} f(p)\,dp = -W\alpha\cot\sigma_0. \quad . \quad . \quad . \quad (12)$$

The discontinuous decrease in v is

$$\sin\sigma_1 \lim_{\epsilon\to 0}\int_{\pi-\sigma_1-\epsilon}^{\pi-\sigma_1+\epsilon} f(p)\,dp = W\alpha\cot\sigma_0\tan\sigma_1. \quad . \quad . \quad . \quad (13)$$

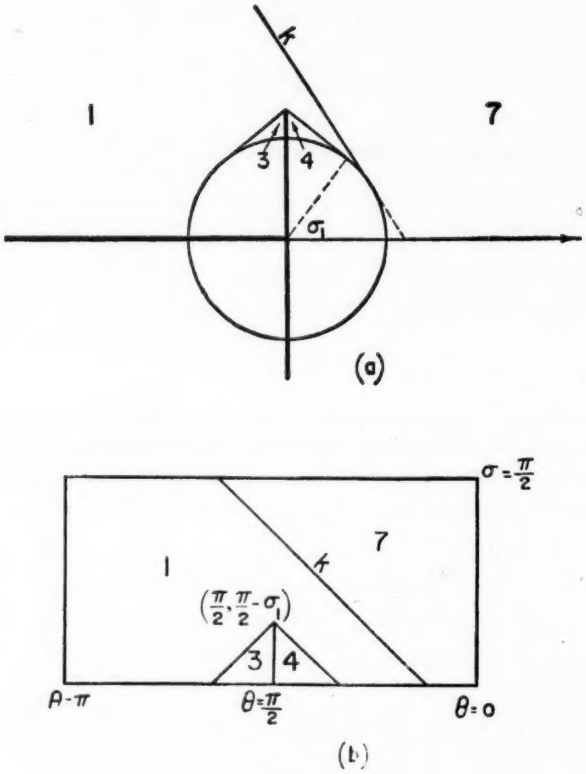

Fig. 3.

and that in w is $-W\alpha\tan\mu\cot\sigma_0\sec\sigma_1$. Hence

$$\left.\begin{aligned} u&=0,\\ v&=-W\alpha(1+\cot\sigma_0\tan\sigma_1)\\ w&=\ W\alpha\tan\mu\,\mathrm{cosec}\,\sigma_0(1+\cos\sigma_0\sec\sigma_1), \end{aligned}\right\} \quad . \quad . \quad . \quad (14)$$

throughout region 3.

The values in region 4 are found similarly to be

$$\left.\begin{aligned} u&=0,\\ v&=-W\alpha(1-\cot\sigma_0\tan\sigma_1),\\ w&=\ W\alpha\tan\mu\,\mathrm{cosec}\,\sigma_0(1-\cos\sigma_0\sec\sigma_1). \end{aligned}\right\} \quad . \quad . \quad . \quad (15)$$

and the velocity components vanish everywhere outside these regions.

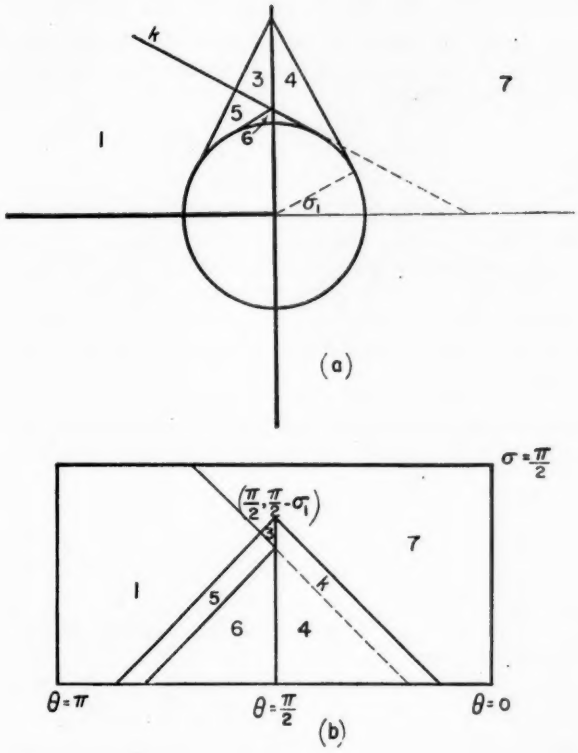

Fig. 4.

Case 3. $c > \operatorname{cosec}\sigma_0$

In this case the simple wave k produced by the wing tip is reflected on the vane (*see* Figs. 4(*a*) and 4(*b*)), thus increasing the number of regions to be considered. In the same way as before, the velocity components are found to be

Region	u	v	w
1	$-W\alpha\cot\sigma_0$	$-W\alpha$	$W\alpha\tan\mu\operatorname{cosec}\sigma_0$
2	0	0	0
3	0	0	0
4	$-W\alpha\cot\sigma_0$	$-W\alpha$	$W\alpha\tan\mu\operatorname{cosec}\sigma_0$
5	0	$-2W\alpha$	$2W\alpha\tan\mu\operatorname{cosec}\sigma_0$

. . . (16)

and outside these regions the velocity components vanish everywhere.

4. The Field Inside the Mach Cone of the Vertex

As in Ref. 1, the velocity components inside the Mach cone (*i.e.* inside the circle $r=1$ in the x_1y_1-plane) are determined by transforming the interior of $r=1$ into a complex t-plane defined by

$$\frac{1}{t}=\frac{\cos\theta-i(1-r^2)^{\frac{1}{2}}\sin\theta}{r}. \qquad (17)$$

The circle $r=1$ is transformed with its interior into the whole of the t-plane, with cuts along the portions of the real axis for which $|t|\geqslant 1$: the upper half $0<\theta<\pi$ is represented on the upper half-plane, $\mathscr{I}(t)>0$, and the lower half $-\pi<\theta<0$ on the lower half-plane, $\mathscr{I}(t)<0$. The axis $x_1=0$ inside the unit circle is transformed into the imaginary axis in the t-plane, while the axis $y_1=0$ inside the unit circle is transformed without any change into the same part of the real axis in the t-plane.

The velocity components u, v, w of the perturbation velocity are found to satisfy Laplace's equations in this t-plane and therefore

$$\left.\begin{aligned} u&=\mathscr{R}\{G_1(t)\},\\ v&=\mathscr{R}\{G_2(t)\},\\ w&=\mathscr{R}\{G_3(t)\}. \end{aligned}\right\} \qquad (18)$$

where $G_1(t)$, $G_2(t)$, $G_3(t)$ are functions of the complex variable t; from the condition of irrotational flow

$$G_1'(t):G_2'(t):G_3'(t)=1:i(1-t^2)^{\frac{1}{2}}:-t\tan\mu. \qquad (19)$$

To obtain the field inside the Mach cone it is necessary to find the complex functions $G_1(t)$, $G_2(t)$, $G_3(t)$, which are related by equation (19) and whose real parts satisfy the boundary conditions on the wing, the vane, and the Mach circle. Since the boundary conditions on the Mach circle differ for the different cases considered before, these functions must be found for each case separately.

Case 1. $c<1$

The projection of the system in the x_1y_1-plane when the vane lies entirely inside the Mach cone is shown in Fig. 2. Transferring to the t-plane, the tips of the vane $x_1=0$, $y_1=\pm c$ are represented by $t=\pm ia$ respectively where

$$a=\frac{c}{(1-c^2)^{\frac{1}{2}}}. \qquad (20)$$

The boundary conditions could be laid down directly in the t-plane; they are:—

$$\left.\begin{aligned} &\text{real axis,} && v=-W\alpha && \text{for } t<0 \text{ and } t>\sec\sigma_0=t_0, \text{ say}\\ &&& w=0 && \text{for } 0<t<t_0,\\ &\text{imaginary axis,} && u=0 && \text{for } |t|<a. \end{aligned}\right\} \qquad (21)$$

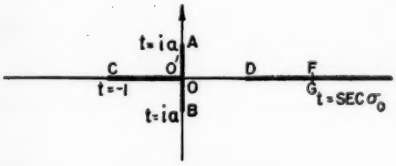

Fig. 5.

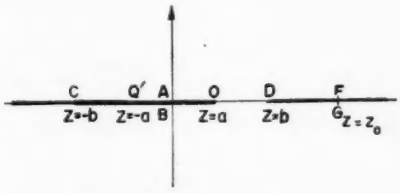

Fig. 6.

These boundary conditions show clearly the convenience of transforming the cut t-plane to a cut z-plane by the transformation

$$z=(a^2+t^2)^{\frac{1}{2}}. \quad . \quad . \quad . \quad . \quad . \quad . \quad . \quad (22)$$

To make the transformation from the t-plane to the z-plane one-to-one, z is taken to be real and positive when t is real and positive, and by following the argument of z

$$\arg z=\tfrac{1}{2}[\arg(t+ia)+\arg(t-ia)],$$

gives for the upper half-planes:—

(*i*) The real axis in the t-plane is transformed to those parts of the real axis in the z-plane for which $|z|>a$.

(*ii*) For the vane OA (Fig. 6), the side $\mathscr{R}(t)=+0$ is mapped on to that part of the real axis for which $0<z<a$ and the side $\mathscr{R}(t)=-0$ is mapped on to $-a<z<0$ on the real axis. The point A is mapped on the origin in the z-plane.

(*iii*) The imaginary axis with $|t|>a$ is mapped on the whole imaginary axis in the z-plane.

The lower half is transformed similarly. The correspondence between the points on the real axis is shown in Figs. 5 and 6.

The boundary conditions in the z-plane are all given on the real axis and are as follows:—

$$\left.\begin{array}{ll} v=-W\alpha & \text{for } z>(a^2+\sec^2\sigma_0)^{\frac{1}{2}}=z_0 \text{ say} \\ & \quad \text{and for } z<-a, \\ v=0 & \text{for } z_0>z>(1+a^2)^{\frac{1}{2}}=b \text{ say}, \\ u=0 & \text{for } -a<z<a, \\ w=0 & \text{for } \quad a<z<b. \end{array}\right\} \quad . \quad . \quad . \quad (23)$$

Since u, v, w are the real parts of functions of t, $G_1(t)$, $G_2(t)$, $G_3(t)$ respectively, they are also the real parts of functions of z, $H_1(z)$, $H_2(z)$, $H_3(z)$ respectively, so that

$$\left.\begin{aligned} u+iu_1 &= H_1(z), \\ v+iv_1 &= H_2(z), \\ w+iw_1 &= H_3(z). \end{aligned}\right\} \quad . \quad . \quad . \quad . \quad . \quad (24)$$

Hence, from equations (14) and (22),

$$H_1'(z) : H_2'(z) : H_3'(z) = 1 : i(b^2-z^2)^{\frac{1}{2}} : -\tan\mu\,(z^2-a^2)^{\frac{1}{2}}. \quad . \quad (25)$$

The boundary conditions (23) lead to the following conditions on $H_2'(z)$:—

$$\left.\begin{aligned} &\mathscr{R}\{H_2'(z)\} = 0 \text{ for } b < z \text{ and } z < -a, \\ &\mathscr{I}\{H_2'(z)\} = 0 \text{ for } -a < z < b. \end{aligned}\right\} \quad . \quad . \quad . \quad (26)$$

The conditions (23) and (26) show that $H_2'(z)$ must have the form

$$H_2'(z) = \frac{(z+a)^{m+\frac{1}{2}}(b-z)^{n+\frac{1}{2}}}{z^l(z-z_0)}\,H(z), \quad . \quad . \quad . \quad (27)$$

where m, n, l are integers and $H(z)$ is an integral function which is real when z is real.

The following restrictions must be imposed in order that the solution may correspond to a physically possible flow.

(*i*) In the physical plane $v = -W\alpha$ at $x_1 = 0$, $y_1 = \pm 1$ and in a neighbourhood of each of these two points, and therefore as in Ref. 1, $H_2'(z)$ must be $O(z^{-2})$ at most as $|z| \to \infty$.

(*ii*) u, v, w must be finite at $z = b$ and $z = -a$. As $H_2'(z)$ contains the factor $(z-b)^{n+\frac{1}{2}}$, $H_1'(z)$ and $H_3'(z)$ contain the factor $(z-b)^n$ and so $n \geqslant 0$; also it can be proved that $m \geqslant -1$.

(*iii*) At the subsonic leading edges of the vane, the velocity normal to the plane of the vane must vary as $r_1^{\frac{1}{2}}$ as $r_1 \to 0$, where r_1 is the normal distance from the edge in the plane of the vane. Therefore in the t-plane, $G_2(t) \sim K(a^2+t^2)^{\frac{1}{2}}$ as $t \to ia$ or $-ia$, the two points corresponding to the two edges of the vane (K is a constant). In the z-plane $H_2(z) \sim K/z$ and therefore $H_2'(z) \sim -K/z^2$ as $z \to 0$; hence $l = 0$.

(*iv*) If condition (*i*) is to be satisfied, then $H(z)$ must be a polynomial of degree p say. The boundary conditions show that there must be no residue at the double pole $z = 0$; hence $p \geqslant 1$.

Thus from these four conditions

$$\begin{aligned} m+n+p &\leqslant 0, \\ m &\geqslant -1, \\ n &\geqslant 0, \\ p &\leqslant -1, \end{aligned}$$

and the unique values of m, n, p satisfying these inequalities are

$$m=-1, \qquad n=0, \qquad p=1.$$

Therefore
$$H_2'(z)=A\frac{(b-z)^{\frac{1}{2}}}{z^2(z-z_0)(z+a)^{\frac{1}{2}}}(z+B), \quad . \quad . \quad . \quad . \quad (28)$$

where A and B are real numbers. The value of B is obtained by equating the residue at $z=0$ to zero and that of A by equating the residue at $z=z_0$ to $iW\alpha/\pi$, whence

$$B=\frac{2abz_0}{z_0(a+b)-2ab}, \quad . \quad . \quad . \quad . \quad . \quad . \quad . \quad (29)$$

$$A=\frac{W\alpha}{\pi}\left(\frac{a+z_0}{z_0-b}\right)^{\frac{1}{2}}\frac{z_0(a+b)-2ab}{a+b}. \quad . \quad . \quad . \quad (30)$$

From equation (25)

$$H_1'(z)=-Ai\frac{z+B}{z^2(z-z_0)(z+a)}\left(\frac{z+a}{z+b}\right)^{\frac{1}{2}}, \quad . \quad . \quad . \quad (31)$$

$$H_3'(z)=-A\tan\mu\frac{z+B}{z^2(z-z_0)}\left(\frac{a-z}{b+z}\right)^{\frac{1}{2}}. \quad . \quad . \quad . \quad . \quad (32)$$

Hence in the upper half-plane

$$H_1(z)=\frac{iW\alpha}{\pi}\left\{\frac{1}{(z_0^2-b^2)^{\frac{1}{2}}}\log\frac{\left(\frac{a+z_0}{b+z_0}\right)^{\frac{1}{2}}+\left(\frac{a+z}{b+z}\right)^{\frac{1}{2}}}{\left(\frac{a+z_0}{b+z_0}\right)^{\frac{1}{2}}-\left(\frac{a+z}{b+z}\right)^{\frac{1}{2}}}-\frac{2}{a+b}\left(\frac{a+z_0}{z_0-b}\right)^{\frac{1}{2}}\frac{(z+a)^{\frac{1}{2}}(z+b)^{\frac{1}{2}}}{z}\right\}$$
$$. \quad . \quad . \quad . \quad (33)$$

$$H_2(z)=\frac{2W\alpha}{\pi}\left\{\frac{b}{(a+b)}\left(\frac{a+z_0}{z_0-b}\right)^{\frac{1}{2}}\frac{(a+z)^{\frac{1}{2}}(b-z)^{\frac{1}{2}}}{z}-\tan^{-1}\left(\frac{a+z_0}{z_0-b}\right)^{\frac{1}{2}}\left(\frac{b-z}{a+z}\right)^{\frac{1}{2}}\right\}$$
$$. \quad . \quad . \quad . \quad (34)$$

$$H_3(z)=\frac{2W\alpha\tan\mu}{\pi}\left\{\left(\frac{z_0^2-a^2}{z_0^2-b^2}\right)^{\frac{1}{2}}\tan^{-1}\left(\frac{b+z_0}{z_0-a}\right)^{\frac{1}{2}}\left(\frac{a-z}{b+z}\right)^{\frac{1}{2}}-\right.$$
$$\left.-\frac{a}{a+b}\left(\frac{a+z_0}{z_0-b}\right)^{\frac{1}{2}}\frac{(z+b)^{\frac{1}{2}}(a-z)^{\frac{1}{2}}}{z}\right\}, \quad (35)$$

where the square roots are positive when their arguments are real and positive, and the inverse tangents are between $-\pi/2$ and $\pi/2$ for real arguments.

The velocity components are obtained by taking the real parts of these expressions for the H's after substituting for z in terms of t, and thence in terms of x_1, y_1. For general points inside the Mach cone this is a very tedious process, but for points on the wing and the vane, that is for points on the real axis in the z-plane, the results follow immediately from equations (33) to (35).

Thus on the upper wing surface w is given by the right hand side of equation (35), which is purely real in the interval $-b<z<-a$, where now

$$z=-(a^2+x_1^2)^{\frac{1}{2}}, \qquad z_0=(a^2+\sec^2\sigma_0)^{\frac{1}{2}}, \qquad a=\frac{c}{(1-c^2)^{\frac{1}{2}}}, \qquad b=\frac{1}{(1-c^2)^{\frac{1}{2}}}.$$

Case 2. $1<c<\operatorname{cosec}\sigma_0$

In this case the edges of the vane are outside the Mach cone. Therefore the fields in the two upper quadrants are independent, and in the t-plane they will be separated by the whole imaginary axis. The two fields have then to be solved separately.

For the left-hand quadrant in the t-plane the boundary conditions are

$$\left.\begin{aligned} &v=-W\alpha && \text{for } -\sec\sigma_1<t<0,\\ \text{and from (14)}\quad &\\ &v=-W\alpha(1+\cot\sigma_0\tan\sigma_1) && \text{for } t<-\sec\sigma_1. \end{aligned}\right\} \quad . \quad . \quad (36)$$

The condition $u=0$ on the vane in the x_1y_1-plane becomes $\mathscr{R}\{G_1'(t)\}=0$ on the imaginary axis. Hence on the imaginary axis $\mathscr{I}\{G_1'(t)\}=0$ and from equation (19) $\mathscr{R}\{G_2'(t)\}=0$. Thus the boundary conditions for $G_2'(t)$ are

$$\left.\begin{aligned} &\mathscr{R}\{G_2'(t)\}=0 \quad \text{on the real axis for } t<0 \quad (t\neq-\sec\sigma_1=-t_1, \text{ say}),\\ &\mathscr{R}\{G_2'(t)\}=0 \quad \text{on the imaginary axis.} \end{aligned}\right\} \quad . \quad (37)$$

The condition that $G_2'(t)$ is $O(t^{-2})$ at most as $t\longrightarrow\infty$ still applies, and the discontinuity at $t=-t_1$ in the value of v along the real axis shows that $G_2'(t)$ has a pole there with residue $(iW\alpha/\pi)\cot\sigma_0\tan\sigma_1$; $G_2'(t)$ has no other singularity in the upper left-hand quadrant of the t-plane or on its boundary.

The solution for $G_2'(t)$ and $G_2(t)$ with these conditions is unique and is

$$G_2'(t)=-\frac{i}{\pi}W\alpha\cot\sigma_0\tan\sigma_1\frac{2t_1}{t^2-t_1^2}. \quad . \quad . \quad . \quad (38)$$

From equation (19)

$$G_1'(t)=\frac{W\alpha}{\pi}\cot\sigma_0\tan\sigma_1\frac{2t_1}{t^2-t_1^2}\frac{1}{(1-t^2)^{\frac{1}{2}}}, \quad . \quad . \quad . \quad (39)$$

$$G_3'(t)=\frac{W\alpha}{\pi}\tan\mu\cot\sigma_0\tan\sigma_1\frac{2t_1}{t^2-t_1^2}\frac{1}{(1-t^2)^{\frac{1}{2}}}. \quad . \quad . \quad (40)$$

Hence in the upper left-hand quadrant:

$$G_1(t)=\frac{W\alpha}{\pi}\cot\sigma_0\left\{\cos^{-1}\frac{1-t_1t}{t_1-t}-\cos^{-1}\frac{1+t_1t}{t_1+t}\right\}. \quad . \quad . \quad . \quad . \quad . \quad (41)$$

$$G_2(t) = -\frac{iW\alpha}{\pi}\cot\sigma_0\tan\sigma_1\log\frac{t-t_1}{t+t_1} - W\alpha(1+\cot\sigma_0\tan\sigma_1), \quad . \quad . \quad (42)$$

$$G_3(t) = -\frac{W\alpha}{\pi}\tan\mu\cot\sigma_0\sec\sigma_1\left\{\cos^{-1}\frac{1-t_1t}{t_1-t} + \cos^{-1}\frac{1+t_1t}{t_1+t}\right\} + \\ + W\alpha\tan\mu\,\mathrm{cosec}\,\sigma_0(1+\cos\sigma_0\sec\sigma_1). \quad (43)$$

The real part of these functions could be obtained easily.

The value of w on $y_1 = +0$, $-1 < x_1 < 0$, *i.e.* on the upper surface of the wing is

$$w = -\frac{W\alpha}{\pi}\tan\mu\cot\sigma_0\sec\sigma_1\left\{\cos^{-1}\frac{1-t_1x_1}{t_1-x_1} + \cos^{-1}\frac{1+t_1x_1}{t_1+x_1}\right\} + \\ + W\alpha\tan\mu\,\mathrm{cosec}\,\sigma_0(1+\cos\sigma_0\sec\sigma_1). \quad (44)$$

In the upper right-hand quadrant, the boundary conditions on $G_2'(t)$ are

$$\left.\begin{aligned} &\mathscr{I}\{G_2'(t)\} = 0 \quad \text{for } 0 < t < 1, \\ &\mathscr{R}\{G_2'(t)\} = 0 \quad \text{for } 1 < t, \\ &\mathscr{R}\{G_2'(t)\} = 0 \quad \text{for } |t| > 0, \end{aligned}\right\} \quad . \quad . \quad . \quad . \quad . \quad (45)$$

when t is real, and

when t is imaginary.

With these boundary conditions, following the method used previously, it is easy to find that

$$G_1'(t) = \frac{iW\alpha}{\pi}(t_1^2 - t_0^2)\cot\sigma_0\frac{2t}{(t^2-t_0^2)(t^2-t_1^2)}, \quad . \quad . \quad . \quad (46)$$

$$G_2'(t) = -\frac{W\alpha}{\pi}(t_1^2 - t_0^2)\cot\sigma_0\frac{2t}{(t^2-t_0^2)(t^2-t_1^2)}(1-\ldots), \quad . \quad . \quad (47)$$

$$G_3'(t) = -\frac{iW\alpha}{\pi}(t_1^2 - t_0^2)\cot\sigma_0\tan\mu\frac{2t^2}{(t^2-t_0^2)(t^2-t_1^2)}. \quad . \quad . \quad (48)$$

Integrating, in the upper right-hand quadrant

$$G_1(t) = \frac{iW\alpha}{\pi}\cot\sigma_0\log\frac{t^2-t_1^2}{t^2-t_0^2}. \quad . \quad . \quad . \quad . \quad . \quad . \quad . \quad . \quad (49)$$

$$G_2(t) = -\frac{2W\alpha}{\pi}\cot\sigma_0\left\{(t_0^2-1)^{\frac{1}{2}}\tan^{-1}\left(\frac{1-t^2}{t_0^2-1}\right)^{\frac{1}{2}} - (t_1^2-1)^{\frac{1}{2}}\tan^{-1}\left(\frac{1-t^2}{t_1^2-1}\right)^{\frac{1}{2}}\right\}, \quad (50)$$

$$G_3(t) = -\frac{iW\alpha}{\pi}\tan\mu\cot\sigma_0\left\{t_1\log\frac{t-t_1}{t+t_1} - t_0\log\frac{t-t_0}{t+t_0}\right\} - W\alpha\tan\mu(t_1-t_0)\cot\sigma_0. \\ . \quad . \quad . \quad . \quad . \quad (51)$$

Case 3. $c > \operatorname{cosec} \sigma_0$

In a similar manner to Case 2, for the upper left-hand quadrant

$$G_1'(t) = -\frac{2W\alpha}{\pi} \frac{t_0}{t^2 - t_0^2} \frac{1}{(1-t^2)^{\frac{1}{2}}}, \quad . \quad . \quad . \quad . \quad . \quad (52)$$

$$G_2'(t) = -\frac{iW\alpha}{\pi} \frac{2t_0}{t^2 - t_0^2}, \quad . \quad . \quad . \quad . \quad . \quad (53)$$

$$G_3'(t) = \frac{W\alpha}{\pi} \tan\mu \frac{2t_0}{t^2 - t_0^2} \frac{t}{(1-t^2)^{\frac{1}{2}}} \quad . \quad . \quad . \quad (54)$$

Integration gives, over the surface of the body,

$$w = -\frac{W\alpha}{\pi} \tan\mu \left\{ \cos^{-1} \frac{1 - t_0 x_1}{t_0 - x_1} + \cos^{-1} \frac{1 + t_0 x_1}{t_0 + x_1} \right\} + 2W\alpha \tan\mu \operatorname{cosec} \sigma_0. \quad . \quad . \quad . \quad . \quad (55)$$

For the upper right-hand quadrant u vanishes on the boundary; hence $G_1(t)$, $G_2(t)$, $G_3(t)$ vanish everywhere in this quadrant.

Having obtained the components of the perturbation velocity in the upper half-plane, outside and inside the Mach cone, the corresponding values of these components for the lower half-plane are obtained for the three cases from the fact that v is even, while u, w are odd, in y_1.

5. Lift Coefficient

The lift force in the direction of the positive y-axis is obtained by integrating the perturbation pressure over the upper and lower sides of the wing. When the wing and the vane have straight trailing edges normal to the direction of the undisturbed stream, the lift coefficient (referred to area and $\frac{1}{2}\rho W^2$) for the part of the wing inside the Mach cone of the vertex is

$$C_L = -2 \int_{-1}^{0} \frac{P}{\frac{1}{2}\rho W^2} \, dx_1 \quad . \quad . \quad . \quad . \quad . \quad (56)$$

where P is the perturbation pressure on the upper surface given in equation (2).

Therefore $$C_L = \frac{4}{W} \int_{-1}^{0} w \, dx_1.$$

On the wing, $x_1 = t$, $w = G_3(t)$, $(-1 < t < 0)$,

and hence $$C_L = \frac{4}{W} \int_{-1}^{0} G_3(t) \, dt.$$

Integrating by parts,

$$C_L = 4\alpha \operatorname{cosec}\sigma_0 \tan\mu - \frac{4}{W}\int_{-1}^{0} G_3'(t)\,t\,dt. \quad . \quad . \quad . \quad (57)$$

For the first case, $c<1$, transform to the z-plane. From equation (22), $z=-(a^2+t^2)^{\frac{1}{2}}$ on the wing, so that $-b<z<-a$. Hence

$$C_L = 4\alpha \operatorname{cosec}\sigma_0 \tan\mu + \frac{4}{W}\int_{-b}^{-a} H_3'(z)\,(z^2-a^2)^{\frac{1}{2}}\,dz. \quad . \quad . \quad (58)$$

An expression for $H_3'(z)$ is obtained for this case in equation (32). Substituting and then performing the integration,

$$C_L = 4\alpha \operatorname{cosec}\sigma_0 \tan\mu \left\{ 1 - \left(\frac{z_0+b}{z_0-a}\right)^{\frac{1}{2}} \left[z_0 - (z_0-a)\left(\frac{z_0+a}{z_0+b}\right)^{\frac{1}{2}} - \frac{2ab}{a+b}\right]\right\}. \quad . \quad . \quad . \quad . \quad (59)$$

When the leading edge of the wing is perpendicular to the stream direction, $z_0=\infty$, $\sigma=\pi/2$,

$$C_L = 4\alpha \tan\mu \left[1 - \frac{1}{2}\frac{(b-a)^2}{b+a}\right]$$

$$= 4\alpha \tan\mu \left[1 - \frac{1}{2}\left(\frac{1-c}{1+c}\right)^{3/2}\right] \quad . \quad . \quad . \quad . \quad (60)$$

which is the value obtained by Stewartson[3] who solved this problem by using a Laplace transform method.

For Case 2, $1<c<\operatorname{cosec}\sigma_0$, substituting for $G_3'(t)$ from equation (40) in (57),

$$C_L = 4\alpha \operatorname{cosec}\sigma_0 \tan\mu \left[1 + t_1 \cos\sigma_0 \tan\sigma_1 \left(\frac{t_1}{(t_1^2-1)^{\frac{1}{2}}} - 1\right)\right],$$

and $t_1 = \sec\sigma_1, \qquad c = \operatorname{cosec}\sigma_1.$

Therefore $C_L = 4\alpha \operatorname{cosec}\sigma_0 \tan\mu \left[1 + \cos\sigma_0 \frac{c}{1+c}\right]. \quad . \quad . \quad . \quad (61)$

For Case 3, $c>\operatorname{cosec}\sigma_0$, C_L can be obtained as in Case 2, giving the result

$$C_L = 4\alpha \operatorname{cosec}\sigma_0 \tan\mu\,[1+\tan\sigma_0(\operatorname{cosec}\sigma_0 - 1)]. \quad . \quad . \quad (62)$$

If $C_L' = 4\alpha \operatorname{cosec}\sigma_0 \tan\mu$ is the two-dimensional value of the lift coefficient, the variation of $(C_L - C_L')/C_L'$ as a function of c is calculated for three different wings, having values of sweepback β of 0, $\tan^{-1}(\tan\mu/2)$ and μ, *i.e.* for $\sigma_0=\pi/2$, $\sec^{-1}2$, $\sec^{-1}1$). The results are shown in Figs. 7 and 8.

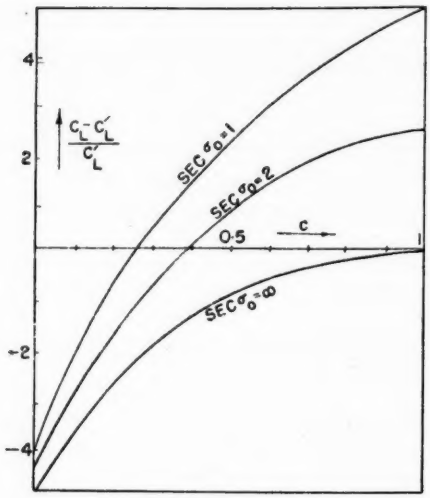

Fig. 7.

It will be seen from these figures that the effect of the vane is to reduce the deficit of lift otherwise caused by the presence of the wing tip. With zero sweepback the value of the lift coefficient tends to the two-dimensional (Ackeret) value as the vertex semi-angle of the vane increases towards the Mach angle, *i.e.* as c increases from 0 to 1. When the wing is swept, the effect of the vane is similar. Its effect is to restore the lift to the two-dimensional value for a vane semi-angle, $\gamma = \gamma_1 < \mu$, depending on the angle of sweep β; so that for $0 < \gamma < \gamma_1$, the lift is less than the two-dimensional value and for $\gamma > \gamma_1$ the lift is greater than this value. It reaches its maximum when the vane edge touches the shock wave produced by the leading edges of the wing.

This result was encouraging, and it was decided to go further and determine the drag and to discuss how the overall performance was affected by the presence of the vane.

6. The Symmetrical Part

This part corresponds to the wing and the vane of small finite thickness, but at zero incidence; the drag exists because of the thickness. The form of wing and vane for this case has already been described and a sketch of it is shown in Fig. 1. The thicknesses of the wing and the vane are represented by the angles δ and ε which their surfaces make with the z-axis. The solution is given here only for the field inside the Mach cone when the edges of the vane lie entirely inside the Mach cone. The other cases can be treated in the same way as the corresponding anti-symmetrical cases if they are needed.

To the degree of approximation assumed, the boundary conditions may be applied on the planes of symmetry of the wing and the vane instead of on the

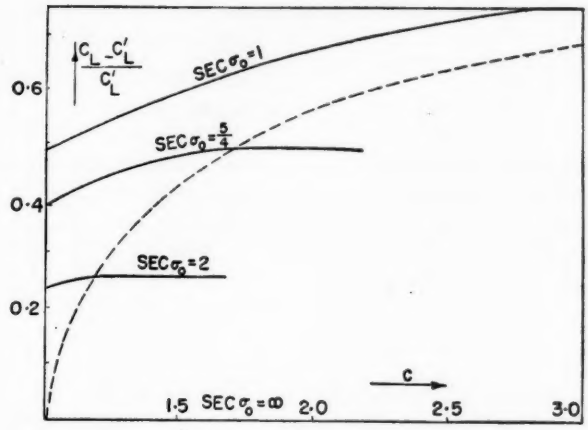

Fig. 8.

actual surfaces. Then, by neglecting quantities of the second and higher orders, the boundary condition on the upper surface of the wing $y_1 = +0$ is

$$v = W\delta,$$

and on the lower surface of the wing $y_1 = -0$ is

$$v = -W\delta,$$

while on the right-hand side of the vane $x_1 = +0$, the boundary condition is

$$u = W\varepsilon,$$

and that on the left-hand side of the vane $x_1 = -0$ is

$$u = -W\varepsilon,$$

where W is the velocity of the main stream in the z-direction.

The velocity components on the Mach cone are similar to those obtained in the lifting case in equation (11) but with $\alpha = -\delta$ in region 1 and $\alpha = \delta$ in region 2.

On transforming into the t-plane defined in equation (17) and then to the z-plane defined in equation (22), the components u, v, w of the perturbation velocity are the real parts of the functions $H_1(z)$, $H_2(z)$, $H_3(z)$ of the complex variable z. The boundary conditions could easily be transformed to the z-plane; they are

$$\left.\begin{aligned} u = \mathscr{R}\{H_1(z)\} &= W\varepsilon && \text{for } 0 < z < a, \\ &= -W\varepsilon && \text{for } -a < z < 0, \\ v = \mathscr{R}\{H_2(z)\} &= W\delta && \text{for } z_0 < z \text{ and for } z < -a, \\ &= 0 && \text{for } a < z < z_0, \end{aligned}\right\} \quad . \tag{63}$$

and hence from equation (28), the boundary conditions on $H_2'(z)$ are

$$\left.\begin{aligned} \mathscr{I}\{H_2'(z)\} &= 0 \quad \text{for } -a < z < a, \\ \mathscr{R}\{H_2'(z)\} &= 0 \quad \text{for } z < -a \text{ and } z > a. \end{aligned}\right\} \quad . \quad . \quad . \quad (64)$$

From these boundary conditions $H_2'(z)$ must have a double pole of residue $2iW\varepsilon/\pi$ at the origin, since it corresponds to the subsonic leading edge of the vane, another pole with residue $iW\delta/\pi$ at $z=z_0$, and a singularity at $z=\pm a$ of the form $(a^2-z^2)^{n+\frac{1}{2}}$ where $n \geqslant -1$. Therefore $H_2'(z)$ must have the form

$$H_2'(z) = \frac{(a^2-z^2)^{n+\frac{1}{2}}}{z^2(z-z_0)} H(z) \quad . \quad . \quad . \quad . \quad (65)$$

where $H(z)$ is an integral function which is real when z is real. Since $H_2'(z)$ must be of $O(z^{-2})$ as $z \longrightarrow \infty$, $H(z)$ must be a polynomial of degree p say. Therefore we have

$$\begin{aligned} 2n+p &\leqslant 0, \\ n &\geqslant -1, \\ p &\geqslant 1. \end{aligned}$$

Then $n=-1$, and either $p=1$ or $p=2$. In either case $H_2'(z)$ can be put in the form

$$H_2'(z) = \left(\frac{C}{z^2} + \frac{C_1}{z} + \frac{C_2}{z-z_0}\right) \frac{1}{(a^2-z^2)^{\frac{1}{2}}} \quad . \quad . \quad . \quad . \quad (66)$$

and from equation (27)

$$H_1'(z) = -i\left(\frac{C}{z^2} + \frac{C_1}{z} + \frac{C_2}{z-z_0}\right) \frac{1}{(a^2-z^2)^{\frac{1}{2}}} \frac{1}{(b^2-z^2)^{\frac{1}{2}}}, \quad . \quad (67)$$

$$H_3'(z) = -\tan\mu \left(\frac{C}{z^2} + \frac{C_1}{z} + \frac{C_2}{z-z_0}\right) \frac{1}{(b^2-z^2)^{\frac{1}{2}}}. \quad . \quad . \quad (68)$$

In these expressions

$$C_1 = -\frac{2Wc}{\pi} ab, \qquad C_2 = \frac{W\delta}{\pi} (z_0^2-a^2)^{\frac{1}{2}}. \quad . \quad . \quad . \quad (69)$$

The value of C is found after integrating $H_1(z)$, from the condition that $u = \mathscr{R}\{H_1(z)\}$ vanishes for $b < z < z_0$.

The expressions (66), (67) and (68) are now integrated. $H_2(z)$ and $H_3(z)$ can be expressed as elementary functions. $H_1'(z)$ can be written in the form

$$H_1'(z) = -i\left(\frac{C}{z^2} + \frac{W\delta(z_0^2-a^2)^{\frac{1}{2}}}{\pi} \frac{z_0}{z^2-z_0^2} + \frac{W\delta(z_0^2-a^2)^{\frac{1}{2}}}{\pi} \frac{z}{z^2-z_0^2} - \frac{2W\varepsilon ab}{\pi z}\right) \times$$

$$\times \frac{1}{(a^2-z^2)^{\frac{1}{2}}(b^2-z^2)^{\frac{1}{2}}}. \quad . \quad . \quad (70)$$

On integration, the first and second terms give elliptic integrals, and the remaining terms give elementary functions.

For the first and second terms, let

$$k=\frac{1}{b}, \qquad k'=(1-k^2)^{\frac{1}{2}}=\frac{a}{b}. \qquad . \quad . \quad . \quad (71)$$

χ is defined by means of Jacobian elliptic functions

$$\mathrm{dn}\,(\chi, k)=z/b, \qquad \mathrm{sn}\,(\chi, k)=(b^2-z^2)^{\frac{1}{2}} \qquad \mathrm{cn}\,(\chi, k)=(z^2-a^2)^{\frac{1}{2}}, \quad . \quad (72)$$

The elliptic integral of the second kind

$$\mathrm{E}(\chi)=\int_0^{\chi} \mathrm{dn}^2(\theta, k)\, d\theta, \quad . \quad . \quad . \quad . \quad . \quad (73)$$

and the elliptic integral of the third kind

$$\mathrm{F}(\chi)=\frac{z_0^2-a^2}{z_0^2-b^2}\int_0^{\Psi} \frac{d\psi}{1+\dfrac{\mathrm{sn}^2\psi}{z_0^2-b^2}}. \qquad . \quad . \quad . \quad (74)$$

If $\chi=\mathrm{K}$, the complete elliptic integral of the first kind to modulus k, $\mathrm{E}(\chi)$ and $\mathrm{F}(\chi)$ will tend to the corresponding complete integrals E and F. The values $z=-\infty$, 0, a, b correspond with $\chi=i\mathrm{K}'$, $\mathrm{K}+i\mathrm{K}'$, K, 0, where K′ is the complete elliptic integral of the first kind to modulus k'. With all these substitutions, the integral for $H_1'(z)$ on the upper half-plane that vanishes at $z=a$ is

$$H_1(z)=\frac{C}{b^2a^2}\left[\frac{(z^2-a^2)^{\frac{1}{2}}(b^2-z^2)^{\frac{1}{2}}}{z}-b\,(\mathrm{E}(\chi)-\mathrm{E})\right]+\frac{W\delta}{\pi b}\frac{z_0}{(z_0^2-a^2)^{\frac{1}{2}}}(\mathrm{F}(\chi)-\mathrm{F})-$$

$$-\frac{W\delta}{\pi(z_0^2-a^2)^{\frac{1}{2}}}\tan^{-1}\left(\frac{z_0^2-b^2}{z_0^2-a^2}\right)^{\frac{1}{2}}\left(\frac{z^2-a^2}{b^2-z^2}\right)^{\frac{1}{2}}+\frac{2iW\varepsilon}{\pi}\log\frac{b(a^2-z^2)^{\frac{1}{2}}+a(b^2-z^2)^{\frac{1}{2}}}{z}+2W\varepsilon. \quad . \quad . \quad . \quad . \quad (75)$$

On the real axis for $b<z<z_0$, χ, $\mathrm{E}(\chi)$, $\mathrm{F}\chi)$ are all purely imaginary, and in order that $\mathscr{R}\{H_1(z)\}=2W\varepsilon$ in this range,

$$\frac{C}{a^2}=\frac{W\delta}{\pi}\left(\frac{z_0}{(z_0^2-a^2)^{\frac{1}{2}}}\frac{\mathrm{F}}{\mathrm{E}}-\frac{b}{(z_0^2-a^2)^{\frac{1}{2}}}\frac{\pi}{2\mathrm{E}}\right). \qquad . \quad . \quad (76)$$

Therefore

$$H_1(z)=\frac{C}{b^2a^2}\left[\frac{(z^2-a^2)^{\frac{1}{2}}(b^2-z^2)^{\frac{1}{2}}}{z}-b\,\mathrm{E}(\chi)\right]+\frac{W\delta}{\pi b}\frac{z_0}{(z_0^2-a^2)^{\frac{1}{2}}}\mathrm{F}(\chi)+$$

$$+\frac{W\delta}{\pi}\frac{1}{(z_0^2-b^2)^{\frac{1}{2}}}\tan^{-1}\left(\frac{z_0^2-a^2}{z_0^2-b^2}\right)^{\frac{1}{2}}\left(\frac{b^2-z^2}{z^2-a^2}\right)^{\frac{1}{2}}+$$

$$+\frac{2iW\varepsilon}{\pi}\log\frac{b(a^2-z^2)^{\frac{1}{2}}+a(b^2-z^2)^{\frac{1}{2}}}{z}+2W\varepsilon. \quad . \quad . \quad . \quad . \quad (77)$$

The integrals for $H_2(z)$ and $H_3(z)$ on the upper half-plane are

$$H_2(z) = -\frac{C}{a^2}\frac{(a^2-z^2)^{\frac{1}{2}}}{z} + \frac{2W\delta}{\pi}\tan^{-1}\left(\frac{a+z_0}{z_0-a}\right)^{\frac{1}{2}}\left(\frac{a-z}{a+z}\right)^{\frac{1}{2}} + \frac{2W\varepsilon b}{\pi}\log\frac{a+(a^2-z^2)^{\frac{1}{2}}}{z}, \quad . \quad . \quad . \quad . \quad (78)$$

$$H_3(z) = \tan\mu\left[\frac{C}{b^2}\frac{(b^2-z^2)^{\frac{1}{2}}}{z} - \frac{2W\delta}{\pi}\left(\frac{z_0^2-a^2}{z_0^2-b^2}\right)^{\frac{1}{2}}\tan^{-1}\left(\frac{b+z_0}{z_0-b}\right)^{\frac{1}{2}}\left(\frac{b-z}{b+z}\right)^{\frac{1}{2}} - \right.$$
$$\left. - \frac{2W\varepsilon a}{\pi}\log\frac{b+(b^2-z^2)^{\frac{1}{2}}}{z}\right]. \quad . \quad . \quad . \quad (79)$$

The velocity components may now be obtained by taking the real parts of these expressions after substituting for z in terms of t and thence in terms of x_1, y_1. The corresponding values for the lower half-plane are obtained from the fact that in this symmetrical case v is odd, while u and w are even in y.

7. The Drag Force

The drag force in the z-direction is due to the perturbation pressure acting normally over the surfaces of the wing and the vane, and to the suction force normal to the leading edges of the vane. The first two parts, the drag over the wing and the drag over the vane, are obtained by integrating the z-component of the force due to the perturbation pressure over their respective surfaces. The third part is obtained by integrating the z-component of the suction force over the two leading edges of the vane.

The drag over the wing

Let P be the perturbation pressure defined in equation (2). The drag over that part of the wing inside the Mach cone which lies between the origin and the plane $z=\cot\mu$, *i.e.* the drag over an area $\frac{1}{2}\cot\mu$ of the wing, is

$$D_1 = -\rho\cot\mu\, W\delta\mathscr{R}\left\{\int_{-1}^{0} G_3(t)\,dt\right\}.$$

Integrating by parts

$$D_1 = -\rho\cot\mu\, W\delta\mathscr{R}\left\{\Big[G_3(t)\,t\Big]_{-1}^{0} - \int_{-1}^{0} G_3'(t)\,t\,dt\right\}.$$

Changing the variable of integration from t to z, from equation (24), $z=-(a^2+t^2)^{\frac{1}{2}}$ on the wing, so that the range of integration is $-b<z<-a$. Hence

$$D_1 = \rho\cot\mu W\delta\left\{\Big[H_3(z)(z^2-a^2)^{\frac{1}{2}}\Big]_{-b}^{-a} - \int_{-b}^{-a} H_3'(z)(z^2-a^2)^{\frac{1}{2}}\,dz.\right\} \quad . \quad (80)$$

The expressions for $H_3'(z)$ or $H_3(z)$ are all real in $-b<z<-a$.

The drag on the wing is composed of two parts; the first part is due to the incidence of the wing, and for this $H_3'(z)$ and $H_3(z)$ are given by equations (32) and (35) respectively. The evaluation of (80) in these circumstances was carried out when the lift on the wing was calculated in equation (59), and hence

$$D_1' = \rho W^2 \alpha^2 \operatorname{cosec} \sigma_0 \left\{ 1 - \left(\frac{z_0+b}{z_0-a} \right)^{\frac{1}{2}} \left[z_0 - (z_0-a) \left(\frac{z_0+a}{z_0+b} \right)^{\frac{1}{2}} - \frac{2ab}{a+b} \right] \right\}. \quad (81)$$

The second part is due to the thickness of the wing and the vane; and here $H_3'(z)$ and $H_3(z)$ are given in equations (68) and (79) respectively. Therefore

$$D_1'' = \rho W \delta \cot \mu \Big[W\delta \operatorname{cosec} \sigma_0 \tan \mu + \tan \mu \int_{-b}^{-a} \left(\frac{C}{z^2} + \frac{W\delta}{\pi} \frac{(z_0^2-a^2)^{\frac{1}{2}}}{z-z_0} \right) \left(\frac{z^2-a^2}{b^2-z^2} \right)^{\frac{1}{2}} dz - \\ - \frac{2abW\varepsilon \tan \mu}{\pi} \int_{-b}^{-a} \frac{1}{z} \left(\frac{z^2-a^2}{b^2-z^2} \right)^{\frac{1}{2}} dz \Big],$$

$$= \rho W^2 \delta^2 \left[\operatorname{cosec} \sigma_0 + \frac{C}{W\delta b} (\mathrm{K}-\mathrm{E}) + \frac{z_0 (z_0^2-a^2)^{\frac{1}{2}}}{\pi b} (\mathrm{K}-\mathrm{F}) + \right. \\ \left. + \tfrac{1}{2} (z_0^2-a^2)^{\frac{1}{2}} \left\{ \left(\frac{z_0^2-a^2}{z_0^2-b^2} \right)^{\frac{1}{2}} - 1 \right\} \right] + \rho W^2 \delta \varepsilon a (b-a). \quad (82)$$

The total drag on the wing is $D_1' + D_1''$. With no sweepback $z_0 \longrightarrow \infty$, $\sigma_0 \longrightarrow \pi/2$. From the definition for F and K given before it is easy to prove that

$$\operatorname*{Lim}_{z_0 \to \infty} \mathrm{F} = \mathrm{K},$$

and

$$\operatorname*{Lim}_{z_0 \to \infty} \frac{z_0 (z_0^2-a^2)^{\frac{1}{2}}}{b\pi} (\mathrm{K}-\mathrm{F}) = \frac{1}{\pi b} (a^2 \mathrm{K} - b^2 \mathrm{E}).$$

Therefore

$$C = \frac{W\delta a^2}{\pi} \frac{\mathrm{K}}{\mathrm{E}},$$

and

$$D_1 = \rho W^2 \delta^2 \left[1 + \frac{1}{\pi (1-c^2)^{\frac{1}{2}}} \left(\frac{c^2 \mathrm{K}^2}{\mathrm{E}} - \mathrm{E} \right) \right] + \rho W^2 \varepsilon \delta \frac{c}{1+c} + \rho W^2 \alpha^2 \left[1 - \frac{1}{2} \left(\frac{1-c}{1+c} \right)^{3/2} \right]. \\ \quad (83)$$

The drag over the vane

In this case the pressure is to be integrated over the two sides of the vane, from the vertex at the origin to the plane $z = \cot \mu$, *i.e.* over an area $c \cot \mu$. The drag will be

$$D_2 = -\rho \varepsilon \cot \mu \, W \int_0^c (w_{x_1=+0} + w_{x_1=-0}) \, dy_1.$$

On the vane, if t' is the imaginary part of t, from equation (17)

$$\frac{1}{t'} = \frac{(1-y_1^2)^{\frac{1}{2}}}{y_1} \quad , \quad \frac{dy_1}{dt'} = \frac{1}{(1+t'^2)^{3/2}} .$$

Therefore $$D_2 = -\rho W \varepsilon \cot \mu \int_0^a (w_{\mathrm{Re}\,(t)=+0} + w_{\mathrm{Re}\,(t)=-0}) \frac{dt'}{(1+t'^2)^{3/2}} .$$

On transforming to the z-plane, $z=(a^2-t'^2)^{\frac{1}{2}}$, $0<z<a$ on the right-hand side of the vane, and $z=-(a^2-t'^2)^{\frac{1}{2}}$, $-a<z<0$ on the left-hand side. The drag will be

$$D_2 = -\rho W \varepsilon \cot \mu \int_{-a}^{0} + \int_a^0 \frac{\mathscr{R}\{H_3(z)\}}{(b^2-z^2)^{3/2}} \frac{z\,dz}{(a^2-z^2)^{\frac{1}{2}}} . \quad . \quad . \quad (84)$$

From the expression (79) for $H_3(z)$ it is clear that it is real in the interval $-a<z<a$. Therefore

$$D_2 = -2\rho \frac{W\varepsilon\delta}{\pi} \int_{-a}^{0} + \int_a^0 \tan^{-1} \left\{ \left(\frac{z_0+b}{z_0-b}\right)^{\frac{1}{2}} \left(\frac{b-z}{b+z}\right)^{\frac{1}{2}} \right\} \frac{z\,dz}{(b^2-z^2)^{3/2}(a^2-z^2)^{\frac{1}{2}}} +$$

$$+ \frac{\rho W \varepsilon C}{b^2} \int_{-a}^{0} + \int_a^0 \frac{dz}{(b^2-z^2)(a^2-z^2)^{\frac{1}{2}}} +$$

$$+ \frac{2\rho W^2 \varepsilon^2 a}{\pi} \int_{-a}^{0} + \int_a^0 \log \frac{a+(a^2-z^2)^{\frac{1}{2}}}{|z|} \frac{z\,dz}{(b^2-z^2)^{3/2}(a^2-z^2)^{\frac{1}{2}}} .$$

Integrate the first term by parts, then divide the integral part into its even and odd parts. The even integrals in D_2 will vanish on integration. Calculating the odd integrals gives

$$D_2 = \frac{4\rho W^2 \varepsilon \delta a}{\pi b} \left(\frac{z_0^2-a^2}{z_0^2-b^2}\right)^{\frac{1}{2}} \tan^{-1} \left(\frac{z_0+b}{z_0-b}\right)^{\frac{1}{2}} -$$

$$- \frac{2\rho W^2 \varepsilon \delta}{\pi (z_0^2-a^2)^{\frac{1}{2}}} \left\{ (z_0^2-a^2)^{\frac{1}{2}} \tan^{-1} \frac{a}{(z_0^2-a^2)^{\frac{1}{2}}} - \tan^{-1} a \right\} +$$

$$+ \frac{4\rho W^2 \varepsilon^2 a}{\pi} \left\{ a \log \frac{b}{a} + \tan^{-1} a \right\} . \quad . \quad . \quad . \quad (85)$$

The last term is the drag over the vane in the absence of the wing, a result obtained by Puckett[4]. The remaining two terms represents the effect of the thickness of the wing.

The drag due to the suction force on the leading edges of the vane

At the subsonic leading edges of the vane, the velocity becomes infinite in the linear theory both in the anti-symmetrical and symmetrical part of the field. If at any point (z, y) on the upper leading edge of the vane, r_1 is the normal distance from

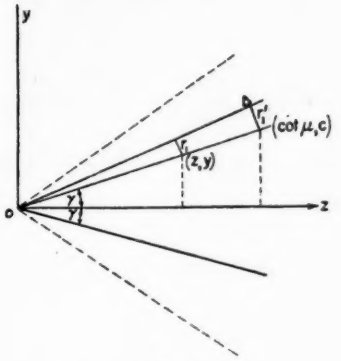

Fig. 9.

this edge in the plane of the vane (*see* Fig. 9) the velocity normal to that plane $\sim \varepsilon_1 r_1^{-\frac{1}{4}}$ as $r_1 \longrightarrow 0$, *i.e.* $u \sim \varepsilon_1 r_1^{-\frac{1}{4}}$ (where ε_1 is a constant proved later to depend on y); there is a suction force on the leading edge and in the plane of the vane, whose magnitude per unit length is[1]

$$\frac{\pi\rho\varepsilon_1^{\,2}}{(1-M^2\sin^2\gamma)^{\frac{1}{2}}}.$$

The drag force due to this suction force over a length $\operatorname{cosec}\gamma$ of the upper edge of the vane is

$$-\int_0^c \frac{\pi\rho\varepsilon_1^{\,2}}{(1-M^2\sin^2\gamma)^{\frac{1}{2}}}\,dy.$$

In conical flows the components of the perturbation velocity u, v, w are constant along straight lines emerging from the vertex of the Mach cone. Let ε_1' be the value of ε_1 at the upper edge of the vane in the plane $z=\cot\mu$, *i.e.* at the point $(\cot\mu, c)$ in Fig. 10, so that $u \sim \varepsilon_1'/r_1'^{\frac{1}{4}}$ as $r_1' \longrightarrow 0$. Therefore along any straight line, Δ say, near the upper edge of the vane,

$$u \sim \frac{\varepsilon_1}{r_1^{\frac{1}{4}}} = \frac{\varepsilon_1'}{r_1'^{\frac{1}{4}}}. \qquad (86)$$

Hence

$$\varepsilon_1 = \varepsilon_1'\left(\frac{r_1}{r_1'}\right)^{\frac{1}{4}} = \varepsilon_1'\left(\frac{y}{c}\right)^{\frac{1}{4}} \qquad (87)$$

Therefore the drag force due to the suction force along the upper edge of the vane is

$$-\frac{\pi\rho\varepsilon_1'^2 c}{2(1-M^2\sin^2\gamma)^{\frac{1}{2}}}.$$

A similar expression is obtained for the lower edge, and the total drag due to the suction force becomes

$$D_s = -\frac{\pi\rho c(\varepsilon_1'^2+\varepsilon_2'^2)}{2(1-M^2\sin^2\gamma)}, \quad . \quad . \quad . \quad . \quad . \quad (88)$$

where ε_2' is the corresponding value of ε_1' at the lower edge of the vane.

To determine ε_1',

$$H_1'(z) \sim \frac{i\lambda}{z^2} \quad \text{as} \quad z \longrightarrow 0 \quad \text{along the imaginary axis.}$$

Then in the t-plane,

$$G_1'(t) \sim \frac{i\lambda t}{(a^2+t^2)^{3/2}} \quad \text{as} \quad t \longrightarrow ia \quad \text{along the imaginary axis.}$$

In transforming to the x_1y_1-plane

$$\frac{du}{dy_1} \sim -\frac{\lambda(1-c^2)^{3/2}}{(y_1^2-c^2)^{3/2}}\frac{y_1}{(1-y_1^2)^{\frac{1}{2}}} \quad \text{as} \quad y_1 \longrightarrow c,$$

$$\sim -\lambda\frac{(1-c^2)}{(8c)^{\frac{1}{2}}}\frac{1}{(y_1-c)^{3/2}} \quad \text{as} \quad y_1 \longrightarrow c.$$

Hence $$u \sim -\lambda\frac{(1-c^2)}{(2c)^{\frac{1}{2}}}\frac{1}{(y_1-c)^{\frac{1}{2}}}. \quad . \quad . \quad . \quad . \quad . \quad (89)$$

Comparing equations (86) and (89),

$$\varepsilon_1' = -\cos^{\frac{1}{2}}\gamma(1-c^2)(2c)^{-\frac{1}{2}}\lambda. \quad . \quad . \quad (90)$$

But from equations (32) and (68) the value of λ corresponding to the upper edge of the vane is

$$\frac{2(ab)^{\frac{1}{2}}}{a+b}\left(\frac{z_0+a}{z_0-b}\right)^{\frac{1}{2}}\frac{W\alpha}{\pi} - \frac{C}{ab},$$

and that for the lower edge is

$$\frac{2(ab)^{\frac{1}{2}}}{a+b}\left(\frac{z_0+a}{z_0-b}\right)^{\frac{1}{2}}\frac{W\alpha}{\pi} + \frac{C}{ab}.$$

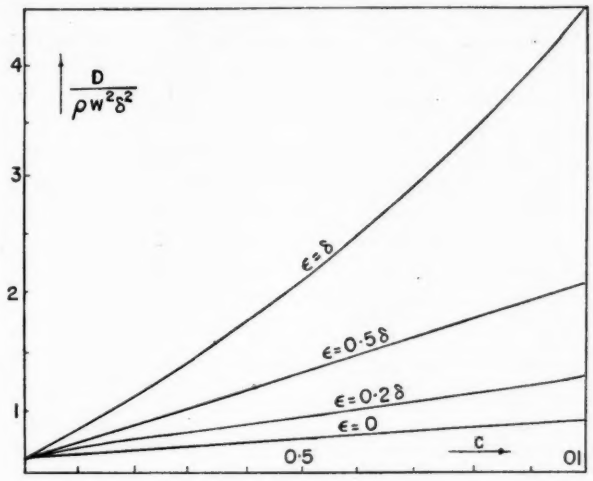

Fig. 10.

Therefore the drag force becomes

$$D_3 = \frac{\pi\rho\cos\gamma}{2(1-M^2\sin^2\gamma)^{\frac{1}{2}}}(1-c^2)^2\left[\left(\frac{C}{ab}\right)^2 + \left\{\frac{2(ab)^{\frac{1}{2}}}{a+b}\left(\frac{z_0+a}{z_0-b}\right)^{\frac{1}{2}}\frac{W\alpha}{\pi}\right\}^2\right].$$

Since $c=\tan\gamma\cot\mu$, $M=\operatorname{cosec}\mu$, hence

$$D_3 = \frac{\pi\rho}{2}(1-c^2)^{3/2}\left[\left(\frac{C}{ab}\right)^2 + \left\{\frac{2(ab)^{\frac{1}{2}}}{a+b}\left(\frac{z_0+a}{z_0-b}\right)^{\frac{1}{2}}\frac{W\alpha}{\pi}\right\}^2\right]. \quad . \quad . \quad . \quad (91)$$

The total drag is now obtained by adding together the expressions obtained for D_1, D_2, D_3. For no sweepback this gives

$$D=\rho W^2\delta^2\left[1+\frac{1}{\pi(1-c^2)^{\frac{1}{2}}}\left(\frac{c^2K^2}{E}-E\right)\right]+c\rho W^2\varepsilon\delta\left(\frac{1}{1+c}+1\right)+$$
$$+\frac{4c}{\pi}\rho W^2\varepsilon^2\left[\sin^{-1}c-\frac{c}{(1-c^2)^{\frac{1}{2}}}\log c\right]+\rho W^2\alpha^2\left[1-\frac{1}{2}\left(\frac{1-c}{1+c}\right)^{3/2}\right]-$$
$$-\frac{c^2(1-c^2)^{3/2}}{2\pi}\rho W^2\left[\frac{K^2}{E^2}\delta^2+\frac{4\alpha^2}{c(1+c)^2}\right]. \quad . \quad . \quad . \quad (92)$$

When α is very small so that α^2 can be neglected,

$$\frac{D}{\delta^2\rho W^2}=1+\frac{1}{\pi(1-c^2)^{\frac{1}{2}}}\left(\frac{c^2K^2}{E}-E\right)-\frac{c^2(1-c^2)^{3/2}}{2\pi}\frac{K^2}{E^2}+$$
$$+\frac{c(2+c)}{1+c}\frac{\varepsilon}{\delta}+\frac{4c}{\pi}\left[\sin^{-1}c-\frac{c\log c}{(1-c^2)^{\frac{1}{2}}}\right]\frac{\varepsilon^2}{\delta^2}. \quad . \quad . \quad . \quad (93)$$

The variation of the drag given in this last equation as a function of $c=\tan\gamma/\tan\mu$ can be seen in Fig. 10.

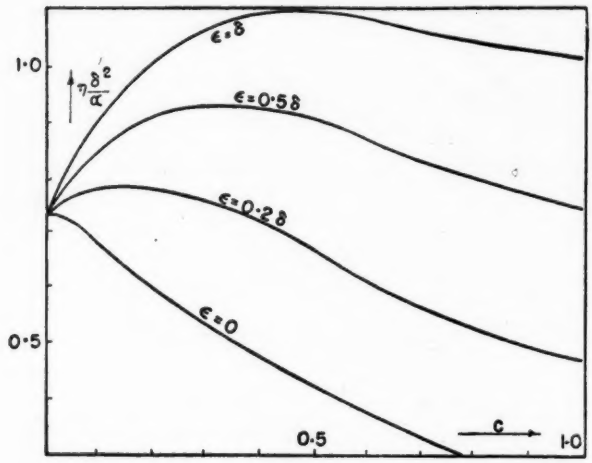

Fig. 11.

8. Performance

It is now possible to discuss how the performance is affected by the presence of the vane. Let L be the lift force at incidence α and D the drag force at zero incidence; the trailing edges of both the wing and the vane are straight lines lying in the plane $z=\cot\mu$. Then the quantity

$$\eta=\frac{L}{D} \qquad . \qquad . \qquad . \qquad . \qquad . \qquad . \qquad . \qquad (94)$$

is a measure of the performance of the wing-vane system.

Consider the only available case, that is when the vane lies entirely inside the Mach cone. The other cases when the vane edges are outside the Mach cone are not important, since in these cases the drag increases without any considerable increase in lift.

η is obtained by substituting for L and D from the values already obtained. To avoid unnecessary complications the case of no sweep ($z_0=\infty$, $\sigma_0=\pi/2$) is considered. η is then given by

$$\eta=\frac{\dfrac{\alpha}{\delta^2}\left[1-\frac{1}{2}\left(\frac{1-c}{1+c}\right)^{3/2}\right]}{\left[1+\dfrac{1}{\pi(1-c^2)^{\frac{1}{2}}}\left(\frac{c^2K^2}{E}-E\right)-\frac{c^2(1-c^2)^{3/2}}{2\pi}\frac{K^2}{E^2}+\frac{4c(2+c)}{\pi(1+c)}\frac{\varepsilon}{\delta}+\right.}$$
$$\left.+\frac{4c}{\pi}\left(\sin^{-1}c-\frac{c}{(1-c^2)^{\frac{1}{2}}}\log c\right)\left(\frac{\varepsilon}{\delta}\right)^2\right] \qquad (95)$$

The variation of $\eta\delta^2/\alpha$ as a function of c, given by equation (95), is shown in Fig. 11. The calculations were made for wings carrying vanes of different thickness in a flow for which the Mach number was $\sqrt{2}$.

It appears, then, that with no sweep, an increase in the performance is made possible by using wing tip vanes, provided that $\varepsilon < \delta$; for each value of ε there is an optimum semi-angle for the vane, this angle increasing as ε decreases. The maximum performance is obtained when $\varepsilon = 0$, which clearly must be the case, the index of merit η then being about $1{\cdot}1\,\alpha/\delta^2$ and the semi-angle of the vane being about 25° when the Mach angle is 45°; with no vane $\eta = 0{\cdot}735\,\alpha/\delta^2$, so that the performance of that part of the wing-vane system which lies inside the Mach cone is increased by a factor of 1·5. In the more practical case when $\varepsilon = 0{\cdot}2\,\delta$, the optimum value of η is $0{\cdot}925\,\alpha/\delta^2$ for a semi-angle of about 18° when the Mach angle is 45°, the performance in this case being better than that with no vane by a factor of 1·26. Or when $\varepsilon = 0{\cdot}5\,\delta$, the optimum semi-angle is about 6·5° when the Mach angle is 45°, and the factor of improvement is 1·07.

It is clear that an increase in performance also occurs when the wing has a swept leading edge, and the indication of Fig. 7 is that this may be greater than in the unswept case.

ACKNOWLEDGMENTS

The author wishes to express his indebtedness to Professor G. N. Ward for his continued help in the preparation of this paper; also to Professor S. Goldstein and Professor M. J. Lighthill for the interest they have shown in it.

REFERENCES

1. GOLDSTEIN, S. and WARD, G. N. (1950). The Linearised Theory of Conical Fields in Supersonic Flow, with Application to Plane Aerofoils. *The Aeronautical Quarterly*, Vol. III, May 1950, pp. 39-84.

2. PUCKETT, A. E. (1946). Supersonic Wave Drag of Thin Aerofoils. *Journal of the Aeronautical Sciences*. Vol. 13, September 1946, pp. 475-484.

3. STEWARTSON, K. (1949). The Effect of a Symmetrical Guide on the Lift of a Semi-infinite Wing, Moving with Supersonic Speed. A.R.C. 12,112, January 1949.

4. WHITTAKER, E. T. and WATSON, G. N. (1927). *Modern Analysis*, Chapter 22. Cambridge University Press. Fourth Edition, 1927.

Estimation of the Effects of Distortion on the Longitudinal Stability of Swept Wing Aircraft at High Speeds (Sub-Critical Mach Numbers)

B. S. CAMPION, B.Sc.(Eng.), D.C.Ae.

(College of Aeronautics, Cranfield)

Summary: The effects of distortion on the longitudinal stability of swept wing aircraft at high speeds (sub-critical Mach numbers) are considered on a quasi-static basis. The method is based on the theory of Gates and Lyon[1] but involves some extension of this theory.

The treatment of wing distortion is considered in some detail and the effects of built-in twist and camber and wing weight are included, using the so-called superposition method.[3] The application of the analysis of Lyon and Ripley[2] for investigating fuselage, tail and control circuit distortion is suggested, but means of modifying and simplifying this procedure where desirable are put forward.

The analysis is illustrated by means of a simple example of a swept wing fighter aircraft for which wing, fuselage and tail distortion effects are considered, and the results are discussed with reference to the individual and combined distortion effects, as well as the effect of compressibility.

1. Introduction

The longitudinal stability of an aircraft is usually considered in terms of "static stability" (measured by the static margins), "manoeuvrability" (measured by the manoeuvre margins) and general dynamic stability. If the stability derivatives are very little modified by frequency effects (*i.e.* they approximate closely to the quasi-static values), then the static and manoeuvre margins as normally defined can be related to the coefficients E_1 and C_1 in the "stability quartic," given by the usual small displacement theory. The values of the static and manoeuvre margins then largely determine the characteristics of the phugoid and short period oscillations.

When structural distortion effects are introduced, it is again necessary to consider whether the motion of the aircraft (in the long and short period oscillations) occurs under quasi-static conditions, or whether the dynamics of the separate aircraft components should be considered, introducing additional degrees of freedom corresponding to oscillations of individual components. This question is discussed in Ref. 4, where it is pointed out that if the frequency of the short period oscillation is of the same order as the lowest natural frequency of any component (*e.g.* the wing) the simple quasi-static approach is suspect. Once the quasi-static approach is abandoned, however, the treatment of dynamic stability when distortion effects are included becomes very difficult[5]. The general treatment of the dynamic stability of

Originally received June 1954.

[The Aeronautical Quarterly, Vol. V, November 1954]

a flexible aircraft can be similar to that used in flutter problems, although the difficulties are enhanced by the fact that coupled oscillations of wing, fuselage, tail, and so on, are combined with the overall "rigid body" motion of the aircraft. An attempt to formulate the equations governing the motion of an aircraft with flexible fuselage and wings is made in Ref. 5, and the problem is considered briefly in Ref. 4.

In this report the "quasi-static" approach only is considered, as in Refs. 1 and 2. By this method the equations of motion for a rigid aircraft are used but the values of the aerodynamic derivatives are modified to include distortion effects.

The basic theory is, in essentials, that of Refs. 1 and 2, with certain modifications and extensions which it is believed will permit of a more logical treatment of the effects of wing distortion in cases where there is built-in twist or camber, and the treatment also permits the ready inclusion of the effects of aircraft weight. The conditions for the balance of aerodynamic, elastic and inertia forces are obtained by the superposition method of Ref. 3, which it is considered has many advantages over other methods.

The analysis is illustrated by means of an example of a high-speed swept wing fighter, and the results of the analysis are discussed in detail. This example presents a number of features of general interest.

For compressibility effects on a rigid aircraft the important parameter is the Mach number, so that the variation of true air speed must be considered. When the aircraft is flexible, however, the distortions produced by aerodynamic loading are dependent on the equivalent air speed. In general, therefore, the two parameters M and $q=\frac{1}{2}\rho V^2$ must be considered. In this report the suffix M indicates that a derivative is taken at constant Mach number (*e.g.* $(\partial C_L/\partial\alpha)_M$), and in such cases it is also implied that q is constant.

The corrections for variations of inertia loading due to normal acceleration, introduced in Section 4, are "quasi-static," *i.e.* it is assumed that the normal accelerations of all parts of the aircraft are the same as that of the c.g. and that the structure is always in equilibrium under the applied aerodynamic and inertia loading. This assumption is similar to the assumption that frequency effects on the aerodynamic derivatives, and so on, may be neglected and will similarly become invalid when the short period frequency is high.

Notation

A wing lift curve slope with compressibility and distortion effects included

A_R rigid wing lift curve slope when compressibility effects are included

A^0 value of A for condition $n=0$ (*i.e.* neglecting inertia loading)

$A_n = (\partial C_{Lnw}/\partial n)_M$

A_S, B_S, C_S superposition coefficients

A_1, A_2, A_3, $\bar{A}_1, \bar{A}_2$ etc. — tail lift coefficient derivatives[1] when compressibility and all distortion effects are included

A_{1T}, B_{1T}, $\bar{A}_{1T}$ — tail lift and hinge moment derivatives corresponding to true tail-setting angle

$\frac{\partial \bar{A}_1}{\partial M}, \frac{\partial \bar{A}_{1T}}{\partial M}$ etc. — defined in Section 4.3

B_0, B_1, B_2, B_3 — tail hinge moment derivatives when compressibility and all distortion effects are included

$\bar{c}$ — standard mean chord

C_{L0} — overall lift coefficient based on wing area in steady level flight, $= W/(\frac{1}{2}\rho V^2 S)$

C_{Lw} — wing lift coefficient

$C_{Lcw}, C_{Ltw}, C_{Lnw}$ — wing lift coefficient increments due to built-in camber and twist and wing weight

C_{Law} — wing lift coefficient due to incidence only

$C_{Lw0} = C_{Lcw} + C_{Ltw}$

C_{mw} — wing pitching moment coefficient about *rigid* wing mean aerodynamic centre

$C_{mcw}, C_{mtw}, C_{mnw}$ — wing pitching moment coefficients corresponding to C_{Lcw}, C_{Ltw}, C_{Lnw}

$(C_{m0})_{wing}$ — wing pitching moment coefficient about *flexible* wing mean aerodynamic centre

C_{mf} — fuselage pitching moment coefficient (based on wing area)

$C_R = W/(\frac{1}{2}\rho V^2 S)$, "resultant vertical force coefficient"

$$F = A_1 \frac{S_T}{S}\left(\frac{1}{A^0} - \frac{\partial \varepsilon}{\partial \alpha}\right)$$

$$\bar{F} = \bar{A}_1 \frac{S_T}{S}\left(\frac{1}{A^0} - \frac{\partial \varepsilon}{\partial \alpha}\right)$$

H_m, H_m' — stick fixed, stick free manoeuvre margins

H_0, H_0^0 — value of h corresponding to position of (flexible) wing mean aerodynamic centre of lift due to incidence only—affix 0 refers to $n=0$.

H_0^n — "inertial aerodynamic centre" position

H_{0R} — value of H_0 for rigid wing

K_n, K_n' — stick fixed, stick free static margins

l — distance from tail aerodynamic centre to wing aerodynamic centre (corresponding to H_0^0)

l_T — distance from tail aerodynamic centre to c.g. of aircraft

n — defined by $(n-1)g$ = normal acceleration

$q = \frac{1}{2}\rho V^2$; also angular velocity in pitch

$\left.\begin{aligned} \overline{V}_{\text{a.c.}} &= \frac{S_T l}{Sc} \\ \overline{V}_{\text{c.g.}} &= \frac{S_T l_T}{Sc} \\ V_T &= \frac{\overline{V}_{\text{a.c.}}}{1+\overline{F}} \\ \overline{V}_T &= \frac{\overline{V}_{\text{a.c.}}}{1+\overline{F}} \end{aligned}\right\}$ tail volume coefficients

α wing incidence measured at root

α_T, α_{T0} tailplane root incidences corresponding to η_T, η_{T0}

β tab angle corresponding to movement of pilot's trimmer control

$\overline{\varepsilon}$ mean downwash angle at tailplane

$\overline{\varepsilon}_\alpha$ mean downwash angle at tailplane due to wing root incidence

$\overline{\varepsilon}_0$ mean downwash angle at tailplane corresponding to C_{Lw0}

$\overline{\varepsilon}_n$ mean downwash angle at tailplane due to distortion of wing under inertia loading

$\dot{\overline{\varepsilon}}_\alpha = \overline{\varepsilon}_\alpha/(A^0\alpha)$

$\dot{\overline{\varepsilon}}_n = \overline{\varepsilon}_n/(A_n n)$

η elevator angle corresponding to movement of control column

η_{T0} tail setting angle corresponding to setting on ground (if "fixed") or to movement of pilot's control (if "variable")

η_T true (root) tail-setting angle

2. Wing Distortion

When considering longitudinal stability it is usual to assume that the ailerons will remain in the neutral position when the wing distorts. Distortion of the main wing structure only is then considered. For most swept wings the loss of incidence due to upward bending is greater than the increase due to twist (referred to an ideal straight flexural axis). Thus wing distortion produces a net loss of lift curve slope, accompanied by forward movement of the aerodynamic centre (*see* Section 2.2).

When the quasi-static approach is used in obtaining stability criteria and derivatives it is assumed that the structure is always in equilibrium under the applied loading. The problem of treating wing distortion is then basically that of solving for the "aeroelastic equilibrium" of a flexible lifting surface.

2.1. Solution of the aeroelastic equilibrium problem for a flexible lifting surface

The problem of calculating the aerodynamic characteristics of a flexible lifting surface is one of some difficulty, due to the fact that distortion under load produces a change of load. Mathematically the problem takes the form of the solution of an integral equation.

It is possible to solve the problem (using strip theory) by successive approximation (*see* Ref. 4) or by the method of semi-rigid representation [4, 8]. These methods are well known and widely used. They suffer from the disadvantage that, since strip theory must be used, induced aerodynamic effects due to the distortion itself are neglected; also with the semi-rigid method, as normally applied using one mode, the accuracy is limited by the closeness with which the mode represents the distortion. However, the semi-rigid method is not in principle limited to one mode and the "superposition" method which is put forward in Ref. 3*, and which has been adopted here as being in some respects superior to previous techniques, can strictly be regarded as a variant of the semi-rigid representation technique. The following is a brief description of it. The usual assumption of linearity between loading and incidence is fundamental to the method.

At any point on the span of an elastic wing in equilibrium under aerodynamic load, the final geometric incidence α_F will be given by

$$\alpha_F = \alpha_I + \alpha_E$$

where α_I = geometric incidence of undistorted wing ("initial" incidence)

α_E = change of incidence due to distortion.

If α_F is known, the final loading is known and α_E may be calculated, giving α_I. Thus the problem is easily solved "backwards." If a number of arbitrary "final" incidence distributions α_{F_1}, α_{F_2}, and so on, are chosen and the corresponding "initial" incidence distributions α_{I_1}, α_{I_2}, and so on, are so obtained, then any given initial incidence distributions may be approximately represented by a linear combination of the arbitrary initial distributions. Thus

$$\alpha_I = A_S\alpha_{I_1} + B_S\alpha_{I_2} + C_S\alpha_{I_3} + \ldots$$

In practice three or four such terms may be sufficient.

The coefficients A_S, B_S, C_S, and so on, are functions of the parameter qA_R, where A_R is the rigid wing lift curve slope allowing for compressibility effects.

But
$$A_S\alpha_{I_1} = A_S\alpha_{F_1} - A_S\alpha_{E_1}$$
$$B_S\alpha_{I_2} = B_S\alpha_{F_2} - B_S\alpha_{E_2}, \text{ etc.}$$

and therefore
$$\alpha_F - \alpha_E = A_S\alpha_{F_1} + B_S\alpha_{F_2} + C_S\alpha_{F_3} + \ldots - (A_S\alpha_{E_1} + B_S\alpha_{E_2} + C_S\alpha_{F_3} + \ldots)$$

so that
$$\alpha_F = A_S\alpha_{F_1} + B_S\alpha_{F_2} + C_S\alpha_{F_3} + \ldots$$

and hence for the given initial incidence distribution, α_I, the final incidence distribution α_F, and hence the final aerodynamic characteristics, can be obtained. By means of this method the aerodynamic and structural problems are separated and may be considered independently.

*The superposition method has also been developed independently at Handley Page Ltd., but this work remains unpublished.

This method is likely to yield more accurate results for many problems than the other methods mentioned previously, due mainly to the fact that induced aerodynamic effects due to distortion are readily included and no sweeping assumptions need be made about the mode of distortion. Once the calculations have been completed for the arbitrary cases chosen, equilibrium conditions for any combination of q and M are quite easily obtained. As with other methods, some difficulty is encountered if the form of the aerodynamic loading varies appreciably with Mach number (*see* Section 5.2).

2.2. *Effects of wing distortion on the wing lift and pitching moment contributions*

2.2.1. WING WITH ZERO BUILT-IN TWIST AND CAMBER; DISTORTIONS DUE TO WING WEIGHT NEGLECTED

If the incidence of the wing α is defined as the angle between the chord line of the wing and the direction of flight, measured at the wing root, then

$$C_{Lw} = \text{wing lift coefficient} = \left(\frac{\partial C_{Law}}{\partial \alpha}\right)_M \alpha = A\alpha \qquad . \quad . \quad . \quad (1)$$

where C_{Law} = wing lift coefficient of flexible wing due to (root) incidence α

$$A = \text{wing lift curve slope (following Ref. 1)} = \left(\frac{\partial C_{Law}}{\partial \alpha}\right)_M.$$

It is possible to find $(\partial C_{Law}/\partial \alpha)_M$ using the superposition method as already described (*see* also Ref. 3).

Similarly, taking moments about the rigid wing aerodynamic centre,

$$C_{mw} = \left(\frac{\partial C_{maw}}{\partial \alpha}\right)_M \alpha \qquad . \quad . \quad . \quad . \quad (2)$$

where C_{maw} is the pitching moment coefficient corresponding to C_{Law} and may also be found by the superposition method. For the "rigid wing" C_{mw} as defined is of course zero, but with the flexible wing there is a pitching moment about the rigid wing mean aerodynamic centre, H_{0R}, which is proportional to incidence, *i.e.* there is a movement of the wing aerodynamic centre given by

$$\Delta H_0 = -\frac{\partial C_{maw}}{\partial \alpha} \Big/ \frac{\partial C_{Law}}{\partial \alpha} \qquad . \quad . \quad . \quad . \quad . \quad (3)$$

giving the mean aerodynamic centre of the flexible wing

$$H_0 = H_{0R} + \Delta H_0.$$

The wing pitching moment coefficient about the aircraft c.g. is then

$$C_{\text{mw c.g.}} = A\alpha(h - H_0) \quad . \quad . \quad (4)$$

and the wing pitching moment coefficient about the new mean aerodynamic centre H_0 is zero,

$$i.e. \qquad (C_{m_0})_{\text{wing}} = 0.$$

2.2.2. WING WITH BUILT-IN TWIST AND CAMBER; DISTORTIONS DUE TO WING WEIGHT NEGLECTED

When the undistorted wing has twist or camber it is possible to consider the effects of incidence, twist and camber separately. Applying the principle of superposition as in Ref. 3,

$$C_{\text{Lw}} = \left(\frac{\partial C_{\text{Law}}}{\partial \alpha}\right)\alpha + C_{\text{Lcw}} + C_{\text{Ltw}}$$

$$= A\alpha + C_{\text{Lw}_0} \quad . \quad . \quad . \quad . \quad . \quad . \quad . \quad (5)$$

where α = root incidence as defined in Section 2.2.1

C_{Law} = lift coefficient due to root incidence α on wing with zero built-in twist and no built-in camber

C_{Lcw} = lift coefficient on wing with zero root incidence and zero built-in twist, but with built-in camber

C_{Ltw} = lift coefficient on wing with zero root incidence and zero built-in camber but with built-in twist

$C_{\text{Lw}_0} = C_{\text{Lwc}} + C_{\text{Ltw}}$

$A = \left(\frac{\partial C_{\text{Law}}}{\partial \alpha}\right)_M$ (as before).

C_{Lcw} and C_{Ltw} may be found using the superposition method and are functions of speed and Mach number.

Thus $$\left(\frac{\partial C_{\text{Lw}}}{\partial \alpha}\right)_M = \left(\frac{\partial C_{\text{Law}}}{\partial \alpha}\right)_M = A \text{ as in Section 2.2.1.}$$

Also, the pitching moment coefficient about the rigid wing mean aerodynamic centre is

$$C_{\text{mw}} = \left(\frac{\partial C_{\text{maw}}}{\partial \alpha}\right)\alpha + C_{\text{mcw}} + C_{\text{mtw}},$$

where C_{maw}, C_{mcw}, C_{mtw} are the pitching moment coefficients corresponding to C_{Law}, C_{Lcw}, C_{Ltw}, and hence

$$\left(\frac{\partial C_{\text{mw}}}{\partial \alpha}\right)_M = \left(\frac{\partial C_{\text{maw}}}{\partial \alpha}\right)_M.$$

i.e. $$\Delta H_0 = -\frac{\partial C_{maw}}{\partial \alpha} \Big/ \frac{\partial C_{Law}}{\partial \alpha}$$ as in Section 2.2.1.

Then $$C_{mw\,c.g.} = \frac{\partial C_{maw}}{\partial \alpha}\alpha + C_{mw_0} + (h - H_{0R})C_{Lw},$$

where $$C_{mw_0} = C_{mcw} + C_{mtw},$$

i.e. $$C_{mw\,c.g.} = A\alpha\Delta H_0 + C_{mw_0} + (h - H_{0R})(A\alpha + C_{Lw_0})$$

$$= (C_{m_0})_{wing} + A\alpha(h - H_0), \quad . \quad . \quad . \quad . \quad (6)$$

where $$(C_{m_0})_{wing} = C_{mw_0} + (h - H_{0R})C_{Lw_0}$$

and $$H_0 = H_{0R} + \Delta H_0.$$

This expression for $C_{mw\,c.g.}$ is different from that normally used in that $C_{Lw} \neq A\alpha$. It will be seen, however, that it is convenient to express quantities in the form $X + Y\alpha$, where X and Y are functions of speed and Mach number but not of incidence.

2.2.3. WING WITH BUILT-IN TWIST AND CAMBER WHEN DISTORTIONS DUE TO WING WEIGHT ARE INCLUDED

Following the method adopted in Section 2.2.2,

$$C_{Lw} = A^0\alpha + C_{Lw_0}{}^0 + n\left(\frac{\partial C_{Lnw}}{\partial n}\right)_M \quad . \quad . \quad . \quad . \quad . \quad . \quad (7)$$

where $n - 1 = (1/g) \times$ normal acceleration of aircraft (positive upwards)

i.e. $n = C_L \frac{1}{2}\rho V^2 S/W$, in flight for which the inclination of the flight path to the horizontal is small

C_{Lnw} = lift coefficient on wing with zero root incidence, zero built-in twist and no built-in camber, due to deflection of the wing under its effective weight.

The affix 0 denotes the condition $n = 0$, so that the effects of wing weight are entirely contained in the last term.

As with C_{Lw_0}, and so on, $\partial C_{Lnw}/\partial n$ may be found using the superposition method.

Similarly, taking moments about the rigid wing aerodynamic centre,

$$C_{mw} = \left(\frac{\partial C_{maw}}{\partial \alpha}\right)_M^0 \alpha + C_{mw_0}{}^0 + n\left(\frac{\partial C_{mnw}}{\partial n}\right)_M \quad . \quad . \quad . \quad (8)$$

and about the c.g.,

$$C_{\mathrm{mw\,c.g.}} = \left(\frac{\partial C_{\mathrm{maw}}}{\partial \alpha}\right)_M^0 \alpha + C_{\mathrm{mw_0}}{}^0 + n\left(\frac{\partial C_{\mathrm{maw}}}{\partial n}\right)_M +$$

$$+ (h - H_{0\mathrm{R}})(A^0\alpha + C_{\mathrm{mw_0}}{}^0) + n\left(\frac{\partial C_{\mathrm{Law}}}{\partial n}\right)_M (h - H_{0\mathrm{R}})$$

$$= (C_{\mathrm{m_0}})_{\mathrm{wing}}{}^0 + (h - H_0{}^0) A^0\alpha + (h - H_0{}^n) A_n{}^n. \quad . \quad . \quad . \quad . \quad . \quad (9)$$

where $H_0{}^0 = H_{0\mathrm{R}} + \Delta H^0$, $\Delta H_0{}^0 = -\left(\frac{\partial C_{\mathrm{maw}}}{\partial \alpha} \Big/ \frac{\partial C_{\mathrm{Law}}}{\partial \alpha}\right)^0$

$$A_n = \left(\frac{\partial C_{\mathrm{Law}}}{\partial n}\right)_M, \quad \Delta H_0{}^n = -\left(\frac{\partial C_{\mathrm{maw}}}{\partial n} \Big/ \frac{\partial C_{\mathrm{Law}}}{\partial n}\right)$$

$$H_0{}^n = H_{0\mathrm{R}} + \Delta H_0{}^n.$$

In practice the affix 0 could be dropped from A^0, $C_{\mathrm{Lw_0}}{}^0$, $C_{\mathrm{mw_0}}{}^0$ and $(C_{\mathrm{m_0}})_{\mathrm{wing}}{}^0$ without confusion occurring.

The effect on existing longitudinal stability theory of using these more complicated expressions for C_{Lw}, $C_{\mathrm{mw\,c.g.}}$ is considered in Section 4.

2.3. *Effect of wing distortion on the downwash at the tail*

The incidence of any point on the rigid tailplane is given by

$$\alpha_{\mathrm{T1}} = \alpha + \eta_{\mathrm{T}} - \varepsilon_1$$

where ε_1 = local downwash angle.

Hence, following the method used in dealing with wing distortion,

$$\Delta C_{\mathrm{LT}} = A_{1\alpha}(\alpha + \eta_{\mathrm{T}}) - A_{1\varepsilon}\varepsilon_{\mathrm{R}}$$

due to tailplane incidence,

where $A_{1\alpha} = \partial C_{\mathrm{LT}} / \partial \alpha_{\mathrm{c}}$

α_{c} = root incidence of tailplane with zero wing downwash

$= \alpha + \eta_{\mathrm{T}}$

$A_{1\varepsilon} = \partial C_{\mathrm{LT}} / \partial \varepsilon_{\mathrm{R}}$

ε_{R} = downwash angle at tailplane root.

Values of $A_{1\alpha}$ and $A_{1\varepsilon}$ might then be found using the superposition method*, provided that the spanwise downwash distribution were known.

*This is strictly true only for an all-moving tailplane (*see* Section 3.2).

Then $$\Delta C_{LT} = A_1 (\alpha + \eta_T - \bar{\varepsilon}_R)$$

due to incidence,

where $$\bar{\varepsilon}_R = \varepsilon_R (A_{1\epsilon}/A_{1\alpha})$$

and $$A_1 = A_{1\alpha}.$$

In practice, however, the downwash distribution is not usually known with any accuracy even for the rigid wing, and since it will change slightly with speed due to wing distortion it will not be possible to carry out a single aeroelastic equilibrium calculation for the tailplane applying to all speeds. In view of these difficulties it seems acceptable to use a mean downwash angle, the mean being weighted in favour of the regions of greatest tailplane lift.

Since the downwash is produced by wing lift it is logical to use an expression for the mean downwash angle $\bar{\varepsilon}$ having the same form as the expression for C_{Lw}.

Then $$\bar{\varepsilon} = A^0\alpha \, \dot{\bar{\varepsilon}}_\alpha + \bar{\varepsilon}_0 + A_n n \, \dot{\bar{\varepsilon}}_n = \bar{\varepsilon}_\alpha + \bar{\varepsilon}_0 + \bar{\varepsilon}_n \quad . \quad . \quad . \quad (10)$$

where the lift distribution corresponding to $A^0\alpha$ produces a mean downwash angle $\bar{\varepsilon}_\alpha$, the lift distribution corresponding to C_{Lw0} produces a mean downwash angle $\bar{\varepsilon}_0$, and the lift distribution corresponding to nA_n produces a mean downwash angle $\bar{\varepsilon}_n$.

The value of $\bar{\varepsilon}$ will approximate to the value of $\bar{\varepsilon}_R$ defined, and

$$\bar{\varepsilon} \simeq \bar{\varepsilon}_R = \bar{\varepsilon}_{\alpha R} + \bar{\varepsilon}_{0R} + \bar{\varepsilon}_{nR},$$

so that the use of $\bar{\varepsilon}$ does not necessarily imply an approximation.

Since the lift distributions $A^0\alpha$, and so on, may be obtained by using the superposition method, it is possible to obtain the downwash distributions corresponding to these lift distributions by superposition of the downwash distributions corresponding to the arbitrary lift distributions employed. This can be a somewhat involved process and in practice it may be acceptable to use estimated values of $\dot{\bar{\varepsilon}}_\alpha$, and so on, with semi-empirical corrections for the effects of wing distortion.

The expression given for $\bar{\varepsilon}$ is more complicated than the usual expressions for downwash angle, and the effect of using it in stability theory is considered in Section 4.

3. Fuselage, Control Circuit and Tail Distortion

Distortion of the fuselage, tail and control circuits modifies the tail lift and pitching moment contributions, and also the elevator hinge moment. This has been considered in Ref. 2, where compressibility effects have not been explicitly considered.

Lyon and Ripley[2] write

$$C_{LT} = A_1 \alpha_{T_0} + A_2 \eta + A_3 \beta$$

$$C_H = B_0 + B_1 \alpha_{T_0} + B_2 \eta + B_3 \beta$$

where $\alpha_{T_0} = \alpha + \eta_{T_0} - \bar{\varepsilon}$

η_{T_0} = tail setting angle at zero wind speed ("built-in" tail setting angle)

η, β are control angles equivalent to movements of the pilot's controls (η_p, β_p of Ref. 2) as is η_{T_0} if a "variable incidence" tailplane is used.

Alternatively

$$C_{LT} = A_{1T}\alpha_T + A_2\eta + A_3\beta$$

$$C_H = B_0 + B_{1T}\alpha_T + B_2\eta + B_3\beta$$

where $\alpha_T = \alpha + \eta_T - \bar{\varepsilon}$,

η_T = true (root) tail-setting angle

$A_{1T} = \partial C_{LT}/\partial \alpha_T$

= value of A_1 when fuselage is rigid*,

and likewise $B_{1T} = \partial C_H/\partial \alpha_T$.

3.1. *Effect of fuselage inertia loading*

The expressions already given in Section 3 may be used to include the effects of all distortion under purely aerodynamic loading, the values of A_1, A_2, etc., being modified to take accounts of these effects. If the effect of bending of the fuselage under its own weight is to be included, a slight modification of the expressions for C_{LT} and C_H is necessary.

Suppose application of a (total) normal acceleration of ng produces a net change of $n\partial\alpha_T/\partial n$ in the value of α_T.

Then
$$C_{LT} = A_{1T}\alpha_T{}^0 + nA_{1T}\frac{\partial \alpha_T}{\partial n} + A_2\eta + A_3\beta \quad . \quad . \quad . \quad . \quad . \quad (11)$$

where $\alpha_T{}^0$ = true root tailplane incidence for $n = 0$.

This may be written

$$C_{LT} = C_{LT}{}^0 + nA_{1T}\frac{\partial \alpha_T}{\partial n} \quad . \quad . \quad . \quad . \quad . \quad . \quad . \quad (12)$$

and similarly
$$\left.\begin{aligned} C_H &= C_H{}^0 + nB_{1T}\frac{\partial \alpha_T}{\partial n} \\ &= B_0 + B_1\alpha_{T_0} + nB_{1T}\frac{\partial \alpha_T}{\partial n} + B_2\eta + B_3\beta. \end{aligned}\right\} \quad . \quad . \quad . \quad (13)$$

*This applies to tailplanes of "fixed" incidence—with a "variable incidence" tailplane A_{1T} is the value of A_1 when both fuselage and incidence control circuit are rigid.

If application of ng produces a net change of tail-setting angle $\Delta\eta_T$, we have

$$\Delta\eta_T = \Delta\eta_{Ti} - \frac{A_{1T}\Delta\eta_T qS_T}{F_f},$$

where $\Delta\eta_{Ti}$ = change of η_T due to ng at zero wind speed

$q = \frac{1}{2}\rho V^2$

F_f = fuselage bending stiffness = $\dfrac{\text{load on tail}}{\text{change in } \eta_T}$.

Then
$$\Delta\eta_T = \frac{\Delta\eta_{Ti}}{1 + \dfrac{A_{1T}qS_T}{F_f}}$$

and
$$\frac{\partial\alpha_T}{\partial n} = \frac{\Delta\eta_T}{n} = \frac{\partial\eta_{Ti}}{\partial n}\left(\frac{1}{1 + A_{1T}\dfrac{qS_T}{F_f}}\right) \quad . \quad . \quad . \quad . \quad . \quad . \quad (14)$$

$$\frac{\partial}{\partial\alpha}\left(\frac{\partial\alpha_T}{\partial n}\right) = 0; \quad \frac{\partial}{\partial M}\left(\frac{\partial\alpha_T}{\partial n}\right) = -\frac{\partial\eta_{Ti}}{\partial n}\frac{\left(\dfrac{\partial A_{1T}}{\partial M}q + A_{1T}\dfrac{2q}{M}\right)}{\left(1 + A_{1T}\dfrac{qS_T}{F_f}\right)^2}\left(\frac{S_T}{F_f}\right) \quad . \quad . \quad (15)$$

3.2. *Calculation of A_1, A_2, etc., including distortion effects*

The analysis of Ref. 2 is adopted here but with certain modifications and with the inclusion of compressibility effects.

FUSELAGE DISTORTION (AERODYNAMIC LOADING)

Formulae are deduced in Ref. 2 for the ratios A_1/a_1, A_2/a_2, allowing for fuselage distortion, and these expressions may be applied in general if a_1, a_2, etc., are interpreted as the values of A_1, A_2, etc., when compressibility and all distortion effects except fuselage distortion are included.

TAILPLANE-ELEVATOR DISTORTION

As pointed out in Ref. 2, tailplane distortion and elevator distortion cannot be considered separately, since the two are completely interdependent. For this reason it is not strictly possible to use the superposition method for the estimation of distortion effects on the tailplane-elevator combination. In Ref. 3 a method of treating the "flap-deflection" case is given which uses the superposition method, but this is based on the assumption that the local flap angle is not changed by distortion of the main surface or flap, so that the form of the spanwise load distribution due to the flap deflection remains the same at all speeds. While this assumption may not lead to serious errors when dealing with the wing-aileron combination (although it seems dubious even in this case), it seems likely that it would lead to appreciable

errors if used for a tailplane and elevator. For the treatment of the tailplane and elevator, therefore, the method of "semi-rigid representation" as given in Ref. 2 would seem to be more suitable. If the effects of tab distortion and elevator skin distortion can be neglected (*see* the next paragraph), the effects of compressibility may be introduced (by means of linearised theory corrections) to the "strip" derivatives used. The corrections applied should be those appropriate to the three-dimensional tail surface, so that the overall lift and hinge moment coefficients vary in the correct way although changes in the form of the lift distribution due to compressibility are ignored, as with the superposition method. It is not possible to carry out the calculations in terms of a "compressibility-distortion" parameter such as qA_R (used in the superposition method), since the aerodynamic coefficients a_1, a_2, a_3, b_1, b_2, b_3 are not all modified by compressibility in the same way. It is, therefore, strictly necessary to carry out calculations for each combination of q and M within the required range.

ELEVATOR TAB AND TAB CIRCUIT DISTORTION

In Ref. 2 it is shown that, if C_1 and C_2 are small (as they usually are), A_1, A_2, B_1 and B_2 are almost unaffected by tab distortion and A_3, B_3 and C_3 are modified by the factor $K/(K-C_3')$ where C_3' is the value of C_3 when tab distortion is ignored and K is proportional to $(1/q)\times$ tab stiffness. On this basis the elevator angle to trim, and hence the stick fixed static margin K_n, is not appreciably changed, while the stick free static margin K_n' is slightly changed. Similarly the stick fixed manoeuvre margin H_m is almost unaffected, while the stick free manoeuvre margin H_m' is slightly changed. If the tab circuit can be designed so that K is large compared with C_3' for all q, tab distortion effects are then obviously negligible. If this cannot be done, tab distortion effects are easily included by applying the factor given to A_3, B_3, C_3, on the reasonable assumption that the secondary effects of tab distortion on elevator and tailplane distortion are negligible.

If power operated controls are fitted this type of distortion does not, of course, arise.

ELEVATOR SKIN DISTORTION

The effect of elevator skin distortion is also considered in Ref. 2, where it is shown that distortion of the elevator skin, caused by pressure differences between the inside and outside of the control surface, can modify A_1, A_2 and A_3 slightly and B_1, B_2 and B_3 to quite a large extent. The treatment is approximate, since skin distortion of a fabric or metal covered surface is not proportional to load.

The curves in Ref. 2 of panel deflection against load show that, for an unstiffened metal skin, the rate of change of deflection with load is small once the small initial deflection required to take any load has been exceeded. If the skin is applied with initial tension (as is normal practice) this small initial deflection can be minimised. In view of this it seems reasonable to ignore the effects of elevator skin distortion for design purposes on the grounds that it should be possible to design the elevator so as to keep the skin distortion and its effects small enough to be negligible.

The main effect of any skin distortion is to decrease the stick free static and manoeuvre margins, so that if powered controls are used the effects are even less serious than with manually operated controls.

ELEVATOR CONTROL CIRCUIT DISTORTION

The treatment of elevator control circuit distortion given in Ref. 2 can be applied in general if a_1, a_2, etc., are interpreted as the values of A_1, A_2, etc., when compressibility and all distortion effects except control circuit distortion are included.

4. Modifications to existing longitudinal stability theory

When the new expressions of Sections 2 and 3 for C_{Lw}, C_{mw}, and so on, are used, we have, in general,

$$C_L = A^0\alpha + C_{Lw0} + nA_n + \frac{S_T}{S}\left\{A_1(\alpha - A^0\dot{\bar{\varepsilon}}_a\alpha - \bar{\varepsilon}_0 - A_n n\dot{\bar{\varepsilon}}_n + \eta_{T0}) + nA_{1T}\frac{\partial\alpha_T}{\partial n} + \right.$$
$$\left. + A_2\eta + A_3\beta\right\} \quad . \quad . \quad . \quad . \quad . \quad (16)$$

$$C_m = C_{mf} + (C_{m0})_{wing} + (h - H_0^0)A^0\alpha + (h - H_0^n)A_n n -$$
$$- \overline{V}_{c.g.}\left\{A_1(\alpha - A^0\dot{\bar{\varepsilon}}_a\alpha - \bar{\varepsilon}_0 - A_n n\dot{\bar{\varepsilon}}_n + \eta_{T0}) + nA_{1T}\frac{\partial\alpha_T}{\partial n} + A_2\eta + A_3\beta\right\} \quad (17)$$

where $C_{mf} = C_m$ contribution from fuselage

$\overline{V}_{c.g.} = S_T l_T / S\bar{c}$

l_T = distance from tailplane mean aerodynamic centre to aircraft c.g.

The other new symbols are defined in Sections 2 and 3.

4.1. *Static margin*

In Ref. 1,
$$K_n = -\left(\frac{dC_m}{dC_R}\right)_{d\eta/dC_R = 0}$$

$$K_n' = -\left(\frac{dC_m}{dC_R}\right)_{C_H = 0}$$

where $C_R\rho V^2 = \text{constant} = W/(\tfrac{1}{2}S)$

i.e. in level flight $n = 1 = \text{constant}$.

Following Ref. 1 the expression for C_m can be modified by the introduction of a new tail volume coefficient V_T. Thus, when $n = 1$,

$$C_m = C_{mf} + (C_{m0})_{wing} + (h - H_0^0)(C_L - C_{Lw0} - A_n) + (h - H_0^n)A_n -$$
$$- V_T\left\{A_1\left[\left(\frac{1}{A^0} - \varepsilon_a\right)(C_L - C_{Lw0} - A_n) - \bar{\varepsilon}_0 - A_n\dot{\bar{\varepsilon}}_n + \eta_{T0}\right] + A_{1T}\frac{\partial\alpha_T}{\partial n} + A_2\eta + A_3\beta\right\}$$
$$. \quad . \quad . \quad . \quad . \quad . \quad . \quad . \quad . \quad (18)$$

where $$V_T = \frac{\overline{V}_{a.c.}}{1 + A_1 \frac{S_T}{S}\left(\frac{1}{A^0} - \dot{\bar{\varepsilon}}_a\right)} = \frac{\overline{V}_{a.c.}}{1+F}$$

and $$\overline{V}_{a.c.} = \overline{V}_{c.g.} + (h - H_0{}^0)\frac{S_T}{S}.$$

Differentiating equation (18) with respect to C_R and making use of the fact that $d\eta/dC_R = 0$, gives, as in Ref. 1,

$$K_n = -V_T A_2 (d\eta/dC_R)_{C_m = 0}.$$

Similarly for the stick free case ($n=1$):—

$$C_m = C_{mf} + (C_{m0})_{wing} + (h - H_0{}^0)(C_L - C_{Lw0} - A_n) + (h - H_0{}^n) A_n -$$

$$- \overline{V}_T \left\{ \overline{A}_1 \left[\left(\frac{1}{A^0} - \dot{\bar{\varepsilon}}_a \right)(C_L - C_{Lw0} - A_n) - \bar{\varepsilon}_0 - A_n \dot{\bar{\varepsilon}}_n + \eta_{T0} \right] + \overline{A}_{1T} \frac{\partial \alpha_T}{\partial n} + \overline{A}_3 \beta - \frac{A_2}{B_2} B_0 \right\} \quad . \quad . \quad . \quad . \quad (19)$$

where $$\overline{V}_T = \frac{\overline{V}_{a.c.}}{1 + \overline{A}_1 \frac{S_T}{S}\left(\frac{1}{A^0} - \dot{\bar{\varepsilon}}_a\right)} = \frac{\overline{V}_{a.c.}}{1+\overline{F}}$$

$$\overline{A}_1 = A_1 - \frac{A_2}{B_2} B_1$$

$$\overline{A}_{1T} = A_{1T} - \frac{A_2}{B_2} B_{1T}$$

$$\overline{A}_3 = A_3 - \frac{A_2}{B_2} B_3.$$

This yields similarly, $K_n' = -\overline{V}_T \overline{A}_3 \left(\frac{d\beta}{dC_R}\right)_{\substack{C_H = 0 \\ C_m = 0}}$

as in Ref. 1.

4.2. *Manoeuvre margin*

The manoeuvre margin, H_m, is given by[1]

$$H_m = -\left(\frac{\partial C_m}{\partial C_L}\right)_M - \frac{l}{\bar{c}} \frac{m_\eta}{\mu_1}.$$

The second term is usually fairly small and decreases with increase of altitude, so that the value of the manoeuvre margin is greatly influenced by the value of $(\partial C_m/\partial C_L)_M$*.

*Note that l = distance between tail and no-tail aerodynamic centres $\neq l_T$.

When n is variable,

$$C_m = C_{mf} + (C_{m0})_{wing} + (h - H_0^0)(C_L - C_{Lw0} - A_n n) + (h - H_0^n) A_n \dot{n} -$$

$$- V_T \left\{ A_1 \left[\left(\frac{1}{A^0} - \dot{\bar{\varepsilon}}_a \right) (C_L - C_{Lw0} - A_n n) - \bar{\varepsilon}_0 - A_n \dot{\bar{\varepsilon}}_n n + \eta_{T0} \right] + \right.$$

$$\left. + A_{1T} \frac{\partial \alpha_T}{\partial n} n + A_2 \eta + A_3 \beta \right\} . \quad . \quad . \quad . \quad (20)$$

Differentiating (20) with respect to C_L, with stick fixed (*i.e.* η and β constant), gives

$$\left(\frac{\partial C_m}{\partial C_L} \right)_M = \left(\frac{\partial C_{mf}}{\partial C_L} \right)_M + (h - H_0^0) \left(1 - A_n \left(\frac{\partial n}{\partial C_L} \right)_M \right) + (h - H_0^n) A_n \left(\frac{\partial n}{\partial C_L} \right)_M -$$

$$- V_T \left\{ A_1 \left(\frac{1}{A^0} - \dot{\bar{\varepsilon}}_a \right) \left(1 - A_n \left(\frac{\partial n}{\partial C_L} \right)_M \right) + A_{1T} \frac{\partial \alpha_T}{\partial n} \left(\frac{\partial n}{\partial C_L} \right)_M \right\} . \quad (21)$$

$$\text{If} \quad C_L = \frac{nW}{\frac{1}{2}\rho V^2 S} \quad \text{and} \quad C_{L0} = \frac{W}{\frac{1}{2}\rho V^2 S}$$

$$C_L = n C_{L0} \quad \text{and} \left(\frac{\partial n}{\partial C_L} \right)_M = \frac{1}{C_{L\eta}} . \quad . \quad . \quad . \quad (22)$$

With stick free,

$$\left(\frac{\partial C_m}{\partial C_L} \right)_M = \left(\frac{\partial C_{mf}}{\partial C_L} \right)_M + (h - H_0^0) \left(1 - A_n \left(\frac{\partial n}{\partial C_L} \right)_M \right) + (h - H_0^n) A_n \left(\frac{\partial n}{\partial C_L} \right)_M -$$

$$- \overline{V}_T \left\{ \overline{A}_1 \left(\frac{1}{A^0} - \dot{\bar{\varepsilon}}_a \right) \left(1 - A_n \left(\frac{\partial n}{\partial C_L} \right)_M \right) + \overline{A}_{1T} \frac{\partial \alpha_T}{\partial n} \left(\frac{\partial n}{\partial C_L} \right)_M \right\} . \quad (23)$$

The tail contribution to $\left(\frac{m_q}{\mu_1} \frac{l}{\bar{c}} \right)$ is, approximately,

$$- \frac{V_T A_1}{2\mu_1} \quad \text{stick fixed}$$

$$\text{and} \quad - \frac{\overline{V}_T \overline{A}_1}{2\mu_1} \quad \text{stick free.}$$

The wing contribution to m_q is not necessarily negligible if the wing is swept.

In the manoeuvre margin theory it is implicitly assumed that m_q is not appreciably changed by movement of the c.g. Thus, in deriving these expressions for the tail contribution to m_q, the tail moment arm used is the distance between the tail and "no-tail" aerodynamic centres. This is not strictly correct since the angular velocity q is about the c.g.

When the tailplane is swept, its centre section and tips may be fairly large distances forward and aft of the mean tail aerodynamic centre, so that more accurately

$$m_{q\,\text{tail}} = -\frac{V_T A_1}{\mu} + m_{qT},$$

where m_{qT} = contribution to m_q due to rotation of tailplane about its mean aerodynamic centre.

In general, however, m_{qT} will be small.

4.3. *Dynamic stability—quasi-static theory*

Dynamic stability and its relation to the static and manoeuvre margins is discussed in Ref. 1, where it is shown that the slow divergence associated with $K_n < 0$ is less serious than the rapid divergence or rapid unstable oscillation corresponding to $H_m < 0$. This means that the value of $(\partial C_m/\partial C_L)_M$ is of greater importance than the value of dC_m/dC_L. In this section the effects of distortion on the quasi-static longitudinal stability derivatives are discussed.

If distortion effects are included on a quasi-static basis, the usual small-displacement equations of motion can be used for the flexible aircraft, but the derivatives have to be suitably modified.

Ignoring the thrust contributions[1],

$$\left.\begin{aligned} x_u &= -C_D - \frac{M}{2}\left(\frac{\partial C_D}{\partial M}\right)_s; & z_u &= -C_L - \frac{M}{2}\left(\frac{\partial C_L}{\partial M}\right)_\alpha \\ m_u &= \frac{M}{2}\frac{\bar{c}}{l}\left(\frac{\partial C_m}{\partial M}\right)_s; & x_w &= \tfrac{1}{2}\left(C_L - \left(\frac{\partial C_D}{\partial \alpha}\right)_M\right) \\ z_w &= -\tfrac{1}{2}\left[\left(\frac{\partial C_L}{\partial \alpha}\right)_M + C_D\right]; & m_w &= \tfrac{1}{2}\frac{\bar{c}}{l}\left(\frac{\partial C_m}{\partial \alpha}\right)_M \end{aligned}\right\} \quad . \quad (24)$$

The largest contributions to m_q and $m_{dw/dt}$ are normally from the tail, and*

$$\mu_1 m_{dw/dt\,(\text{tail})} \simeq -\frac{A^0}{2(1+F)}\frac{S_T}{S} A_1 \dot{\bar{\varepsilon}}_\alpha, \quad m_{q\,(\text{tail})} \simeq -\frac{A_1}{2(1+F)}\frac{S_T}{S}. \quad . \quad (25)$$

These expressions are approximate only and correspond to those given in Ref. 1. The wing contribution to $m_{dw/dt}$ is normally very small at subsonic sub-critical speeds, but the wing contribution to m_q may be appreciable for a swept wing. An estimate of m_q (wing) may be obtained by the method described in Appendix III.

The derivatives x_q and z_q occur in the stability equations divided by μ_1 and are then normally small enough to be neglected.

*For the stick free case, A_1 is replaced by $\bar{A}_1$.

If the distortions of the aircraft components are small, it seems reasonable to ignore distortion effects on the drag derivatives, so that C_D, $(\partial C_D/\partial\alpha)_M$ and $(\partial C_D/\partial M)_\alpha$ may be estimated for the rigid aircraft. It remains to determine $(\partial C_L/\partial\alpha)_M$, $(\partial C_L/\partial M)_\alpha$, $(\partial C_m/\partial\alpha)_M$ and $(\partial C_m/\partial M)_\alpha$ in terms of A^0, A_1, $H_0{}^0$, etc.

Differentiating the expression for C_L given in equation (16),

$$\left(\frac{\partial C_L}{\partial\alpha}\right)_M = A^0 + A_n\left(\frac{\partial n}{\partial\alpha}\right)_M + \frac{S_T}{S}\left\{A_1\left[1 - A^0\,\dot{\bar{\varepsilon}}_a - A_n\left(\frac{\partial n}{\partial\alpha}\right)_M\dot{\bar{\varepsilon}}_n\right] + \right.$$

$$\left. + \left(\frac{\partial n}{\partial\alpha}\right)_M A_{1T}\frac{\partial\alpha_T}{\partial n} + A_2\left(\frac{\partial\eta}{\partial\alpha}\right)_M\right\},$$

assuming $\left(\frac{\partial\eta_{T0}}{\partial\alpha}\right)_M = \left(\frac{\partial\beta}{\partial\alpha}\right)_M = 0$

$$\left(\frac{\partial n}{\partial\alpha}\right)_M = \left(\frac{\partial n}{\partial C_L}\right)_M\left(\frac{\partial C_L}{\partial\alpha}\right)_M = \frac{1}{C_{L0}}\left(\frac{\partial C_L}{\partial\alpha}\right)_M \quad . \quad (26)$$

Therefore

$$\left(\frac{\partial C_L}{\partial\alpha}\right)_M = \frac{A^0 + \frac{S_T}{S}\left\{A_1(1 - A^0\,\dot{\bar{\varepsilon}}_a) + A_2\left(\frac{\partial\eta}{\partial\alpha}\right)_M\right\}}{1 - \frac{A_n}{C_{L0}} + \frac{S_T}{S}\frac{1}{C_{L0}}\left\{A_1A_n\,\dot{\bar{\varepsilon}}_n - A_{1T}\frac{\partial\alpha_T}{\partial n}\right\}} \quad . \quad (27)$$

With stick fixed $\left(\frac{\partial\eta}{\partial\alpha}\right)_M = 0$, so that

$$\left(\frac{\partial C_L}{\partial\alpha}\right)_M \text{stick fixed} = \frac{A^0 + \frac{S_T}{S}A_1(1 - A^0\,\dot{\bar{\varepsilon}}_a)}{1 - \frac{A_n}{C_{L0}} + \frac{S_T}{S}\frac{1}{C_{L0}}\left\{A_1A_n\,\dot{\bar{\varepsilon}}_n - A_{1T}\frac{\partial\alpha_T}{\partial n}\right\}} \quad . \quad (28)$$

With stick free, using equation (13),

$$\left(\frac{\partial\eta}{\partial\alpha}\right)_M = -\frac{B_1}{B_2}(1 - A^0\,\dot{\bar{\varepsilon}}_a) + \left(\frac{\partial n}{\partial\alpha}\right)_M\left(\frac{B_1}{B_2}A_n\,\dot{\bar{\varepsilon}}_n - \frac{B_{1T}}{B_2}\frac{\partial\alpha_T}{\partial n}\right)$$

$$= -\frac{B_1}{B_2}(1 - A^0\,\dot{\bar{\varepsilon}}_a) + \frac{1}{C_{L0}}\left(\frac{\partial C_L}{\partial\alpha}\right)_M\left(\frac{B_1}{B_2}A_n\,\dot{\bar{\varepsilon}}_n - \frac{B_{1T}}{B_2}\frac{\partial\alpha_T}{\partial n}\right),$$

giving

$$\left(\frac{\partial C_L}{\partial\alpha}\right)_M \text{stick free} = \frac{A^0 + \frac{S_T}{S}\overline{A}_1(1 - A^0\,\dot{\bar{\varepsilon}}_a)}{1 - \frac{A_n}{C_{L0}} + \frac{S_T}{S}\frac{1}{C_{L0}}\left(\overline{A}_1A_n\,\dot{\bar{\varepsilon}}_n - \overline{A}_{1T}\frac{\partial\alpha_T}{\partial n}\right)} \quad . \quad (29)$$

Similarly

$$\left(\frac{\partial C_L}{\partial M}\right)_s = \alpha\frac{\partial A^0}{\partial M} + \frac{\partial C_{Lw0}}{\partial M} + \left(\frac{\partial n}{\partial M}\right)_s A_n + n\frac{\partial A_n}{\partial M} +$$

$$+ \frac{S_T}{S}\left\{\frac{\partial A_1}{\partial M}\left(\alpha - A^0\dot{\bar{\varepsilon}}_a\alpha - \bar{\varepsilon}_0 - A_n n\dot{\bar{\varepsilon}}_n + \eta_{T0}\right) +\right.$$

$$+ A_1\left[-\alpha\left(\frac{\partial A^0}{\partial M}\dot{\bar{\varepsilon}}_a + A^0\frac{\partial\dot{\bar{\varepsilon}}_a}{\partial M}\right) - \frac{\partial\bar{\varepsilon}_0}{\partial M} - \frac{\partial A_n}{\partial M}n\dot{\bar{\varepsilon}}_n - A_n\left(\dot{\bar{\varepsilon}}_n\left(\frac{\partial n}{\partial M}\right)_s + n\frac{\partial\dot{\bar{\varepsilon}}_n}{\partial M}\right)\right] +$$

$$\left. + A_{1T}\frac{\partial\alpha_T}{\partial n}\left(\frac{\partial n}{\partial M}\right)_s + nA_{1T}\frac{\partial}{\partial M}\left(\frac{\partial\alpha_T}{\partial n}\right) + n\frac{\partial\alpha_T}{\partial n}\frac{\partial A_{1T}}{\partial M} + \frac{\partial A_2}{\partial M}\eta + A_2\left(\frac{\partial\eta}{\partial M}\right)_s + \frac{\partial A_3}{\partial M}\beta\right\}$$

assuming $\left(\dfrac{\partial\beta}{\partial M}\right)_s = 0.$

Since $$n = \frac{C_L}{C_{L0}}\ ,\ \left(\frac{\partial n}{\partial M}\right)_s = \frac{1}{C_{L0}}\left(\frac{\partial C_L}{\partial M}\right)_s \quad . \quad . \quad . \quad . \quad (30)$$

and initially $n = 1$.

With stick fixed $\left(\dfrac{\partial\eta}{\partial M}\right)_s = 0$, so that finally

$$\left(\frac{\partial C_L}{\partial M}\right)_s \text{ stick fixed} = \frac{\left[\begin{array}{l}\alpha\dfrac{\partial A^0}{\partial M} + \dfrac{\partial C_{Lw0}}{\partial M} + \dfrac{\partial A_n}{\partial M} + \dfrac{S_T}{S}\left\{\dfrac{\partial A_1}{\partial M}\left(\alpha - A^0\dot{\bar{\varepsilon}}_a\alpha - \bar{\varepsilon}_0 - A_n\dot{\bar{\varepsilon}}_n + \eta_{T0}\right) +\right.\\ + A_1\left[-\alpha\left(\dfrac{\partial A^0}{\partial M}\dot{\bar{\varepsilon}}_a + A^0\dfrac{\partial\dot{\bar{\varepsilon}}_a}{\partial M}\right) - \dfrac{\partial\bar{\varepsilon}_0}{\partial M} - \dfrac{\partial A_n}{\partial M}\dot{\bar{\varepsilon}}_n - A_n\dfrac{\partial\dot{\bar{\varepsilon}}_n}{\partial M}\right] +\\ \left. + \dfrac{\partial\alpha_T}{\partial n}\dfrac{\partial A_{1T}}{\partial M} + A_{1T}\dfrac{\partial}{\partial M}\left(\dfrac{\partial\alpha_T}{\partial n}\right) + \dfrac{\partial A_2}{\partial M}\eta + \dfrac{\partial A_3}{\partial M}\beta\right\}\end{array}\right]}{1 - \dfrac{A_n}{C_{L0}} + \dfrac{S_T}{S}\dfrac{1}{C_{L0}}\left(A_1A_n\dot{\bar{\varepsilon}}_n - A_{1T}\dfrac{\partial\alpha_T}{\partial n}\right)}$$

. . . . (31)

With stick free, it can be shown that, using equation (13),

$$\left(\frac{\partial\eta}{\partial M}\right)_s = -\frac{1}{B_2}\frac{\partial B_2}{\partial M}\eta - \frac{1}{B_2}\left\{\frac{\partial B_0}{\partial M} + \frac{\partial B_1}{\partial M}(\alpha + \eta_{T0} - A^0\dot{\bar{\varepsilon}}_a\alpha - \bar{\varepsilon}_0 - A_n\dot{\bar{\varepsilon}}_n) +\right.$$

$$+ B_1\left(-\alpha\left[\frac{\partial A^0}{\partial M}\dot{\bar{\varepsilon}}_a + A^0\frac{\partial\dot{\bar{\varepsilon}}_a}{\partial M}\right] - \frac{\partial\bar{\varepsilon}_0}{\partial M} - A_n\frac{\partial\dot{\bar{\varepsilon}}_n}{\partial M} - \frac{\partial A_n}{\partial M}\dot{\bar{\varepsilon}}_n\right) + B_{1T}\frac{\partial}{\partial M}\left(\frac{\partial\alpha_T}{\partial n}\right) +$$

$$\left. + \frac{\partial B_{1T}}{\partial M}\frac{\partial\alpha_T}{\partial n} + \beta\frac{\partial B_3}{\partial M}\right\} + \frac{1}{C_{L0}}\left(\frac{\partial C_L}{\partial M}\right)_s\left(B_1\frac{A_n}{B_2}\dot{\bar{\varepsilon}}_n - \frac{B_{1T}}{B_2}\frac{\partial\alpha_T}{\partial n}\right) \quad . \quad . \quad (32)$$

and hence finally

$$\left(\frac{\partial C_L}{\partial M}\right)_a \text{ stick free} = \frac{\left[\begin{array}{l} \alpha\frac{\partial A^0}{\partial M} + \frac{\partial C_{Lw0}}{\partial M} + \frac{\partial A_n}{\partial M} + \frac{S_T}{S}\left\{\frac{\partial \bar{A}_1}{\partial M}\left(\alpha + \eta_{T0} - A^0\dot{\bar{\varepsilon}}_a\alpha - \bar{\varepsilon}_0 - A_n\dot{\bar{\varepsilon}}_n\right) + \right. \\ + \bar{A}_1\left(-\alpha\left[\frac{\partial A^0}{\partial M}\dot{\bar{\varepsilon}}_a + A^0\frac{\partial \dot{\bar{\varepsilon}}_a}{\partial M}\right] - \frac{\partial \bar{\varepsilon}_0}{\partial M} - \frac{\partial A_n}{\partial M}\dot{\bar{\varepsilon}}_n - A_n\frac{\partial \dot{\bar{\varepsilon}}_n}{\partial M}\right) + \\ \left. + \frac{\partial \alpha_T}{\partial n}\frac{\partial \bar{A}_{1T}}{\partial M} + \bar{A}_{1T}\frac{\partial}{\partial M}\left(\frac{\partial \alpha_T}{\partial n}\right) + \frac{\partial \bar{A}_2}{\partial M}\eta + \frac{\partial \bar{A}_3}{\partial M}\beta - \frac{A_2}{B_2}\frac{\partial B_0}{\partial M}\right\} \end{array}\right]}{1 - \frac{A_n}{C_{L0}} + \frac{S_T}{S}\frac{1}{C_{L0}}\left(\bar{A}_1 A_n\dot{\bar{\varepsilon}}_n + \bar{A}_{1T}\frac{\partial \alpha_T}{\partial n}\right)} \quad . \quad . \quad . \quad (33)$$

where $$\frac{\partial \bar{A}_1}{\partial M} = \frac{\partial A_1}{\partial M} - \frac{A_2}{B_2}\frac{\partial B_1}{\partial M} \neq \frac{\partial \bar{A}_1}{\partial M}, \quad \frac{\partial \bar{A}_{1T}}{\partial M} = \frac{\partial A_{1T}}{\partial M} - \frac{A_2}{B_2}\frac{\partial B_{1T}}{\partial M} \neq \frac{\partial \bar{A}_{1T}}{\partial M}$$

$$\frac{\partial \bar{A}_2}{\partial M} = \frac{\partial A_2}{\partial M} - \frac{A_2}{B_2}\frac{\partial B_2}{\partial M} \neq \frac{\partial \bar{A}_2}{\partial M}, \quad \frac{\partial \bar{A}_3}{\partial M} = \frac{\partial A_3}{\partial M} - \frac{A_2}{B_2}\frac{\partial B_3}{\partial M} \neq \frac{\partial \bar{A}_3}{\partial M}.$$

Similarly

$$\left(\frac{\partial C_m}{\partial \alpha}\right)_M \text{ stick fixed} = \left(\frac{\partial C_{mf}}{\partial \alpha}\right)_M + (h - H_0^0)A^0 - \bar{V}_{c.g.}A_1(1 - A^0\dot{\bar{\varepsilon}}_a) +$$

$$+ \frac{1}{C_{L0}}\left(\frac{\partial C_L}{\partial \alpha}\right)_M\left\{(h - H_0^n)A_n + \bar{V}_{c.g.}\left[A_1 A_n\dot{\bar{\varepsilon}}_n - A_{1T}\frac{\partial \alpha_T}{\partial n}\right]\right\} \quad . \quad . \quad (34)$$

and

$$\left(\frac{\partial C_m}{\partial \alpha}\right)_M \text{ stick free} = \left(\frac{\partial C_{mf}}{\partial \alpha}\right)_M + (h - H_0^0)A^0 - \bar{V}_{c.g.}\bar{A}_1(1 - A^0\dot{\bar{\varepsilon}}_a) +$$

$$+ \frac{1}{C_{L0}}\left(\frac{\partial C_L}{\partial \alpha}\right)_M\left\{(h - H_0^n)A_n + \bar{V}_{c.g.}\left[\bar{A}_1 A_n\dot{\bar{\varepsilon}}_n - \bar{A}_{1T}\frac{\partial \alpha_T}{\partial n}\right]\right\} \quad . \quad . \quad (35)$$

Also

$$\left(\frac{\partial C_m}{\partial M}\right)_a \text{ stick fixed} = \left(\frac{\partial C_{mf}}{\partial M}\right)_a + \frac{\partial (C_{m0})_{wing}}{\partial M} + \alpha\left\{(h - H_0^0)\frac{\partial A^0}{\partial M} - A^0\frac{\partial H_0^0}{\partial M}\right\} +$$

$$+ (h - H_0^n)\frac{\partial A_n}{\partial M} - A_n\frac{\partial H_0^n}{\partial M} - \bar{V}_{c.g.}\left\{\frac{\partial A_1}{\partial M}(\alpha - A^0\dot{\bar{\varepsilon}}_a\alpha - \bar{\varepsilon}_0 - A_n\dot{\bar{\varepsilon}}_n + \eta_{T0}) +\right.$$

$$+ A_1\left[-\alpha\left(\frac{\partial A^0}{\partial M}\dot{\bar{\varepsilon}}_a + A^0\frac{\partial \dot{\bar{\varepsilon}}_a}{\partial M}\right) - \frac{\partial \bar{\varepsilon}_0}{\partial M} - \frac{\partial A_n}{\partial M}\dot{\bar{\varepsilon}}_n - A_n\frac{\partial \dot{\bar{\varepsilon}}_n}{\partial M}\right] +$$

$$\left. + \frac{\partial A_{1T}}{\partial M}\frac{\partial \alpha_T}{\partial n} + A_{1T}\frac{\partial}{\partial M}\left(\frac{\partial \alpha_T}{\partial n}\right) + \eta\frac{\partial A_2}{\partial M} + \beta\frac{\partial A_3}{\partial M}\right\} +$$

$$+ \frac{1}{C_{L0}}\left(\frac{\partial C_L}{\partial M}\right)_a\left\{A_n(h - H_0^n) + \bar{V}_{c.g.}\left[A_n\dot{\bar{\varepsilon}}_n A_1 + A_{1T}\frac{\partial \alpha_T}{\partial n}\right]\right\}. \quad . \quad (36)$$

$$\left(\frac{\partial C_m}{\partial M}\right)_{\text{stick free}} = \left(\frac{\partial C_{mf}}{\partial M}\right)_{\alpha} + \frac{\partial (C_{m0})_{\text{wing}}}{\partial M} + \alpha \left\{ (h - H_0^0) \frac{\partial A^0}{\partial M} - A^0 \frac{\partial H_0^0}{\partial M} \right\} +$$

$$+ (h - H_0^n) \frac{\partial A_n}{\partial M} - A_n \frac{\partial H_0^n}{\partial M} - \overline{V}_{c.g.} \left\{ \frac{\partial \overline{A_1}}{\partial M} \left(\alpha - A^0 \dot{\bar{\varepsilon}}_\alpha \alpha - \bar{\varepsilon}_0 - A_n \dot{\bar{\varepsilon}}_n + \eta_{T0} \right) + \right.$$

$$+ \overline{A}_1 \left[-\alpha \left(\frac{\partial A^0}{\partial M} \dot{\bar{\varepsilon}}_\alpha + A^0 \frac{\partial \dot{\bar{\varepsilon}}_\alpha}{\partial M} \right) - \frac{\partial \bar{\varepsilon}_0}{\partial M} - \frac{\partial A_n}{\partial M} \dot{\bar{\varepsilon}}_n - A_n \frac{\partial \dot{\bar{\varepsilon}}_n}{\partial M} \right] +$$

$$\left. + \frac{\partial \overline{A}_{1T}}{\partial M} \frac{\partial \alpha_T}{\partial n} + \overline{A}_{1T} \frac{\partial}{\partial M} \left(\frac{\partial \alpha_T}{\partial n} \right) + \frac{\partial \overline{A_2}}{\partial M} \eta + \frac{\partial \overline{A_3}}{\partial M} \beta - \frac{A_2}{B_2} \frac{\partial B_0}{\partial M} \right\} +$$

$$+ \frac{1}{C_{L0}} \left(\frac{\partial C_L}{\partial M} \right)_{\alpha} \left\{ A_n (h - H_0^n) + \overline{V}_{c.g.} \left[A_n \dot{\bar{\varepsilon}}_n \overline{A}_1 + \overline{A}_{1T} \frac{\partial \alpha_T}{\partial n} \right] \right\} \quad . \quad . \quad (37)$$

The value of β (initial value) to be used in these expressions will be given by equation (19) with $C_m = 0$. The initial value of η may then be found from (18), again with $C_m = 0$. Equation (16) then gives α. It is assumed here that $\overline{V}_{c.g.}$ is constant, *i.e.* that l_T is constant. This is not strictly true, since in general the mean aerodynamic centre of the tailplane will move, but the error involved is probably small.

4.4. *Application of the theory*

STATIC MARGINS

Perhaps the simplest way of determining the static margins is to use the formulae

$$K_n = -V_T A_2 \left(\frac{d\eta}{dC_R} \right)_{C_m = 0},$$

$$K_n' = -\overline{V}_T \overline{A}_3 \left(\frac{d\beta}{dC_R} \right)_{\substack{C_m = 0 \\ C_H = 0}}.$$

The values of η and β to trim for a given value of $C_R \simeq C_L$ are given by equations (18) and (19) with $C_m = 0$. These values can then be plotted against C_R (or M) and values of $(d\eta/dC_R)_{C_m=0}$ and $(d\beta/dC_R)_{\substack{C_m=0 \\ C_H=0}}$ are then obtained by graphical or numerical differentiation. This procedure is suggested in Ref. 2, and must involve some loss of accuracy although, since the trim curves can be obtained by calculation, this loss can be minimised by the use of a sufficiently large number of ordinates. When the trim curves are plotted against C_R the high-speed end of the range becomes "compressed" and the low-speed end elongated, so that it is probably better to plot control angles against Mach number. Then

$$\frac{d\eta}{dC_R} = -\frac{M}{2C_R} \frac{d\eta}{dM}, \quad \text{since} \quad C_R M^2 = \text{constant}.$$

It would be possible to find the value of dC_m/dC_R from the relation

$$\frac{dC_m}{dC_R}=\frac{\left(\frac{\partial C_m}{\partial \alpha}\right)_M\left(1+\frac{M}{2C_R}\left(\frac{\partial C_R}{\partial M}\right)_\alpha\right)-\frac{M}{2C_R}\left(\frac{\partial C_R}{\partial \alpha}\right)_M\left(\frac{\partial C_m}{\partial M}\right)_\alpha}{\left(\frac{\partial C_R}{\partial \alpha}\right)_M}.$$

This method, however, suffers from the disadvantage that values of $\partial A_1/\partial M$, $\partial A_2/\partial M$, etc., must be obtained by graphical differentiation (in general) so that the loss of accuracy is likely to be greater than that involved in finding $d\eta/dC_R$.

In general

$$\frac{T_N}{\frac{1}{2}\rho V^2 S}+C_L=C_R\cos\gamma_e$$

$$\frac{T_T}{\frac{1}{2}\rho V^2 S}-C_D=C_R\sin\gamma_e$$

where T_N = component of thrust force normal to flight direction

T_T = component of thrust force in flight direction

γ_e = angle between flight path and horizontal.

Thus in level flight $C_R=C_L$ for $T_N=0$. This result is not, as is suggested in Ref. 6, dependent upon the drag being small compared with the lift.

MANOEUVRE MARGINS

The manoeuvre margins may be obtained by direct substitution of values for A^0, A_1, etc., in the equations of Section 4.2. It is thus a simpler matter to obtain the manoeuvre margins than to obtain the static margins, because of the absence of derivatives with respect to forward speed in the expressions for the manoeuvre margins.

5. Miscellaneous Refinements

5.1. *Inclusion of effects of change of density with altitude on stability*

The effect of density variation with altitude on longitudinal stability is considered by Neumark in Ref. 18. Only the level flight condition is there considered, so that $C_L\simeq C_R$.

STATIC AND MANOEUVRE MARGINS

Neumark gives

$$K_n=-\left(\frac{\partial C_m}{\partial C_L}\right)_M+\frac{M}{2C_L}\left(\frac{\partial C_m}{\partial M}\right)_{C_L},$$

$$K_{n\beta}=-\left(1+\frac{\gamma M^2}{2N}\right)\left(\frac{\partial C_m}{\partial C_L}\right)_M+\left(1-\frac{\gamma M^2}{2}\frac{N-1}{N}\right)\frac{M}{2C_L}\left(\frac{\partial C_m}{\partial M}\right)_{C_L}$$

where $N = \dfrac{g}{g - RK_\phi}$

and R = gas constant for air, K_ϕ = lapse rate.

The static margin (stick fixed or free) as defined by Gates and Lyon[1] is K_n (for $C_L = C_R$); $K_{n\beta}$ is the "generalised static margin" (stick fixed or free) which is proportional to E_1, the last term in the stability quintic, when density variation with height is included. However, the quantity $K_{n\beta}$ is no longer a measure of the stick movement (or force) to change speed.

From these formulae, given K_n and $(\partial C_m/\partial C_L)_M$ (which is found when calculating the manoeuvre margin) $K_{n\beta}$ can be evaluated.

There are no effects of density variations with altitude on the manoeuvre margins.

EFFECT ON STABILITY DERIVATIVES

Additional stability derivatives x_β, z_β are introduced which are derived in full in Ref. 18. These are, however, functions of C_D, $\partial C_D/\partial M$, C_L, $\partial C_L/\partial M$ and of quantities unaffected by distortion, so that they are readily determined.

5.2. *Inclusion of effects of changes in the form of the wing lift distribution and movement of aerodynamic centre due to compressibility*

If distortion effects are to be included, it is very difficult to allow correctly for variations in the form of the wing lift distribution or in the aerodynamic centre position of the rigid wing. If they are functions of Mach number it is strictly necessary to perform a complete set of calculations for each combination of M and q. To avoid the heavy labour of such a procedure, it is suggested that if the shift of aerodynamic centre is not very large then the aeroelastic equilibrium calculations can be made first ignoring the shift of aerodynamic centre. Then allowance for the shift can be made without correcting for the secondary distortion effects introduced. If the movement of the aerodynamic centre is large, however, it might be advisable to perform calculations with a range of representative positions, and then to interpolate.

If the tailplane aerodynamic centre shift is also appreciable it may be necessary to modify the tail arm.

6. A Simple Example

As an example the hypothetical aircraft illustrated in Fig. 1 was considered. It has a wing of 45° sweep, an aspect ratio of 3·81, and an "all-moving" tailplane of similar plan form to the wing. For simplicity the structural characteristics of the wing and tailplane were assumed to be similar, so that calculations of lift curve slope, and so on, made for the flexible wing apply also to the tailplane. Compressibility effects were allowed for by applying linearised theory corrections to the wing

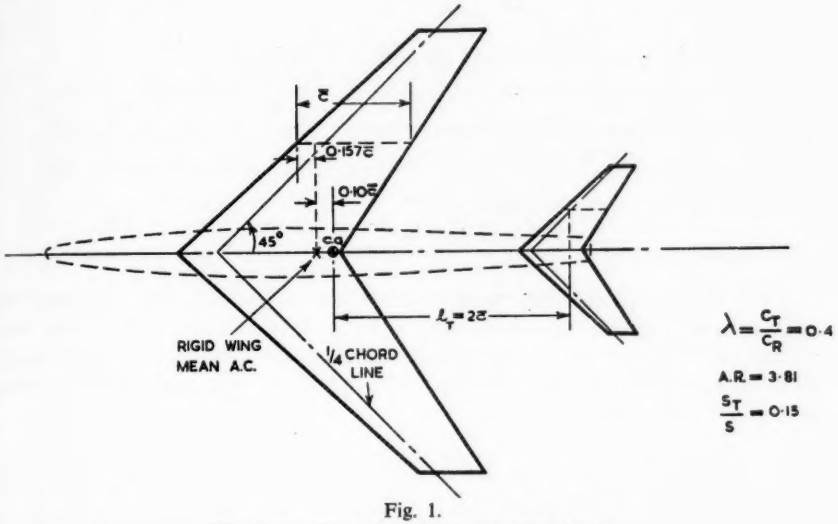

Fig. 1.
Plan form of hypothetical aircraft of Section 6.

and tail lift curve slopes, and also to an assumed value of C_{m_0} introduced into the calculations as an extra "fuselage" pitching moment contribution—the distorted wing has zero twist at all sections and is of symmetrical section, giving zero contribution to C_{m_0}. No other fuselage or thrust contributions to pitching moment or lift were included. Tail lift was included in the total C_L, but wing weight effects were neglected.

Distortion of the wing, fuselage and tailplane was taken into account, but not control circuit distortion, and there is no tab. This is consistent with a system of completely rigid power operated controls, and hence the "stick fixed" case only was considered.

6.1. *Calculation of lift and pitching moment coefficients for the flexible wing and tailplane*

The first problem was to find values of $A = (\partial C_{Lw}/\partial\alpha)_M = (\partial C_{Law}/\partial\alpha)_M$ and ΔH_0 for a suitable range of values of $q\ (=\frac{1}{2}\rho V^2)$ and Mach number. The wing is an example of the case considered in Section 2.2.1, and hence the superposition method was used.

The method used was exactly as described in Ref. 3, as follows:—

(*i*) The method of Küchemann[7] was used to give (for incompressible flow) the lift distributions corresponding to incidence distributions $\alpha = \eta_1$, $\alpha = \eta_1^2$, $\alpha = \eta_1^3$, α = a constant = 1 radian on the rigid wing. $(\eta_1 = y/\{b/2\})$. These lift distributions were integrated graphically to give values of C_{LR}/A_R, C_{L1}/A_R, C_{L2}/A_R, C_{L3}/A_R,

where

C_{LR} = rigid wing lift coefficient per radian of incidence

C_{L_1} = rigid wing C_L corresponding to $\alpha = \eta_1$, with $\alpha = 1$ radian at the tip

C_{L_2} = rigid wing C_L corresponding to $\alpha = \eta_1^2$, with $\alpha = 1$ radian at the tip

C_{L_3} = rigid wing C_L corresponding to $\alpha = \eta_1^3$, with $\alpha = 1$ radian at the tip

A_R = lift curve slope of rigid wing.

It was found that $C_{LR}/A_R = 1{\cdot}0$, $C_{L_1}/A_R = 0{\cdot}435$, $C_{L_2}/A_R = 0{\cdot}264$, $C_{L_3}/A_R = 0{\cdot}184$.

(*ii*) In stage (*i*) the locus of aerodynamic centres was obtained, and hence the pitching moment distributions corresponding to $\alpha = \eta_1$, $\alpha = \eta_1^2$, and so on, were plotted and integrated to give the position of the mean aerodynamic centre of the rigid wing, and the pitching moment coefficients about that point for the various incidence distributions considered.

Then $\dfrac{C_{mR}}{A_R} = 0$, $\dfrac{C_{m_1}}{A_R} = -0{\cdot}0775$, $\dfrac{C_{m_2}}{A_R} = -0{\cdot}0730$, $\dfrac{C_{m_3}}{A_R} = -0{\cdot}0675$,

where C_{mR}, C_{m_1}, etc., are the pitching moment coefficients about the rigid wing mean aerodynamic centre corresponding to C_{LR}, C_{L_1}, etc.

(*iii*) A relation between A_R and Mach number was obtained using the method of Collingbourne[16].

(*iv*) The lift distributions for the rigid wing were integrated to give shear force and bending moment distributions, it being assumed initially that the wing had a straight flexural axis lying along the 0·45 chord line. Torque distributions about this flexural axis were also obtained.

(*v*) Twist and slope distributions for the four cases were obtained using assumed stiffness distributions, and these distributions were then modified at the root in an attempt to introduce corrections corresponding roughly to the root constraint effects on a swept wing.

(*vi*) The elastic incidence changes of (*v*) were matched as described in Ref. 3 and in Section 2.1.1 to give the superposition coefficients A_S, B_S, C_S for a range of values of qA_R.

(*vii*) Using (*iii*) and (*vi*), a graph of A and ΔH_0 against Mach number was produced for the condition $q/\hat{q} = M^2$, where $\hat{q}$ is the value of q corresponding to the maximum allowable equivalent air speed (Fig. 2).

It was assumed that compressibility effects modified the two- and three-dimensional lift curve slopes without appreciably modifying the form of the lift distribution, or the position of the mean aerodynamic centre, of the rigid wing. The relation referred to in (*iii*) connects two- and three-dimensional lift curve slopes, so that when compressibility corrections are applied to the aspect ratio, sweep angle and two-dimensional slope, the required relation between M and A_R is obtained.

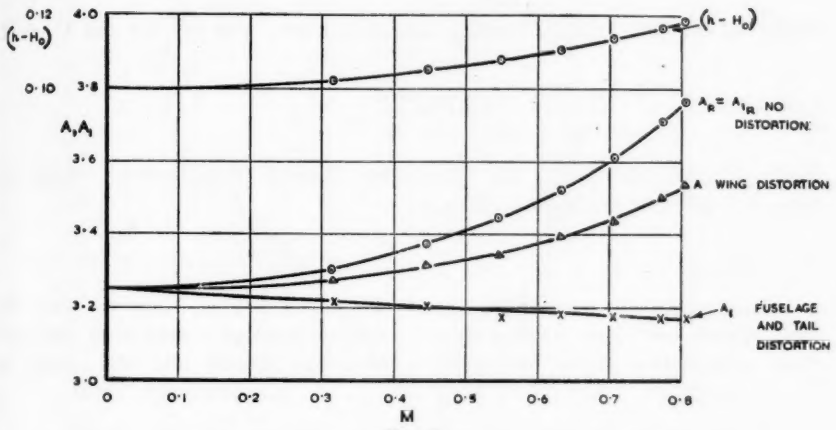

Fig. 2.
Variation of A, A_1, $h-H_0$ with Mach number with and without distortion.

In (*iv*) and (*v*) it was first assumed that, with a straight flexural axis at 0·45*c*, the ratio (bending stiffness)/(torsional stiffness) was constant along the span, and that each stiffness varied as the cube of the local chord. On the basis of information given in Royal Aircraft Establishment Structures Reports 9 and 58 it was decided that a representative value of this ratio was 4·0, and that a representative root torsional stiffness was given by

$$\text{twist per unit torque at root} = \frac{Sl_f^2\hat{q}}{6{\cdot}6}$$

where l_f = length of flexural axis.

It is shown in Ref. 19 that with a swept wing of moderate aspect ratio and conventional construction, the concept of an effective root may be used. The wing may be considered to behave like an unswept wing outboard of this effective root, but inboard of this the root restraint effects are predominant. The information given in Ref. 19 suggests that for a wing of 45° sweep the effective root might be about 0·2 semi-span out from the root. On this basis the twist and slope distributions were modified as shown in Fig. 11. Since this modified the overall values of twist and slope considerably, the root stiffness used was decreased from the value previously quoted, giving

$$(GJ)_R = \frac{Sl_f^2\hat{q}}{10}.$$

Methods of calculating the rigid wing lift distributions and the elastic distortions of swept wings are discussed in Appendices I and II.

6.2. *Introduction of fuselage distortion*

Following the treatment in Ref. 2,

$$A_1 = \frac{A_{1T}}{1+JA_{1T}q}$$

where J = a constant, inversely proportional to the fuselage bending stiffness.

Using the A.P.970* fuselage bending stiffness criterion, with $M=0{\cdot}8$ and $K=0{\cdot}12$,

$$J \simeq \frac{0{\cdot}05}{\hat{q}}$$

where $\hat{q}$ corresponds to V_D, the "maximum allowable diving speed." Since the wing and tailplane are similar, $A_{1T}=A$.

6.3. *Trim curves*

Trim curves for the example aircraft are shown in Figs. 3 and 4. Two sets were plotted, one corresponding to $C_{m_0}=0$ (zero fuselage contribution and zero wing contribution about corrected aerodynamic centre) and the other to $C_{m_0}=-0{\cdot}015/\sqrt{(1-M^2)}$ (taken as $(C_{m_0})_{\text{fuselage}}$, $(C_{m_0})_{\text{wing}}$ remaining zero).

It was assumed for simplicity that $\dot{\bar{\varepsilon}}_a=0{\cdot}1=$constant, and the relation

$$C_L=0{\cdot}0420\left(\frac{\hat{q}}{q}\right)=\frac{0{\cdot}0420}{M^2}$$

was used, corresponding to $W/S=50$ lb./ft.^{2} and $\hat{q}=\frac{1}{2}\rho_0 V^2$, where $V=1{,}000$ ft./sec.

Curves of η_{T_0} (tail-setting angle equivalent to movement of pilot's control) against C_L were produced for the rigid aircraft and for the following cases of distortion:—

(*i*) Wing distortion only
(*ii*) Fuselage distortion only
(*iii*) Tail distortion only
(*iv*) Wing, fuselage and tail distortion.

6.3.1. TRIM CURVES WITH $C_{m_0}=0$

The curves are shown in Fig. 3, and it is clear that the distortion and compressibility effects introduced have had little effect on the slope of the trim curves, except at the highest speeds. These effects are considered in turn.

The effect of compressibility in the absence of distortion is to displace the trim curve a small amount which is nearly constant for all values of C_L. The curve, which is linear and passes through the origin when no compressibility effects are included, remains very nearly linear down to $C_L \simeq 0{\cdot}1$. Below this value of C_L, the slope of the curve becomes slightly more positive, *i.e.* a stabilising effect occurs. Ref. 6 predicts that for $C_{m_0}=0$ the increment of elevator angle to trim due to compressibility is very nearly constant over the whole speed range, the approximation becoming less exact as Mach number increases. This in agreement with the present results.

*Ministry of Supply Air Publication 970. Design Requirements for Aeroplanes for the Royal Air Force and Royal Navy.

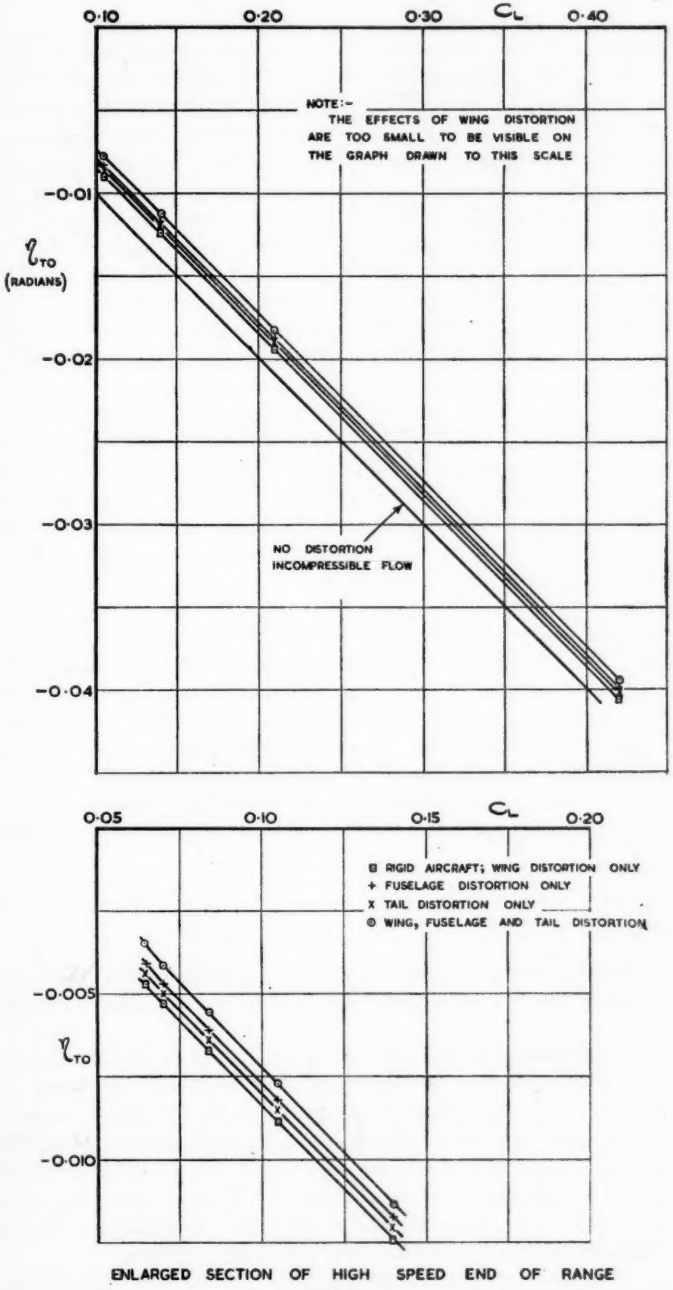

Fig. 3.
Trim curves $C_{m0}=0$.

The distortion of the wing alone then produces a negligible change in the trim curve. The reason for this appears to be that the effect of the loss of lift curve slope due to distortion (the wing tips bend upwards) is offset by the forward movement of the wing aerodynamic centre. Thus, for a given C_L, wing distortion makes it necessary to fly at a slightly higher incidence, so that for a given value of η_T the nose-down tail contribution is increased. This effect is almost exactly cancelled by the extra nose-up moment resulting from the forward movement of the wing aerodynamic centre, so that the value of η_T to trim is unchanged.

Distortion of the fuselage alone produces a constant increment of η_T to trim over the whole range, thus leaving the slope unchanged. This is because, with $C_{m_0}=0$ and a fixed c.g. position, the tailplane load is constant over the whole speed range.

Distortion of the tailplane alone also again produces a constant increment of tail angle to trim and the reason for this is again that the tail load is constant at all speeds. Since the form of the lift distribution due to any given twist distribution of the tailplane is assumed independent of Mach number, the twist due to a given overall load is the same at all speeds and hence the increment of tail-setting angle to trim arising from twist is constant.

When all the distortion effects are combined, the total increment of η_{T_0} to trim is slightly greater than the algebraic sum of the separate increments taken individually. This is because wing distortion makes necessary a slight increase in incidence for a given C_L which, for a given η_{T_0}, causes an increase in the tail load. When the tailplane and fuselage are rigid this has little effect on η_{T_0} to trim, since it is largely cancelled by forward movement of the wing aerodynamic centre. When the tailplane and fuselage are flexible, however, the increased tail load causes extra tail and fuselage distortion, which in turn require a small additional increment of η_{T_0}.

6.3.2. TRIM CURVE WITH $C_{m_0}=-0{\cdot}015/\sqrt{(1-M^2)}$

The curves are shown in Fig. 4 and it will be seen that in this case distortion and compressibility effects have modified the form of the trim curves considerably.

The effects of compressibility alone are very marked at the higher Mach numbers considered. As the lift coefficient decreases and the Mach number increases, C_{m_0} becomes more and more negative, *i.e.* the tail-setting angle to trim out C_{m_0} becomes more and more negative, and at high speeds this contribution to η_{T_0} is large compared with that required to trim out the other wing and tail pitching moment contributions. At low speeds the reverse is the case, so that as speed increases, and the C_{m_0} contribution becomes more dominant, the slope of the trim curve becomes less negative, then zero, and finally positive.

The effect of wing distortion alone, however, then makes no further appreciable difference to the trim curve, as in the case when $C_{m_0}=0$. Again, the forward

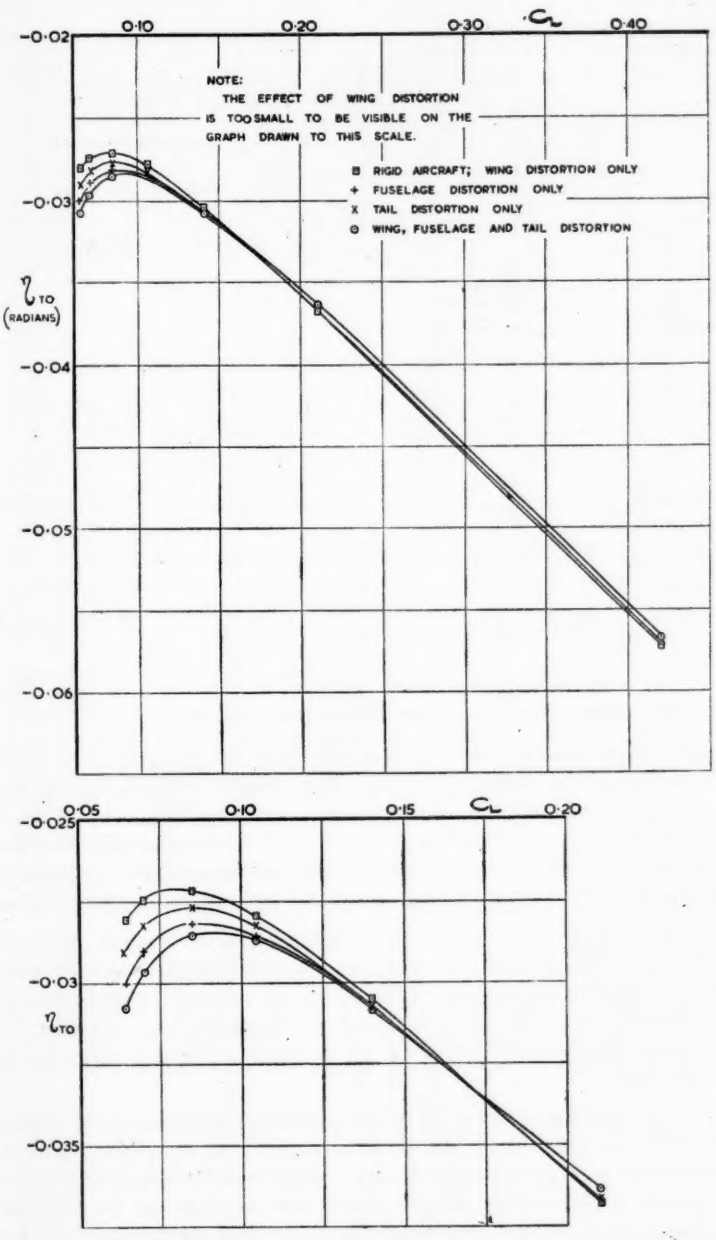

ENLARGED SECTION OF HIGH SPEED END OF RANGE

Fig. 4.

Trim curves $C_{m_0} = \dfrac{-0{\cdot}015}{\sqrt{(1-M^2)}}$

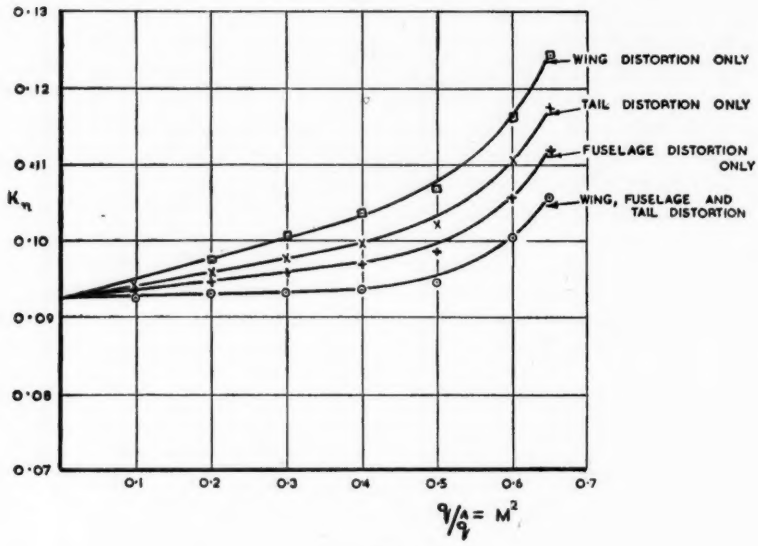

Fig. 5.
Variation of stick fixed static margin with $q/\hat{q}$. $C_{m_0}=0$.

movement of the wing aerodynamic centre is offset by the increased nose-down pitching moment contribution due to the higher tail incidence.

Distortion of the fuselage alone makes the slope of the trim curve more positive (destabilising), the effect increasing with speed. The change in C_{m_0} produces a change in tail load, which becomes more and more negative (tail down) as the Mach number increases. As the speed increases the fuselage distortion due to the increasingly negative tail load produces an increasingly positive incidence of the tail, and therefore an increasingly negative increment of η_{T_0} is required to trim.

Tail distortion alone has a very similar effect to that of fuselage distortion. The all-moving tail behaves like a wing, unlike the usual tailplane-elevator combination. Thus a positive tail load causes the tips of the tailplane to bend upwards, producing a positive increment of η_{T_0} to trim, and conversely for a negative tail load. The changes in η_{T_0} to trim are therefore in the same sense as those caused by fuselage bending.

It will be seen that the result of the combined distortion effects at the highest speeds is slightly less than the algebraic sum of the separate effects. This is because, as for $C_{m_0}=0$, wing distortion causes a slight positive change in tail load which in this case at high speeds reduces slightly the magnitude of the tail load, which is negative, being largely determined by C_{m_0}. Thus the fuselage and tail distortions are slightly reduced and there is a small reduction in the overall (negative) increment of η_{T_0} due to distortion when the distortion effects are combined.

6.4. *Stick fixed static margin*

For an aircraft fitted with an all-moving tailplane,

$$K_n = -V_T A_1 \left(\frac{d\eta_{T0}}{dC_L}\right)_{C_m=0} \text{(for } C_L = C_R\text{)}.$$

Values of $(d\eta_{T0}/dC_L)_{C_m=0}$ were accordingly obtained from the trim curves for the cases $C_{m0}=0$ and $C_{m0}=-0{\cdot}015/\sqrt{(1-M^2)}$.

6.4.1. $C_{m0}=0$

The resulting curves of K_n against $q/\hat{q}$ for $C_{m0}=0$ are given in Fig. 5. Consider first the effects of compressibility. It will be seen that the static margin increases slightly with increase of Mach number. This is because $(d\eta_{T0}/dC_L)_{C_m=0}$ is very nearly constant, except at the highest speeds where it becomes slightly more negative, while A_1 is increased by compressibility*. This result is in agreement with that predicted in Ref. 6 for the case $C_{m0}=0$. When K_n is positive in incompressible flow, the restoring tail pitching moment due to a change of speed and corresponding change of incidence ($C_R V^2 = \text{constant}$) will exceed the destabilising wing contribution. The difference between these contributions will be increased if both wing and tail lift curve slopes are increased by compressibility in roughly the same ratio, C_{m0} remaining zero.

Considering now the effects of distortion, it is seen that, since wing distortion alone does not appreciably change the slope of the trim curve or the value of V_T or of A_1 for the aircraft considered, K_n is almost completely unaffected by wing distortion.

The effect of fuselage and tail distortion, however, is to decrease the value of A_1 (V_T still remains very nearly constant) so that, although for $C_{m0}=0$ the trim curve slopes are not appreciably modified by these effects, the value of K_n is decreased progressively as $q/\hat{q}$ increases compared with the value for the rigid aircraft.

In this example the loss of static margin due to fuselage distortion is greater than that due to tail distortion, and the combined effects produce a maximum loss of static margin of the order of 10-15 per cent. at a Mach number of about 0·8.

6.4.2. $C_{m0}=-0{\cdot}015/\sqrt{(1-M^2)}$

Curves of K_n against $q/\hat{q}$ for the case when $C_{m0}=-0{\cdot}015/\sqrt{(1-M^2)}$ are given in Fig. 6.

Here it will be seen that compressibility effects alone produce a large loss of static margin at high Mach numbers. The static margin, which at low values of M

*V_T is very nearly constant.

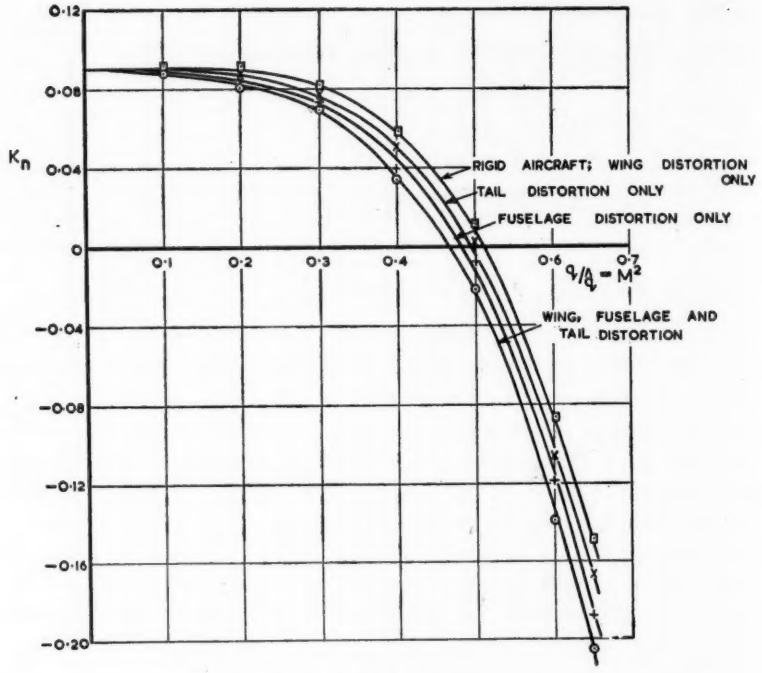

Fig. 6.

Variation of stick fixed static margin with $q/\hat{q}$ $C_{m0} = \dfrac{-0{\cdot}015}{\sqrt{(1-M^2)}}$

is approximately 0·10, becomes zero at $q/\hat{q} \simeq 0{\cdot}5$ ($M \simeq 0{\cdot}7$) and rapidly increases negatively at higher speeds. This loss of K_n with increase of M is predicted in Ref. 6, where it is shown that the loss of K_n due to compressibility depends on the value of $(C_{m0}/K_n)_{M=0}$. As shown already, the static margin is increased by compressibility for $C_{m0}=0$ by an amount dependent on the low-speed value of K_n. When $C_{m0} < 0$, however, the value of dC_{m0}/dC_L is positive and increases rapidly as M increases, producing an increasing loss of static margin. These two effects are in opposition, but the latter is dominant in this example. The loss of static margin will depend on the relative size of the two effects, *i.e.* on the value of $(C_{m0}/K_n)_{M=0}$.

Considering now distortion effects, it will be seen that wing distortion alone causes no appreciable change in K_n as in the case $C_{m0}=0$, and the reason is the same as in that case. Fuselage and tail distortion, however, cause a reduction in A_1 and also make the value of $(d\eta_{T0}/dC_L)_{C_m=0}$ more positive (*see* Fig. 4) so that they produce a large loss of K_n. This reduction in K_n due to fuselage and tail distortion is actually greater than with $C_{m0}=0$, but since here the reduction due to compressibility is very great, the distortion effects appear less important.

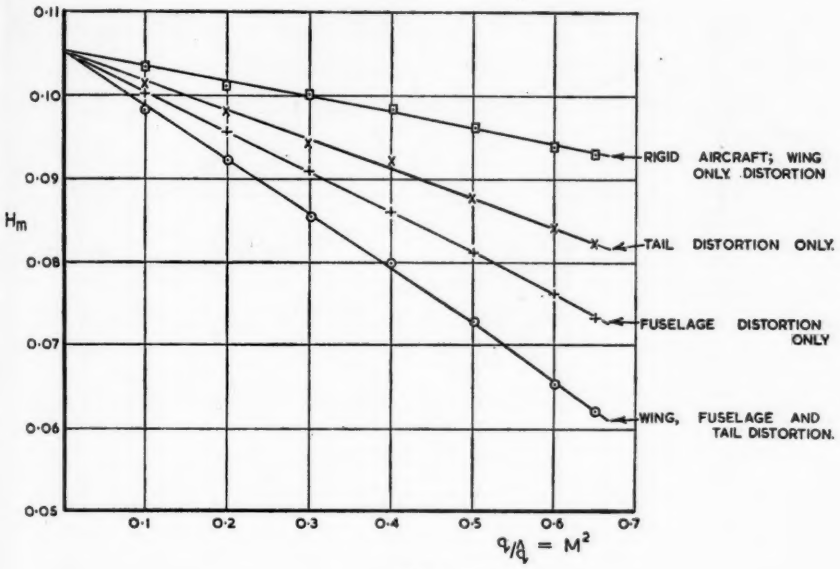

Fig. 7.
Variation of stick fixed manoeuvre margin with $q/\hat{q}$.

6.5. *Stick fixed manoeuvre margin*

For this simple example the formula of Section 4.2 (equation (21)) becomes

$$-\left(\frac{\partial C_m}{\partial C_L}\right)_M = -(h-H_0)+V_T A_1\left(\frac{1}{A}-\frac{\dot{\varepsilon}_\alpha}{}\right)$$

and $$\left(\frac{m_q}{\mu_1}\frac{l}{\bar{c}}\right) \simeq -\frac{V_T A_1}{2\mu_1}+\frac{m_{qw}}{\mu_1}\frac{l}{\bar{c}}.$$

The value of μ_1 was taken as 50. The wing contribution to m_q (m_{qw}) was estimated as described in Appendix III.

The resulting values of H_m as functions of $q/\hat{q}$ are shown in Fig. 7.

It will be seen that compressibility alone produces a loss of H_m which steadily increases as M increases, and this is in agreement with the results of the analysis of Ref. 6.

It can be seen how this arises from the formula

$$H_m = -(h-H_0)+V_T A_1\left(\frac{1}{A}-\frac{\dot{\varepsilon}_\alpha}{}\right)-\frac{m_q}{\mu_1}\frac{l}{\bar{c}}.$$

The effect of compressibility is to increase A_1, A and m_q. The net result is a reduction in the second term, which is large, and an increase in the third term, which is small.

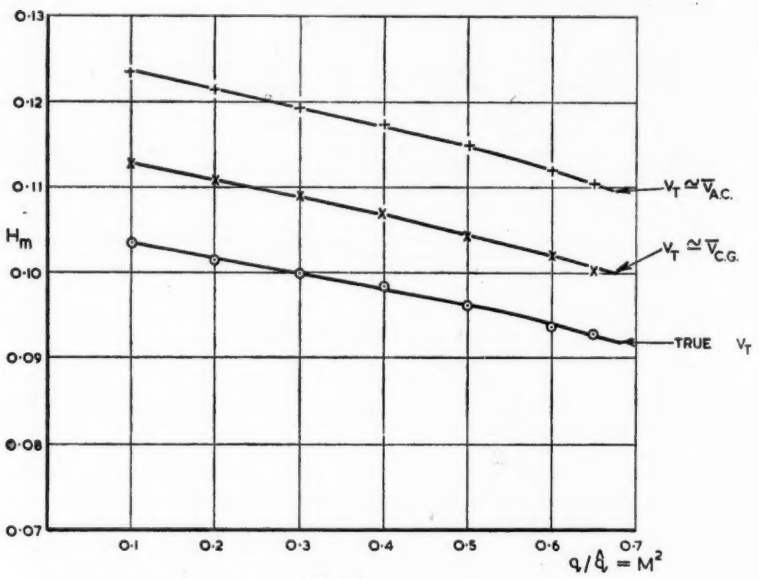

Fig. 8.

Comparison of values of stick fixed manoeuvre margin obtained using approximate and correct tail volume coefficients.

As with the static margin, it is found that wing distortion alone has no effect on manoeuvre margin for the example considered. Wing distortion reduces the values of H_0 and A, so that both the first and second terms in the expression for H_m are increased, but the two changes almost exactly cancel each other.

Both the fuselage and tail distortion effects, on the other hand, leave H_0 unchanged but reduce A_1 and m_q, so that there is a resulting decrease of H_m which, in this example, is greater for fuselage distortion than for tail distortion.

The combined effect of wing, fuselage and tail distortion is very nearly the algebraic sum of the effects taken separately. This suggests that it might be possible to calculate the loss of manoeuvre margin due to each and to add the separate contributions, but in fact this would take longer than the single calculation for the combined effects.

To assess the error in H_m due to using $\overline{V}$ instead of V_T (*i.e.* due to neglecting tail lift in obtaining C_L) values of H_m were calculated using the formula just quoted, but substituting (*i*) $\overline{V}_{c.g.}$ and (*ii*) $\overline{V}_{a.c.}$ for V_T. The results are shown in Fig. 8, where the curve corresponding to the true value of V_T is also shown for comparison. It is interesting to note that the error due to using $\overline{V}_{a.c.}$ instead of V_T is roughly twice that due to using $\overline{V}_{c.g.}$, and that the error due to using $\overline{V}_{c.g.}$ is roughly equal to the magnitude of the value of m_q/μ_1 (in this example).

6.6. *Quasi-static stability derivatives*

For an aircraft with all-moving tail and no tab, the equations of Section 4.3, with stick fixed and taking $\dot{\bar{\varepsilon}}_\alpha$ as constant, simplify to

$$\left(\frac{\partial C_L}{\partial \alpha}\right)_M = A + \frac{S_T}{S} A_1 (1 - A \dot{\bar{\varepsilon}}_\alpha)$$

$$\left(\frac{\partial C_L}{\partial M}\right)_\alpha = \alpha \frac{\partial A}{\partial M} + \frac{S_T}{S} \left\{ \frac{\partial A_1}{\partial M} (\alpha + \eta_{T_0} - \bar{\varepsilon}) - A \alpha \dot{\bar{\varepsilon}}_\alpha \frac{\partial A}{\partial M} \right\}$$

$$\left(\frac{\partial C_m}{\partial \alpha}\right)_M = A (h - H_0) - \bar{V}_{c.g.} \left\{ A_1 (1 - A \dot{\bar{\varepsilon}}_\alpha) \right\} = \left(\frac{\partial C_m}{\partial C_L}\right)_M \left(\frac{\partial C_L}{\partial \alpha}\right)_M$$

$$\left(\frac{\partial C_m}{\partial M}\right)_\alpha = \frac{\partial C_{m_0}}{\partial M} + \alpha \frac{\partial A}{\partial M} (h - H_0) - A \alpha \frac{\partial H_0}{\partial M} - \bar{V}_{c.g.} \left\{ \frac{\partial A_1}{\partial M} (\alpha + \eta_{T_0} - \bar{\varepsilon}) - A_1 \alpha \dot{\bar{\varepsilon}}_\alpha \frac{\partial A}{\partial M} \right\}.$$

Values of α, η_{T_0}, $\bar{\varepsilon}$ were calculated when determining the static margin.

The longitudinal stability derivatives involve the partial derivatives just given (*see* Section 4.3). If it is assumed, as suggested in Section 4.3, that the drag contributions are unaffected by distortion, then the effects of distortion on the stability derivatives may be demonstrated by evaluating $(\partial C_L/\partial \alpha)_M$, $(\partial C_L/\partial M)_\alpha$, $(\partial C_m/\partial \alpha)_M$, $(\partial C_m/\partial M)_\alpha$ with and without distortion effects. This was done for the aircraft considered, using the values of A, A_1, H_0, etc., previously calculated, and these partial derivatives are plotted against $q/\hat{q}$ ($=M^2$ in this case) in Figs. 9 and 10. Only the case $C_{m_0}=0$ is considered, and curves are given for the rigid aircraft and for the aircraft with all distortion effects included (wing, fuselage and tail distortion).

THE DERIVATIVE $(\partial C_L/\partial \alpha)_M$

As might be expected, the curves describing the variation of $(\partial C_L/\partial \alpha)_M$ with $g/\hat{q}$ are very similar to those of A against $q/\hat{q}$. The tail contribution is of the order of 10-15 per cent. of the wing contribution, so that it is not negligible.

THE DERIVATIVE $(\partial C_m/\partial \alpha)_M$

The curves for $(\partial C_m/\partial \alpha)_M$ were obtained from the values of $(\partial C_m/\partial C_L)_M$ calculated when determining the manoeuvre margin and the values of $(\partial C_L/\partial \alpha)_M$ already derived.

It will be seen that, for the rigid aircraft, $(\partial C_m/\partial \alpha)_M$ is very nearly constant over the whole range. Since $(\partial C_m/\partial C_L)_M$ is decreased by increase of M (*see* Section 6.5) and $(\partial C_L/\partial \alpha)_M$ is increased at the same time, the resultant change of $(\partial C_m/\partial \alpha)_M$ is small. Distortion effects reduce both $(\partial C_m/\partial C_L)_M$ and $(\partial C_L/\partial \alpha)_M$ as speed is increased, so that $(\partial C_m/\partial \alpha)_M$ decreases steadily with increase of M for the flexible aircraft.

THE DERIVATIVE $(\partial C_L/\partial M)_\alpha$

Since $(\partial C_L/\partial M)_\alpha$ is a "constant incidence" derivative, the expression for it contains terms of the type $\alpha\partial A/\partial M$. The magnitude of $(\partial C_L/\partial M)_\alpha$ therefore depends on the magnitudes of α, α_T and $\partial A/\partial M$, $\partial A_1/\partial M$. For small values of $q/\hat{q}$, $\partial A/\partial M$ is small but α changes rapidly, while for high values of $q/\hat{q}$, $\partial A/\partial M$ changes rapidly but α then changes slowly. The net result is $(\partial C_L/\partial M)_\alpha$ has a maximum value for moderate values of $q/\hat{q}$.

Distortion increases α and reduces $\partial A/\partial M$; the latter effect is dominant and there is consequently a reduction in $(\partial C_L/\partial M)_\alpha$ due to distortion which is nearly constant over the whole range.

THE DERIVATIVE $(\partial C_m/\partial M)_\alpha$

Since $\partial C_{m0}/\partial M = C_{m0} = 0$, and for the rigid aircraft $(h-H_0)$ is constant, *i.e.* $\partial H_0/\partial M = 0$, therefore the expression for $(\partial C_m/\partial M)_\alpha$ quoted is reduced to two terms:—

$$\alpha\frac{\partial A}{\partial M}(h-H_0) \qquad \text{and} \qquad \overline{V}_{c.g.}\left\{\frac{\partial A_1}{\partial M}\alpha_{T0} - A_1\alpha\frac{\dot{\varepsilon}_\alpha}{}\frac{\partial A}{\partial M}\right\}.$$

The second term is small compared with the first (*i.e.* the wing contribution is large compared with that from the tail) so that

$$\left(\frac{\partial C_m}{\partial M}\right)_\alpha \simeq \alpha\frac{\partial A}{\partial M}(h-H_0).$$

Since $(h-H_0)$ is constant, the form of the curve of $(\partial C_m/\partial M)_\alpha$ for the rigid aircraft is very similar to that of $(\partial C_L/\partial M)_\alpha$, and thus

$$\left(\frac{\partial C_m}{\partial M}\right)_\alpha \simeq (h-H_0)\left(\frac{\partial C_L}{\partial M}\right)_\alpha.$$

When distortion effects are introduced, $\partial H_0/\partial M$ is no longer zero, and in fact the term $(-A\alpha\partial H_0/\partial M)$ is dominant, being large and positive. At low speeds, where α increases rapidly as $q/\hat{q}$ is reduced, this term causes a large increase in $(\partial C_m/\partial M)_\alpha$. At higher speeds the increase is somewhat less although still considerable.

EFFECTS OF DISTORTION ON STABILITY DERIVATIVES

For the aircraft considered, with $C_{m0}=0$, it is seen that distortion reduces $(\partial C_L/\partial\alpha)_M$, $(\partial C_m/\partial\alpha)_M$ and $(\partial C_L/\partial M)_\alpha$ so that z_w, m_w and z_u are decreased. The effects on z_w and m_w are appreciable even at moderate speeds, but the effect on z_u will be serious only at high M and low C_L. Distortion increases $(\partial C_m/\partial M)_\alpha$ so that m_u is increased, and this effect is most marked at the lowest speeds. Tail contributions to m_q, $m_{dw/dt}$ will be decreased by distortion since both A and A_1 are reduced. On the assumption that drag derivatives are unchanged by distortion, x_u and x_w will not be affected.

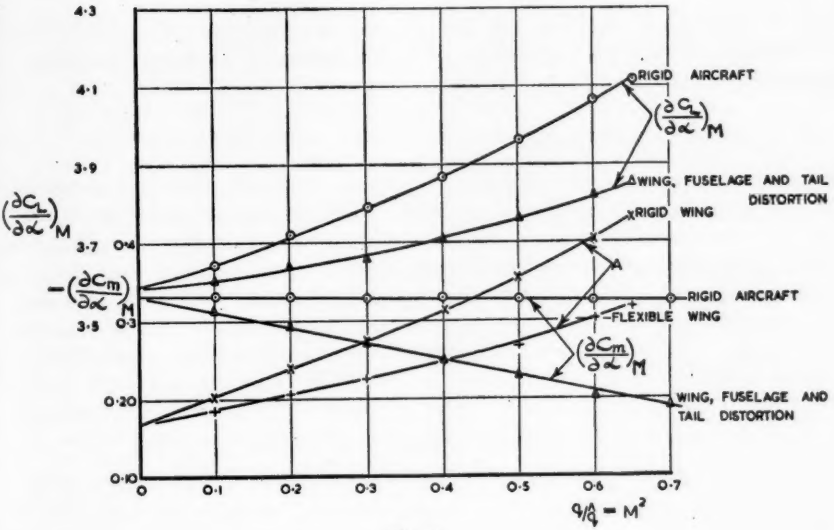

Fig. 9.

Variation of $\left(\frac{\partial C_L}{\partial \alpha}\right)_M$, $\left(\frac{\partial C_m}{\partial \alpha}\right)_M$ with $q/\hat{q}$ with and without distortion.

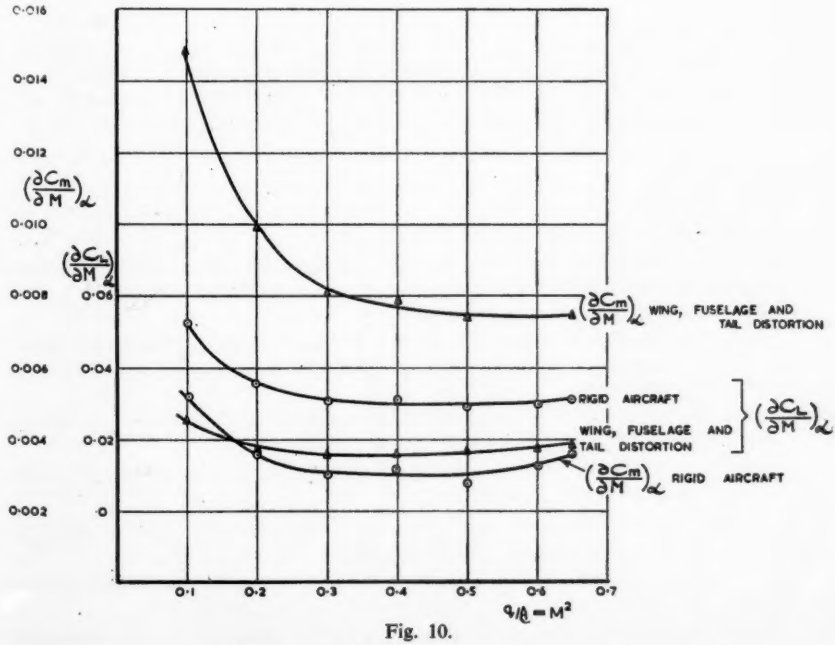

Fig. 10.

Variation of $\left(\frac{\partial C_L}{\partial M}\right)_\alpha$, $\left(\frac{\partial C_m}{\partial M}\right)_\alpha$ with $q/\hat{q}$ with and without distortion.

It must be emphasised that the foregoing results apply only to the aircraft considered and for the condition $C_{m_0}=0$, and caution is needed in attempting to generalise from them.

7. Concluding Remarks

There is no intrinsic difficulty in including distortion effects on longitudinal stability if frequency effects are neglected. The amount of calculation involved may be considerable, however, especially if wing twist, camber and weight effects have to be included. If, therefore, there is good reason to believe that distortion effects are small (as they may be on a fighter-type aircraft with high stiffnesses) a simple crude assessment may be adequate. On a large bomber or transport aircraft, for which load factors and hence stiffnesses are likely to be lower, and which are likely to have higher aspect ratio wings, it may be essential to make a detailed analysis of distortion effects on the lines discussed. This is particularly true of the "podded engine" layouts used in conjunction with thin swept wings.

For the aircraft considered in Section 6 the results show that if $C_{m_0}=0$ neither compressibility nor distortion effects modify the static margin to any serious extent. When C_{m_0} is negative, however, both effects are heavily destabilising as far as the static margin is concerned. It therefore seems advisable to give a high-speed aircraft a layout which is as nearly symmetrical as possible about the plane of the wings.

Acknowledgment

The author wishes to thank Professor A. D. Young, of the Department of Aerodynamics, for his guidance in the preparation of the original thesis and in its revision for publication.

References

1. Gates, S. B. and Lyon, H. M. (1944). A Continuation of Longitudinal Stability and Control Analysis. Part I. R. & M. 2027, February 1944.
2. Lyon, H. M. and Ripley, J. (1945). A General Survey of the Effects of Flexibility of the Fuselage, Tail Unit and Control Systems on Longitudinal Stability and Control. R. & M. 2415, July 1945.
3. Brown, R. B., Holtby, K. F. and Martin, H. C. A Superposition Method for Calculating the Aeroelastic Behaviour of Swept Wings. *Journal of the Aeronautical Sciences*, Vol. 18. August 1951, pp. 531-42.
4. Duncan, W. J. (1952). *The Principles of the Control and Stability of Aircraft*. Cambridge University Press, 1952.
5. Radok, J. R. M. (1952). Dynamic Aeroelasticity of Aircraft with Swept Wings. College of Aeronautics Report No. 58, April 1952.
6. Owen, P. R. (1944). The Effect of Compressibility on Longitudinal Stability Below the Shock Stall. R.A.E. Report Eero. 1829, March 1944.
7. Küchemann, D. (1950). A Simple Method for Calculating the Span and Chordwise Loadings on Thin Swept Wings. R.A.E. Report Aero. 2392, August 1950.
8. Duncan, W. J. (1943). The Representation of Aircraft Wings, Tails and Fuselages by Semi-rigid Structures in Dynamic and Static Problems. R. & M. 1904, February 1943.

9. MULTHOPP, H. (1950). Methods for Calculating the Lift Distribution of Wings (Subsonic Lifting Surface Theory). R.A.E. Report Aero. 2353, January 1950.

10. GARNER, H. C. (1949). Theoretical Calculations of the Distribution of Aerodynamic Loading on a Delta Wing. R. & M. 2819, May 1949.

11. WEISSINGER, J. (1947). The Lift Distribution of Swept-back Wings. N.A.C.A. T.M. 1120, March 1947.

12. DE YOUNG, J. (1947). Theoretical Additional Span Loading Characteristics of Wings with Arbitrary Sweep, Aspect Ratio and Taper Ratio. N.A.C.A. T.N. 1491, December 1947.

13. DIEDERICH, F. W. (1947). A Simple Method for Obtaining the Spanwise Lift Distribution on Swept Wings. N.A.C.A. R.M. L7107, September 1947.

14. STANTON-JONES, R. (1950). An Empirical Method for Rapidly Estimating the Loading Distributions on Swept-back Wings. College of Aeronautics Report No. 32, January 1950.

15. FALKNER, V. M. (1943). The Calculation of Aerodynamic Loading on Surfaces of Any Shape. A.R.C. R. & M. 1910, August 1943.

16. COLLINGBOURNE, J. R. (1952). The Estimation of Lift Curve Slope at Subsonic Mach Numbers. R.A.E. T.N. Aero. 2145, January 1952.

17. GOLDSTEIN, S. and YOUNG, A. D. (1943). Linear Perturbation Theory of Compressible Flow with Application to Wind Tunnel Interference. R. & M. 1909, July 1943.

18. NEUMARK, S. (1948). Dynamic Longitudinal Stability in Level Flight including the Effects of Compressibility and Variations of Atmospheric Characteristics with Height. R.A.E. Report Aero. 2265, August 1948.

19. HALL, A. H. (1951). An Experimental Study of the Static Stiffness and Deformation of Swept Wings with Uniform Chord. *Third Anglo-American Aeronautical Conference*, Brighton, 1951. Royal Aeronautical Society.

20. DIEDERICH, F. W. and FOSS, K. A. (1951). Charts and Approximate Formulæ for the Estimation of Aeroelastic Effects on the Loading of Swept and Unswept Wings. N.A.C.A. T.N. 2608, September 1951.

21. MARTIN, H. C. and GURSAHANEY, H. J. (1951). Deflection of Swept Cantilever Surfaces. *Journal of the Aeronautical Sciences*, Vol. 18, December 1951.

22. McDonnell Aircraft Corporation (1949). Stress Analysis and Stress Measurements for Swept Wings having Ribs Parallel to the Airstream. Report No. 1127, June 1949.

23. HEMP, W. S. (1950). On the Application of Oblique Co-ordinates to Problems of Plane Elasticity and Swept-back Wings. College of Aeronautics Report No. 31, January 1950.

24. WILLIAMS, M. L. (1952). A Review of Certain Analysis Methods for Swept Wing Structures. *Journal of the Aeronautical Sciences*, Vol. 19, September 1952, pp. 615-629.

25. PINSKER, W. J. G. (1950). A Note on the Dynamic Stability of Aircraft at High Subsonic Speeds when Considering Unsteady Flow. R.A.E. Report Aero. 2378, May 1950.

APPENDIX I

CALCULATION OF AERODYNAMIC LOADING ON RIGID SWEPT WINGS

Several methods of calculating the lift distribution on swept wings have been produced. Among these are those due to Multhopp,[9] Garner,[10] Falkner, Weissinger,[11] De Young,[12] Küchemann [7] and Diederich.[13] Stanton-Jones[14] has derived empirical formulæ based on the results of Weissinger which enable lift distribution to be calculated very rapidly for trapezoidal untwisted wings. None of these methods includes thickness, viscosity or compressibility effects.

Of the methods quoted, those due to Falkner, Multhopp and Garner might be described as "lifting surface" theories, by means of which estimates of span and chordwise lift distributions, lift curve slope and aerodynamic centre locus position may

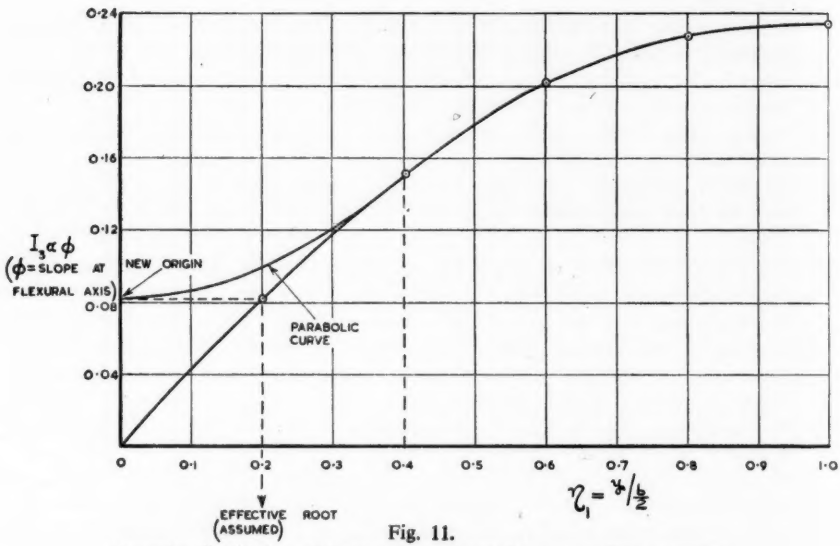

Fig. 11.
Spanwise distribution of slope at flexural axis for $\alpha = 1$ radian = constant.

be obtained. All three methods require a considerable amount of computation if the full advantages of the " lifting surface " method are to be obtained.

The other methods quoted are mainly modifications of the Prandtl " lifting line " theory used for unswept wings and suffer from the disadvantage that reliable estimates of the aerodynamic centre locus cannot be obtained. However, they require less computation than the true lifting surface methods. The method of Küchemann is different from the others in that it uses assumed chordwise lift distributions for the tip, approximately mid-span, and root sections, with distributions at the intermediate sections based on an empirical interpolating relation. A modified version of the flat plate " loading law " is used. It is thus possible to obtain an estimate of the aerodynamic centre locus, although the estimate cannot be more accurate than the initial assumptions involved. The method is, however, simple to apply and provides a reasonably accurate estimate of the spanwise lift distribution, and it was used in the example of Section 6 in this paper.

APPENDIX II

CALCULATION OF DISTORTION OF SWEPT WING UNDER GIVEN AERODYNAMIC LOADING

The mode of distortion of a swept wing under load is different from that of an unswept wing, because of the effects of the oblique restraint at the root. Whereas an unswept wing can be treated as a simple cantilever beam in bending and as a tube in torsion, if the concept of a straight flexural axis is accepted, a swept wing presents a more difficult problem and the flexural axis concept cannot strictly be used. Near the root the wing tends to bend about the root (streamwise) chord, due to the restraint, but the outer portion of the wing behaves more like a straight wing, *i.e.* it bends about a line roughly normal to the leading and trailing edges. Just outboard of the root there is a " transition " between these two types of distortion, so that the overall mode of distortion is complicated.

To estimate deflections for aeroelastic calculations it is possible to use the simple beam theory for a high aspect ratio swept wing. The root restraint effects are confined to a small fraction of the semi-span when the aspect ratio is high. The wing is then

treated as a straight wing from the structural point of view, but the slopes and twists are resolved into the line of flight to give the incidence changes. There is some ambiguity about the position of the effective root, and this method can only be approximate. It is, however, quite widely used and it is put forward in Refs. 3, 20 and 21.

Experimental evidence[19] shows that as the aspect ratio is decreased and the sweep angle is increased this "effective root" method ceases to yield useful results, because the region in which root restraint effects are large now occupies a large fraction of the semi-span. The deflections of quite a large portion of the wing cannot then be estimated by this simple approach. It is possible to make a correction for moderate aspect ratio[20] but for low aspect ratios (or where root stress distributions are required) it is necessary to use a more refined approach. The simple beam theory can be applied together with a "self-equilibrating" stress system,[22] and this method has been used successfully in practice. More exact methods have been put forward (*e.g.* Ref. 23) but these are somewhat more complicated. Once the simple beam theory is discarded, the simple integrations previously used to obtain deflections can no longer be used, and matrix or some other methods must be employed in conjunction with influence coefficients. A review of recent methods considered in the United States is given in Ref. 24.

Finally, it must be noted that with a very low aspect ratio (delta) wing, there may be changes of camber which produce effects of the same order of magnitude as the twist effects.

APPENDIX III

ESTIMATION OF WING CONTRIBUTION TO m_q

With a swept wing, the wing contribution to m_q may be appreciable compared with the tail contribution. For the example of Section 6, m_{qw} was estimated as follows.

Following Ref. 1, a change of manoeuvre margin is obtained for an increment of wing pitching moment ΔC_{mw}, arising from the wing contribution to m_q. This is given by

$$\Delta H_m = -\frac{\Delta C_{mw}}{nC_L} = -\frac{m_{qw}}{\mu}\frac{l}{\bar{c}}$$

ΔC_{mw} is the pitching moment increment due to rotating the wing with constant angular pitching velocity q. Suppose all the wing lift to be generated at the quarter-chord line, and that the wing is rotating about the point A, distant x_0 from the root quarter-chord point taken as the origin.

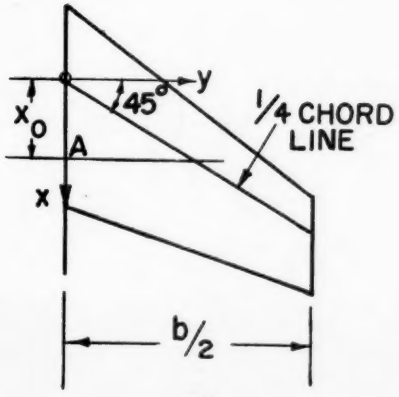

The incidence change at the point (x, y) on the quarter-chord line due to q is then

$$\Delta\alpha = + \frac{q\,(x - x_0)}{V},$$

and $$x = y \tan 45° = y,$$

i.e. $$\Delta\alpha = \frac{q\,(y - x_0)}{V}.$$

The component $-qx_0/V$ is constant along the span.

For the purpose in hand it is sufficient to neglect distortion effects, *i.e.* m_{qw} is determined for the rigid wing.

The constant incidence change $-qx_0/V$ provides zero pitching moment contributions about the rigid wing mean aerodynamic centre. Therefore only the incidence change

$$+\frac{qy}{V} = \frac{ql}{V}\frac{y}{l}$$

need be considered. This is an incidence distribution that increases linearly with spanwise distance from the root.

The calculations of (*ii*) in Section 6.1 for the case $\alpha = \eta_1$, give $C_{m1}/A_R = -0{\cdot}0775$ per radian incidence at the tip. Hence the pitching moment coefficient about the rigid wing mean aerodynamic centre due to the rotation at angular velocity q is

$$\Delta C_{mw} = -0{\cdot}0775\, A_R \frac{b/2}{l}\left(\frac{ql}{V}\right)$$

In this case, $$\frac{b/2}{l} = 0{\cdot}907.$$

Also $$q = \frac{ng}{V} = \frac{nC_L}{2\mu_1}\frac{V}{l},$$

i.e. $$nC_L = 2\mu_1\left(\frac{ql}{V}\right).$$

Therefore $$\Delta H_m = -\frac{\Delta C_{mw}}{nC_L} = + \frac{0{\cdot}0775\, A_R \times 0{\cdot}907}{2\mu_1}$$

$$= + \frac{0{\cdot}070\, A_R}{2\mu_1}.$$

The corresponding tail contribution is $+V_T A_1/(2\mu_1)$. A_1 and A_R are of the same order. and $V_T \simeq 0{\cdot}3$, so that in this case $m_{qw} \simeq 0{\cdot}25\, m_{q\,\text{tail}}$.

Note that ΔC_{mw} is the pitching moment about the mean aerodynamic centre and not the centre of gravity. This is consistent with the use of l instead of l_T in the formula $\Delta\alpha_T = ql/V$ and also with the assumption already made in Section 4.2 that m_{qw} is independent of c.g. position.

INDEX TO VOLUME V

AERODYNAMICS

See also Boundary Layer, Downwash, Electrical Potential Analyser, Secondary Flows, Vanes on Wings.

A Theory of Uniform Supersonic Flow Past a Thin Oscillating Aerofoil at Appreciable Incidence to the Main Stream, Geoffrey L. Sewell, p. 185 (September 1954).

Effects of Wire Length in Turbulence Investigations with a Hot-Wire Anemometer, F. N. Frenkiel, p. 1 (May 1954).

Estimation of the Effects of Distortion on the Longitudinal Stability of Swept Wing Aircraft at High Speeds (Sub-Critical Mach Numbers), B. S. Campion, p. 280 (November 1954).

Subsonic Compressible Flow Past Bluff Bodies, A. L. Longhorn, p. 144 (July 1954).

The Delta Wing in a Non-Uniform Supersonic Stream, G. N. Lance, p. 55 (May 1954).

The Design of Thin Finite Wings in Incompressible Flow, G. J. Hancock, p. 119 (July 1954).

Theory of an Accelerated Slender Supersonic Aerofoil, Geoffrey L. Sewell, p. 52 (May 1954).

BOUNDARY LAYER

On a Simple Method for Calculating Laminar Boundary Layers, K. E. G. Wieghardt, p. 25 (May 1954).

Some Examples of Three-Dimensional Effects in Boundary Layer Flow, J. Wilkinson, p. 73 (May 1954).

The Compressible Laminar Boundary Layer on a Yawed Infinite Wing, L. F. Crabtree, p. 85 (July 1954).

BUCKLING OF PLATES

See Structures.

CAMPION, B. S.

Estimation of the Effects of Distortion on the Longitudinal Stability of Swept Wing Aircraft at High Speeds (Sub-Critical Mach Numbers), p. 280 (November 1954).

CHILVER, A. H.

The Frequency of Failures within a Group of Similar Structures, p. 235 (November 1954).

CRABTREE, L. F.

The Compressible Laminar Boundary Layer on a Yawed Infinite Wing, p. 85 (July 1954).

DELTA WINGS

See Aerodynamics.

DIFFERENTIAL EQUATIONS

A Note on the Numerical Solution of Fourth Order Differential Equations, L. C. Woods, p. 176 (September 1954).

DISTORTION ON SWEPT WINGS

See Aerodynamics.

DOWNWASH

A Note on the Evaluation of the Supersonic Downwash Integral, B. A. Hunn, p. 111 (July 1954).

ELECTRICAL POTENTIAL ANALYSER

The Use of an Electrical Potential Analyser for the Calculation of the Pressures on Lifting Surfaces, S. C. Redshaw, p. 163 (September 1954).

FAILURE RATE

The Frequency of Failures within a Group of Similar Structures, A. H. Chilver, p. 235 (November 1954).

FLAME STABILISATION

Flame Stabilisation in High Velocity Gas Streams and the Effect of Heat Losses at Low Pressures, D. B. Spalding and B. S. Tall, p. 195 (September 1954).

FRENKIEL, F. N.

Effects of Wire Length in Turbulence Investigations with a Hot-Wire Anemometer, p. 1 (May 1954).

GORGUI, M. A.

The Effect of Delta Vanes on Supersonic Wings, p. 251 (November 1954).

HANCOCK, G. J.

The Design of Thin Finite Wings in Incompressible Flow, p. 119 (July 1954).

HOT-WIRE ANEMOMETER

See Aerodynamics.

HUNN, B. A.

A Note on the Evaluation of the Supersonic Downwash Integral, p. 111 (July 1954).

LANCE, G. N.

The Delta Wing in a Non-Uniform Supersonic Stream, p. 55 (May 1954).

LONGHORN, A. L.
Subsonic Compressible Flow Past Bluff Bodies, p. 144 (July 1954).

OSCILLATING AEROFOIL
See Aerodynamics.

PALMER, P. J.
The Natural Frequency of Vibration of Curved Rectangular Plates, p. 101 (July 1954).

PRESTON, J. H.
A Simple Approach to the Theory of Secondary Flows, p. 218 (September 1954).

REDSHAW, S. C.
The Use of an Electrical Potential Analyser for the Calculation of the Pressures on Lifting Surfaces, p. 163 (September 1954).

SECONDARY FLOWS
A Simple Approach to the Theory of Secondary Flows, J. H. Preston, p. 218 (September 1954).

SEWELL, GEOFFREY L.
A Theory of Uniform Supersonic Flow Past a Thin Oscillating Aerofoil at Appreciable Incidence to the Main Stream, p. 185 (September 1954).
Theory of an Accelerated Slender Supersonic Aerofoil, p. 52 (May 1954).

SPALDING, D. B. and B. S. TALL
Flame Stabilisation in High Velocity Gas Streams and the Effect of Heat Losses at Low Pressures, p. 195 (September 1954).

STABILITY
See Aerodynamics.

STRUCTURES
See also Failure Rate.
Buckling of Oblique Plates with Clamped Edges under Uniform Shear, W. H. Wittrick, p. 39 (May 1954).
Symmetrical Buckling of Right-Angled Isosceles Triangular Plates, W. H. Wittrick, p. 131 (July 1954).
The Natural Frequency of Vibration of Curved Rectangular Plates, P. J. Palmer, p. 101 (July 1954).

TALL, B. S. and D. B. SPALDING
Flame Stabilisation in High Velocity Gas Streams and the Effect of Heat Losses at Low Pressures, p. 195 (September 1954).

VANES ON WINGS
The Effect of Delta Vanes on Supersonic Wings, M. A. Gorgui, p. 251 (November 1954).

WIEGHARDT, K. E. G.
On a Simple Method for Calculating Laminar Boundary Layers, p. 25 (May 1954).

WILKINSON, J.
Some Examples of Three-Dimensional Effects in Boundary Layer Flow, p. 73 (May 1954).

WITTRICK, W. H.
Buckling of Oblique Plates with Clamped Edges under Uniform Shear, p. 39 (May 1954).
Symmetrical Buckling of Right-Angled Isosceles Triangular Plates, p. 131 (July 1954).

WOODS, L. C.
A Note on the Numerical Solution of Fourth Order Differential Equations, p. 176 (September 1954).